УДК 550.838:551.14 DOI: https://doi.org/10.24028/gj.v48i1.347053

Magnetic model of the crystalline crust and heterogeneity of the lithosphere in the junction zones between the East European Craton and surrounding structures. Part I. The SW border

I.K. Pashkevich, M.I. Orlyuk, M.I. Bakarzhieva, A.V. Marchenko, 2026

S. Subbotin Institute of Geophysics of National Academy of Sciences of Ukraine, Kyiv, Ukraine
Received 20 December 2025

This article is the first attempt to establish a connection between magnetic heterogeneities in the crystalline crust in the Teisseyre-Tornquist Line region of the SW edge of the East European Craton and heterogeneities in the mantle. A 3D magnetic model of the crystalline crust was created using near-surface anomalous magnetic fields, velocity and structural sections from seismic profiles. The sources are attributed to two levels: local sources to the entire thickness of the upper crust, and deep ones to the middle and lower crust. Magnetization is assumed to be homogeneous, equilibrium, and constant to the depth of the Moho discontinuity or until the Curie temperature of magnetite is reached. This model parameterization led to the estimation of the minimum possible values of source magnetization. The total effect of crustal sources was matched to the observed field by trial and error with an error of no more than 30 nT. The relationship between crustal magnetic heterogeneities and mantle structure is based on the use of compiled diagrams of the main features of the crystalline crust, of the heterogeneity of the subcrustal mantle, and the transition layer from the upper to the middle mantle. The main feature of the 3D magnetic model is the presence of deep magnetic bodies accompanying Teisseyre-Tornquist Line, the Sörgenfrey-Tornquist Zone and the Thor-Tornquist Suture. The strip of magnetic bodies from NE is limited by the lineament L subparallel Teisseyre-Tornquist Line, which we have identified based on the magnetic field structure. It correlates with the Caledonian deformation front in Fennoscandia and the Rava-Ru'ska fault in Sarmatia. This allows us to link magnetic sources with the activation of the Teisseyre-Tornquist Line system and mafic intrusions. The magmatic genesis of these magnetic sources is also evidenced by their location above the overthrust of the subcrustal mantle of the East European Craton onto the mantle of the West European Platform. The overthrust was established based on seismotomography data. It correlates with the underthrust of the lower crust of the East European Craton under the crust of the West European Platform. It is assumed that these structures are connected with their synchronous movement from the NE to the SW, the formation of a stretchingzone, and the intrusions. The stretching regime along the Teisseyre-Tornquist Line may also be caused by SW subduction, which is confirmed by the identified high-speed inclined layers (slabs).The magmatic origin of magnetic sources does not exclude the formation of 'secondary' magnetic minerals due to the penetration of deep fluids into the crystalline

Citation: Pashkevich, I.K., Orlyuk, M.I., Bakarzhieva, M.I., & Marchenko, A.V. (2026). Magnetic model of the crystalline crust and heterogeneity of the lithosphere in the junction zones between the East European Craton and surrounding structures. Part I. The SW border. *Geofizychnyi Zhurnal*, *48*(1), 41—95. https://doi.org/10.24028/gj.v48i1.347053.

crust. This process is facilitated by the increased permeability of the lithosphere, the 'blurring' of the main geodynamic boundary, and the disturbance inthe transition layerstructure of the upper mantle. The nature of deep magnetic sources associated with Teisseyre-Tornquist Line can thus be explained by both primary magnetic minerals of mafic rocks and secondary minerals brought up from the depths.

Key words: East European Craton, 3D magnetic modelling, magnetic field, lithosphere heterogeneity, magnetic anomalies, magmatism, Teisseyre-Tornquist Line, mantle, subduction zones.

Introduction. The deep structure of the Earth's crust and upper mantle of the East European Craton (EEC) and adjacent regions, including its southwestern border, has been intensively studied. In these large-scale national and international programs and projects, seismic methods played a leading role (EUROPROBE Program, POLONAISE-97, BABEL; European GeoTravers (EGT) Project, MONA LISA, DECORP-BASIN, CELEBRATION 2000, ESTRID и др.).

The edges and boundaries of the craton were described in numerous publications; however, they leave a number of points open to debate. Among them are the position of the boundary of the craton's crystalline crust and its subcrustal mantle, 'buried' under younger formations, and their tectonic position. An exception may be the craton's SW border studied most extensively for over a century since its discovery as the Teisseyre-Tornquist Line (TTL).

TTL is named after Polish geologist Wawrzyniec Teisseyre and German geologist and palaeontologist Alexander Tornquist. These researchers independently discovered the southeastern and northwestern parts of TTL. In the southeast, the Berdo-Narol Line was noted by W. Teisseyre in publications in 1893 and 1903 (see references in [Grad, 2019]) as the southwestern border of Podillia. In the northwest, A. Tornquist mapped the southwestern border of the Baltic Plate along the Scania-Lysagory line in 1908 and 1910 (see ibid.). Both lines joined near Sandomierz and formed the TTL, first published by A. Tornquist in his Tectonic Map of Europe in 1913. The TTL was considered a fault or fault zone delimiting the EEC. It was then named the Teisseyre-Tornquist Zone, later, the term Trans-European Suture Zone (TESZ) was introduced, as a collage of collided terrains 100—200 km wide. The NW spreading of the TTZ was named the Songenfrei-Tornquist Zone (STZ).

It is appropriate here to clarify the terminology used: TTL, TTZ and TESZ, since in the literature these terms are incorrectly used interchangeably.

To quote from [Grad, 2019, p. 432]:

« – Teisseyre-Tornquist Line (TTL) conceived as a linear feature is border of crystalline, "granitic" line;

– Teisseyre-Tornquist Zone (TTZ) is zone in sedimentary cover related to the edge of craton;

– Trans-European Suture Zone (TESZ) is a term for the assemblage of suspect terranes boarded by the EEC and WEP; TESZ should not be mistaken with previous ones».

S.V. Bogdanova has repeatedly addressed questions about the nature of the junction between the EEC and the surrounding geological provinces (for example [Bogdanova et al., 2016]). We hope that the results of 3D magnetic modelling of the EEC and surrounding areas, presented here with an emphasis on the characteristics of its boundaries and the heterogeneity of the lithosphere, will add a new dimension to the explanation of the craton's borders' deep structure and its connection with the tectonics of the craton's segments' the marginal parts.

1. State of the problem. As is well known, the EEC, consists of three segments —Fennoscandia, Sarmatia, and Volga-Uralia [Bogdanova, 1993] and is surrounded by younger tectonic units of varying ages with different developmental histories. Thus, its marginal parts and the boundaries of the consolidated crust have their own characteristics of lithosphere structure, including the nature of deep

magnetic heterogeneities. Fig. 1 shows the main tectonic units of the EEC against the background of the anomalous magnetic field. In the southwest, along the complex TESZ, the EEC borders the Caledonides, Variscan Mountains, and Carpathians.

The northwestern boundary of the craton is hidden beneath the Caledonides, which were thrust onto the Precambrian foundation. The source of the Caledonides is unknown, but probably located far from the modern western coast of Scandinavia. The pre-Caledonian basement can be traced more than 400 km towards the Atlantic Ocean according to geophysical data [Bogdanova et al., 2016]. To the NNE, the EEC is surrounded by the Timanides Belt, which formed on the passive continental margin. To the east, the boundary of the craton is defined by the collision zone of the European and Asian terrains and the Late Palaeozoic Ural orogen that formed here. The southern edge of the EEC borders the Scythian Platform (microcontinent), complicated by the Caledonian and Alpine orogeny.

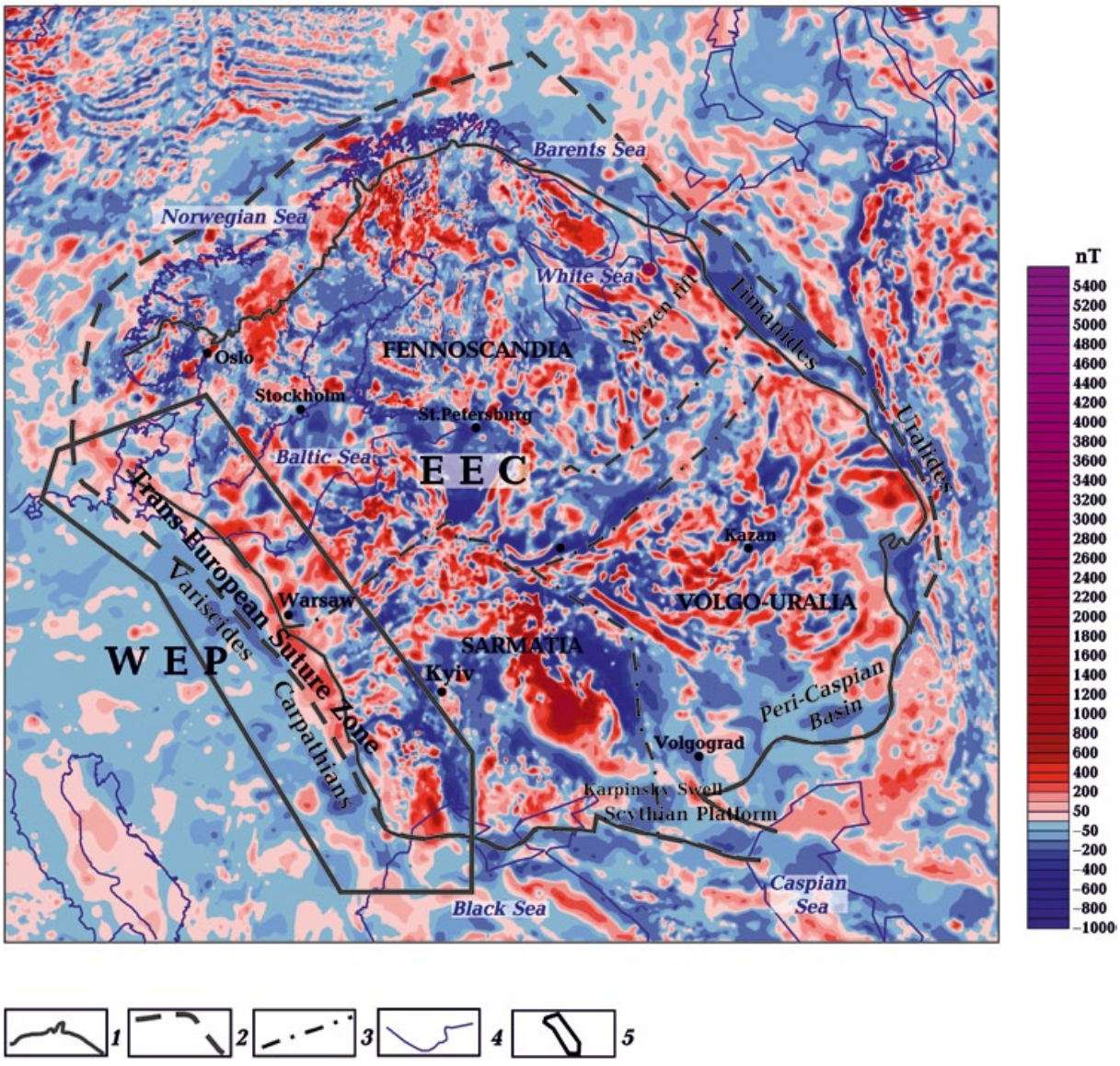

Fig. 1. Anomalous magnetic field of the East European Craton and its surroundings [Meyer et al., 2017]. Craton zoning according to [Bogdanova et al., 2016]: *1* — EEC border; *2* — outer border of the EEC; *3* — borders of the crust segments of the craton; *4* — coastline; *5* — area of the studied region.

A number of fundamental summaries [Artemieva et al., 2006, Grad et al., 2009, 2018; Artemieva, 2011, 2019; Artemieva, Thybo, 2013; Bogdanova et al., 2016; Grad, 2019; Narkiewicz, Petecki, 2019; Majorowicz et al., 2019, etc.] are based on a complex of geological data and the results of interpretation of seismic observations, potential fields, and heat flow.They provide a general characterization of changes in the structure of the Earth's crust and lithosphere of the EEC as a whole and its surroundings.

As shown by [Artemieva et al., 2006; Artemieva, Thybo, 2013], the generalized parameters of the lithosphere, the average velocities of the crust, its thickness, and the thickness of the lithosphere of the EEC and Palaeozoic structures in the southwest vary widely. However, the general pattern is a sharp change in crust thickness from 35 to 65 km within the EEC from 28 to 38 km in the Caledonides and Viriscides, and from 45 to 50 km at the transition from the EEC to the Pre-Carpathian Trough and the Carpathians. The lithosphere thickness in the Caledonides ranges from 90 to 140 km and within the craton from 135 to 300 km, while in the Variscides it is 70—140 km. The average crustal velocities in the Caledonides are 6.0—6.4 km/s, in the Variscides — 6.3—6.7 km/s, with the maxima significantly lower than the maxima in the EEC. In the east, the Ural orogen is an exception to this pattern, with the thickness of the crust increasing from west to east from 45 km in the Pre-Ural Trough to 65 km in the central part, and the thickness of the lithosphere estimated at 175—200 km.

As for the characteristics, the crystalline crust of EEC has a high average magnetization, while the crust of the surrounding structures is weakly or non-magnetic [Pashkevich et al., 1990 and references to it; Krutikhovskaya, 1984; Pechersky, 1994; Taylor, Ravat, 1995; Hahn, Wonik, 1990; Orlyuk, Pashkevich, 1995; Thybo, 1997, 2001; Orlyuk, 2000; Grabowska, Bojdys, 2001; Wonik et al., 2001; Banka et al., 2002; Pharaoh et al., 2006; Thébault et al., 2010; Mazur et al., 2015; Vervelidou, Thébault, 2015; Milano et al., 2016, 2019; Grabowska et al., 2017, etc.].

Using the global-scale magnetic field of the Earth's lithosphere in the form of a series of 16—120 harmonics, generalized data on the thickness of the magnetically active layer and its magnetization have been obtained [Thébault et al., 2010; Vervelidou, Thébault, 2015]. According to these data, the thickness of the magnetically active layer of the ECC is 32—70 km, and for the West European Platform (WEP), 20—27 km. The weighted average magnetization of the Earth's crust varies between 0.1 and 1.0 A/m for the craton and between 0.02 and 0.5 A/m for the WEP. At the same time, the change in the thickness of the magnetically active layer and its magnetization occurs along the TTZ.

The aforementioned general contrasts in lithosphere parameters at the boundaries of the EEC reveal their peculiarities upon closer examination along each of the boundaries.

2. The anomalous magnetic field $(\Delta T)_a$ EEC and its flanking. It should be note that the authors adhere to the convention established in magnetometric work of denoting geomagnetic field induction with the symbol T instead of B.

The anomalous magnetic field of the craton (see Fig. 1) is characterised by a wide range of sizes, intensities (from the first tens to the first hundreds and thousands of nanotesla above iron ore deposits), morphology, and the strike of the anomalies. Two components can be distinguished in the field $(\Delta T)_a$: one of the local upper crustal origin and one regional, caused by deep heterogeneities in the crystalline crust. The anomalous magnetic field of the EEC reflects the tripartite crustal-segment structure (Fennoscandia, Sarmatia, Volga-Ural) and the suture zones separating the segments [Bogdanova et al., 1996].

Various sections of the border areas of the craton are characterized by orderly linear anomalies, zones of increased anomalous magnetic field, consistent with the strike of the border. At the same time, magnetic anomalies and their zones can be located either on the inner side of the craton, on its outer side, or on both sides of the assumed position of the modern boundary of the ancient craton.

In some cases, there is a butt joint of the strike of the anomalies of the craton itself and the suture zones, or a continuation of the craton strike under the foothill depressions.

Let us consider the distribution of magnetic anomalies along various sections of the EEC boundary.

The southwestern boundary of the craton runs through the eastern part of the North Sea and the southern part of the Jutland Peninsula, north of the island of Rügen, along the TTZ along the northeastern edge of the Świętokrzyskie Mountains, southeast of which it extends under the Pre-Carpathian Trough. This border is fixed by a continuous linear zone of a high gradient separating the differentiated anomalous magnetic field of the EEC and the calm, slightly negative field of the WEP. Directly adjacent to the high-gradient zone on the craton side, there is a marginal strip of magnetic maxima of varying intensity with the same strike as the zone. It has a butt joint with the predominant northeast strike of anomalies within the craton and accompanies the high-gradient field zone almost along its entire length. The strike of magnetic anomalies corresponds to the dip of the Precambrian basement to 8.0—9.0 km in the zone of pericraton lowering of the Baikal, Caledonian and Hercynian stages of development.

The emergence of this anomalous zone is probably associated with the processing of the material composition of the Precambrian basement during the process of lowering or enrichment of rocks with magnetite, the transformation of the Precambrian structural plan and, accordingly, the morphology of the magnetic field.

The SW boundary of the EEC in the form of the TTZ and its NW strike (STZ and Thor-Tornquist Suture (Thor-TS)) were formed during a long and multiphase development process. The structure of the lithosphere reflects various stages of intraplate regime activation from the Variscan transgression to the Neogene Carpathian orogenic compression [Narkiewicz, Petecki, 2019; Grad, 2019; Gintov et al., 2022, etc.]. As a result, the junction of the EEC and WEP in the modern tectonic setting appears as a sharp change in the structure of the lithosphere, its thickness, and the types of consolidated crust.

Without touching upon controversial issues concerning the possible continuation of the TTZ to the SE and NW as part of the global Trans-Eurasian, Greenland-Zagros, Baltic-Iranian [Pokalyuk et al., 2020] Lineaments, we will only note that since its discovery, the TTL, and subsequently the TTZ, has been considered as a zone limiting the EEC from the SW. The TTL records a sharp change in the composition and thickness of the ancient crystalline crust at the contact with the young crust. In the Carpathian region, for example, it can be considered as the Pre-Carpathian Fault [Gintov et al., 2022; Orlyuk et al., 2022] in the form of a drop with an amplitude of more than 5 km [Zayats, 2013]. The change in these parameters is accompanied by the formation of a trough (Subcarpathian, for example), made up of Palaeozoic and Mesozoic sediments, covered by Mesozoic–Cenozoic sediments, thrusted over the Main Carpathian Thrust. In the Carpathian region, the trough is bounded by the Pre-Carpathian and Uzhok Faults (folds).

An important argument in favour of the collision-related Precambrian structure of EEC—WEP is the keel in the Moho section beneath it. In [Mazur et al., 2018], the keel is interpreted as a relic of the Precambrian collision suture from the time of Rodinia amalgamation. The TESZ structure includes TTL, TTZ, and Mesozoic-Cenozoic structures along TTZ, forming a zone 150—200 km wide [Gintov et al., 2022, etc.].

The NW-SE changes in the structure and parameters of the lithosphere along the TTL in Poland is shown in Figs. 2—5 and 9—14, 16 in [Majorowicz et al., 2019]. The temperature calculations, including the depth to the Curie isotherm of magnetite (580 °C) at various depths for four models, showed the main patterns of their change during the transition from the VEC to the Variscides and Alpides. The depth of the lithosphere-asthenosphere thermal boundary (LAB) varies from 200 km in the NE to 90 km in the SW. The position of the LAB in the Seis-Grav model presented in this work is closest in morphology to the

thermal LAB, although the difference in depth reaches 50 km.

The southern boundary of the EEC in the Black Sea region is not as continuous and distinct in the magnetic field as the southwestern boundary. Regional magnetic anomalies, predominantly of sublatitudinal strike, are located on the outer side of the craton, forming a transition zone. They also have a butt joint with the anomalies of the craton itself, which are usually of submeridional strike.

The transition from the southern border of the craton to the eastern one is marked by a transregional zone of minimum magnetic field from Donbass to Karpinsky Ridge, where it is conjugated with a zone of echeloned positive regional anomalies of the Ridge.

Further to the east, the platform boundary is a subject of debate. Its position in the magnetic field is not pronounced. The southeastern corner of the craton is most clearly visible in the magnetic field. Here, large anomalies are noted, located on the outer southeastern side of the Caspian Depression and along the Uralids, as well as a positive anomaly from the satellite.

The eastern boundary of the craton manifests itself as a zone of weak magnetic field gradients from the satellite, combining with linear local anomalies of the Ural strikes. The magnetic anomalies of the edge of the Volga-Ural region do not it.

The northern and northeastern boundary of the craton correspond to the strike of the craton boundary and in some cases have a butt joint with boundaries of the craton are marked by the most complex combination of extended linear magnetic anomalies. In general, these boundaries are conjugated with a magnetic minimum that can be traced from the northwestern corner of the craton to the Uralids. Within the marginal part of the craton, the extensive strictly linear magnetic anomalies have two directions: one is associated with the strike of the Khibiny transblock zone of faults with a width of about 500 km from the Karpinsk Fault on the coast of the Barents Sea to the southern border of the Mezen' rifts in the south, the other with the strike of the northwestern part of the Pre-Timan Trough. The eastern part of the trough is accompanied by an anomaly in the outer southeastern edge zone. Anomalies with such a strike can be traced within the Pre-Ural Trough as a continuation of the northern border of the Pre-Timan Trough.

The northwestern edge of the East European Craton is the least pronounced in the magnetic field. It is difficult to establish a clear boundary between the submeridional plane of regional magnetic anomalies in Scandinavia, extending into the Caledonian covers, and the northeastern strikes of linear magnetic anomalies on the Norwegian Sea's shelf. Most likely, this transition can be traced approximately along the 500 m isobath.

Analysis of magnetic anomalies in the marginal parts of the platform indicates that its modern boundaries were formed in stages and differed significantly in different regions. Magnetic anomalies in the marginal parts should probably be considered as a manifestation of basic magmatism or reworking of the composition of the Earth's crust, accompanied by an increase in the concentration of magnetite. As shown by [Orlyuk, 1984, 1986; Pashkevich et al., 1986], such reworking of material can occur in geodynamic conditions of predominant stretching and bending of the Earth's crust.

It is possible to note the uneven distribution of ground magnetic anomalies and anomalies obtained from satellites (see Fig. 1) in different marginal parts of the craton, and the different positions of magnetic anomalies at the edges of the EEC in relation to its boundary established on the surface of the crystalline crust [Pashkevich et al., 1985; Pashkevich, 1989; Orlyuk, 2000].

Based on the structural relationships between magnetic anomalies and EEC boundaries, the following types of anomaly ensembles can be distinguished:

– a virtually continuous series of anomalies along the southwestern boundary of the craton with a butt joints connecting them to anomalies in its interior, a linear zone of high-gradient Magsat and CHAMP anomalies;

– parallel anomalies that 'intersect' the edge of the craton, discordant with its main

structural elements and forming a wide zone (NW boundary);

– anomalies of the edge of the craton and adjacent regions, consistent with the strike of the craton boundary, combined with a positive satellite anomaly within the continental and shelf parts of the EEC (N-NE boundary);

– a sharp break in the ground and satellite anomalies of the inner part of the craton at its border (eastern and southern borders).

Since the 1970s, research has been conducted on the regional component of the anomalous magnetic field at ground level and satellite anomalies in various tectonic regions [Riddihough, 1972; Krutikhovskaya et al., 1973, 1982, 1984; Hall, 1974; Bulina, 1976; Krutikhovskaya, 1976, 1982, 1984; Krutikhovskaya, Pashkevich, 1977, 1979; Coles et al., 1976, 1982; Wasilewski et al., 1979; Schnetzler, Allenby, 1983; 1984; Orlyuk, 1984, 1986; Genshaft, Pecherskyi, 1986; Arkani-Hamed, Strangway, 1986; Mundt et al., 1986; Buryanov et al., 1987; Toft, Haggerty, 1988; Pashkevich et al., 1990 and references to it; Purucker et al., 2002; Milano et al., 2016; Williams, Gubbins, 2019; Maksymchuk et al., 2024; Kis et al., 2024, etc.]. The possibility of deep magnetic sources has been substantiated and the lower limit of the magnetically active layer has been estimated, which has provided additional information for a comprehensive characterization of the deep structure of the crystalline crust.

Deep crustal origin of long-wave magnetic anomalies does not exclude the possibility of mantle magnetic sources [Orlyuk et al., 2020]. This issue is related to the interpretation of satellite magnetic anomalies, the nature of which has been debated in recent decades. This discussion covers the problem of the cumulative effect of crustal sources at satellite altitudes and the problem of determining the maximum depths at which magnetic minerals exist, with an assessment of the preservation of their magnetization. New experimental data indicate the stability of iron oxides to depths of at least 660 km [Ferré et al., 2020]. Fresh samples of mantle xenoliths usually contain magnetite. In subduction zones, hematite is the predominant iron oxide at depths of 300—600 km. Studies of magnetic transitions and critical temperatures in hematite at ultra-high pressures and temperatures (P up to 90 GPa, T up to 1300 K) have shown that hematite remains magnetic at transition zone depths in cold or very cold subduction settings [Kupenko et al., 2019]. In recent decades, new iron oxides have been discovered that are stable at these depths. It cannot be ruled out that below these depths, justite may be present as a magnetic mineral; however, its Curie temperature behaviour at high pressures is unknown.

The most favourable tectonic regions for mantle sources are 'cold' ancient cratons and subduction zones and their relatively cold slabs, where the Curie isotherm deviates downward. In these regions, a serpentinized magnetic wedge can also be a magnetic source. The subduction setting also provides transport of iron oxide-enriched hydrothermal fluids into the subcrustal mantle and crust. Due to changes in magnetic mineralogy, the nature of the source in the slab may vary [Ferré et al., 2020].

Satellite anomalies are associated with subduction zones [Clark et al., 1985; Arkani-Hamed, Strangway, 1986; McEnroe et al., 2018; Williams, Gubbins, 2019; Ferré et al., 2020, etc.]. Several models of magnetization distribution are considered with that: increasing (the «wedge» model), decreasing (the «slab» model), and uniform.

In view of the above, 3D magnetic modelling of crustal sources and assessment of their contribution to satellite anomalies is relevant.

2D magnetic models of the EEC Earth's crust were constructed based on separate GSZ profiles [Krutikhovskaya et al., 1982; Burianov et al., 1987; Sollogub, 1988a, b; Thybo, 2000, 2001; Grabovska, Bojdysg, 2001, 2004; Williamson et al., 2002; Petecki, 2008; Grabovska et al., 2011, 2017; Petecki, Rosowiecka, 2017, etc.]. 3D magnetic modelling was carried out for several regions of the EEC [Orlyuk et al., 2017 and references therein; Orlyuk, 1984, 1986, 1993; Orlyuk, Pashkevich, 1995; Grabowska et al., 2017, etc.].

The work [Pashkevich et al., 1990 and references to it] represents the first attempt to

create a 3D magnetic model of Europe, including the EEC. However, it was constructed without taking into account the sphericity of the Earth, which is necessary to obtain realistic shapes of sources and magnetization values in areas larger than 5,000 km^2.

The previously obtained 3D magnetic model [Orlyuk et al., 2017] of the middle-lower crust of the EEC, taking into account the sphericity of the Earth and the craton's surroundings in the form of projections of the upper edges of deep magnetic sources onto the Earth's surface, gives an idea of the magnetic heterogeneity of the middle and lower crust of the region. It highlights the different saturations of deep magnetic sources in the Precambrian crust of the EEC and the crust of the surrounding regions and, consequently, their different average magnetizations. Within the craton, the highest concentration of sources and their maximum magnetization is observed in its southwestern part.

The aim of this article was to detail the magnetic model of the southwestern edge of the EEC directly in the TTL area and to analyze the relationship between the magnetic heterogeneity of the middle and lower parts of the consolidated crust and the features of its structure and the structure of the upper mantle.

3. Data and methods. A 3D magnetic model of the EEC Earth's crust in the TTZ area and its surroundings, taking into account the sphericity of the Earth, was constructed on a scale of 1:5,000,000. The following data were used to create it: World Digital Magnetic Anomaly Map (WDMAM) at an altitude of 5 km (2007), heat flow and temperature distribution in the lithosphere, relief diagrams of the surface of the basement and the Moho boundary, as well as other geological and geophysical data [Chekunov, 1992; Kutas, 1993; Artemieva, Mooney, 2001; Artemieva, Thybo, 2013; Orlyuk, 2000; Korhonen et al., 2007; Grad et al., 2009; Bogdanova et al., 2015, 2016; Orlyuk et al., 2017, etc]. For magnetic modelling, regional anomalies were obtained by averaging the initial field of the entire EEC with a 40×40 km window [Orlyuk et al., 2024b].

The magnetically active layer of the Earth's crust was limited to depths where the Curie temperature of magnetite (580 °C) — the main magnetic mineral of the crystalline crust — is reached. Since most of the EEC has a 'cold' regime [Kutas, 1993; Artemieva, Mooney, 2001], the lower boundary of the magnetically active layer is taken to be the Mohorovičić discontinuity as a petrological boundary. The upper boundary of deep magnetic sources is attributed to the roof of the middle crust ('diorite' layer), lying at depths of 8 to 15 km. The exceptions are the Dnieper-Donets Aulakogen and the Caspian Depression, where the depth to the crystalline basement reaches 20 km.

The direction of the total magnetization vector is assumed to coincide with the direction of the total vector of geomagnetic field intensity as a consequence of the equilibrium state of rocks magnetization with multidomain ferromagnetic grains in the deep parts of the crust [Pechersky, 1994]. The modelling incorporated the actual values of the power and angular components of the geomagnetic field induction vector DGRF-IGRF [Meyer et al., 2017; Brown et al., 2021]. These data were taken into account using an algorithm for solving a direct magnetic survey problem for the spherical surface of the Earth [Kovalenko-Zavoyskiy, Ivashchenko, 2006; Orlyuk et al., 2007; Orlyuk, Marchenko, 2008].

To construct a magnetic model of the EEC at a scale of 1:5,000,000, it is entirely justified to use uniform averaging parameters for the initial field. However, since anomalies are attenuated variably with source depthit is unacceptable to divide the field into parts with constant transformation parameters for more detailed modelling within the southwestern edge of the craton with differentiated relief of the Precambrian basement and middle crust roof. In this regard, magnetic modelling was performed by trial and error using the well-known and widely used approach of reducing the initial field by exclusion the influence of upper crust sources. The effects of local sources were evaluated at fixed depths of the upper and lower edges, at the depth to the crystalline basement and the roof of the middle crust. The regional component of the field was determined by progressive

approximation to a 'smooth' form. All other principles of magnetic model construction described above were also applied to detailed modelling.

The source materials for modelling this stage were published 1:500,000 and 1:1,000,000 maps of ground-level anomalous magnetic field compiled from data on the following territories: Ukraine [Nechaeva et al., 2002; Orlyuk et al., 2024a], Poland [Petecki et al., 2003], Germany [Gabriel et al., 2011], Denmark [Lyngsie, Thybo, 2007], Sweden [Stephens, 2020], Slovakia [Kubeš et al., 2010], Romania [Airinei et al., 1983], Hungary [Kiss, Gulyás, 2006], as well as sections along seismic profiles, and data on the depths of the Moho and Curie isotherms of magnetite. At the same time, the available modelling results for individual regions were analyzed.

As a basis for constructing a 3D magnetic model of the middle-lower crust, 2.5D models were constructed using seismic profiles: Transect1, P2, P4, CEL01, PANCAKE, and RomUkrSeis. The magnetization values obtained from the profiles were then corrected after the results of 3D modelling. The data from seismic profiles in the area, which were carried out as part of international and national programs and projects, were taken into account.

4. Results. The magnetic model of the middle-lower crystalline crust of the EEC, previously constructed [Orlyuk et al., 2017] on the basis of the averaged magnetic field, was supplemented by more detailed magnetic modelling of the SW edge of the craton. The results are presented as the distribution of projections of the upper edges of deep magnetic sources along the TTL and in sections along the most representative seismic profiles. To analyze the relationship between the crust's magnetic heterogeneity and the structure of the lithosphere, we constructed a diagram of the main tectonic elements of the crust, a diagram of the heterogeneity of the upper mantle, and a diagram of the types of transition layer from the upper to the middle (lower) mantle based on seismotomography (Fig. 2, 3, 4).

4.1. ***Features of the crystalline crust structure***. The ratio of the EEC's crust to the surrounding provinces, crust types, and some elements of fault tectonics are shown in Fig. 2. The diagram is based on published materials.

Published materials were used to describe of faults [Thybo, 1997, 2001; Grad et al., 2002; Bayer et al., 2002; Gurskyi, Kruglov, 2007; Seghedi, 2012; Zayats, 2013, Grabowska et al., 2017; Petecki, Rosowecka, 2017; Mazur et al., 2021; Gintov et al., 2022, etc]. Due to the 'rejuvenation' of the tectonic units that make up the mosaic of the SW environment of the EEC, the nature of the change in lithospheric parameters varies from NW to SE. The TTL strike changes in the same direction: 305° along Fennoscandia (Fs) in the NW, 330° in the SE along Sarmatia (Sm) (see Fig. 2, *b*). The change in the strike of the TTL branches occurs in the zone where the TTL and FSS intersect.

In the extreme NW of the SW edge of the EEC, the junction of the Baltic and Eastern Avalonia occurs along the NW branching of the TTZ in the so-called Tornquist Fan region, bounded by the TEF and the SW Baltic Marginal Fault [Thybo, 1997]. The fault zones that were activated with the change of tectonic regimes in the Mesozoic, Cretaceous, and early Tertiary periods are branching in the area.

Within this area, two suture zones are directly relevant to assessing the nature of the junction between the Baltic and Eastern Avalonia: the Thor Suture (ThorS) (we use the term Thor-Tornquist Suture, Thor-TS) and the Sorgenfrei-Tornquist Zone (STZ). Thor-TS marks the closure of the Tornquist Ocean in the Ordovician. The absence of signs of subduction magmatism in the Baltic indicates SW subduction. According to seismic data, the suture is crustal with a dip angle of 10—12° to the SW.

The STZ has a long history of activation dating back to the Neoproterozoic and has no direct connection with Thor-TS. It represents the northern boundary of the Variscan crustal deformations. In the deep structure of the crust, the STZ fixes the Moho discontinuity within the EEC with an amplitude of ~5 km. The entire Tornquist Fan area and surrounding regions are characterized by Carboniferous-Permian extension and metamorphism,

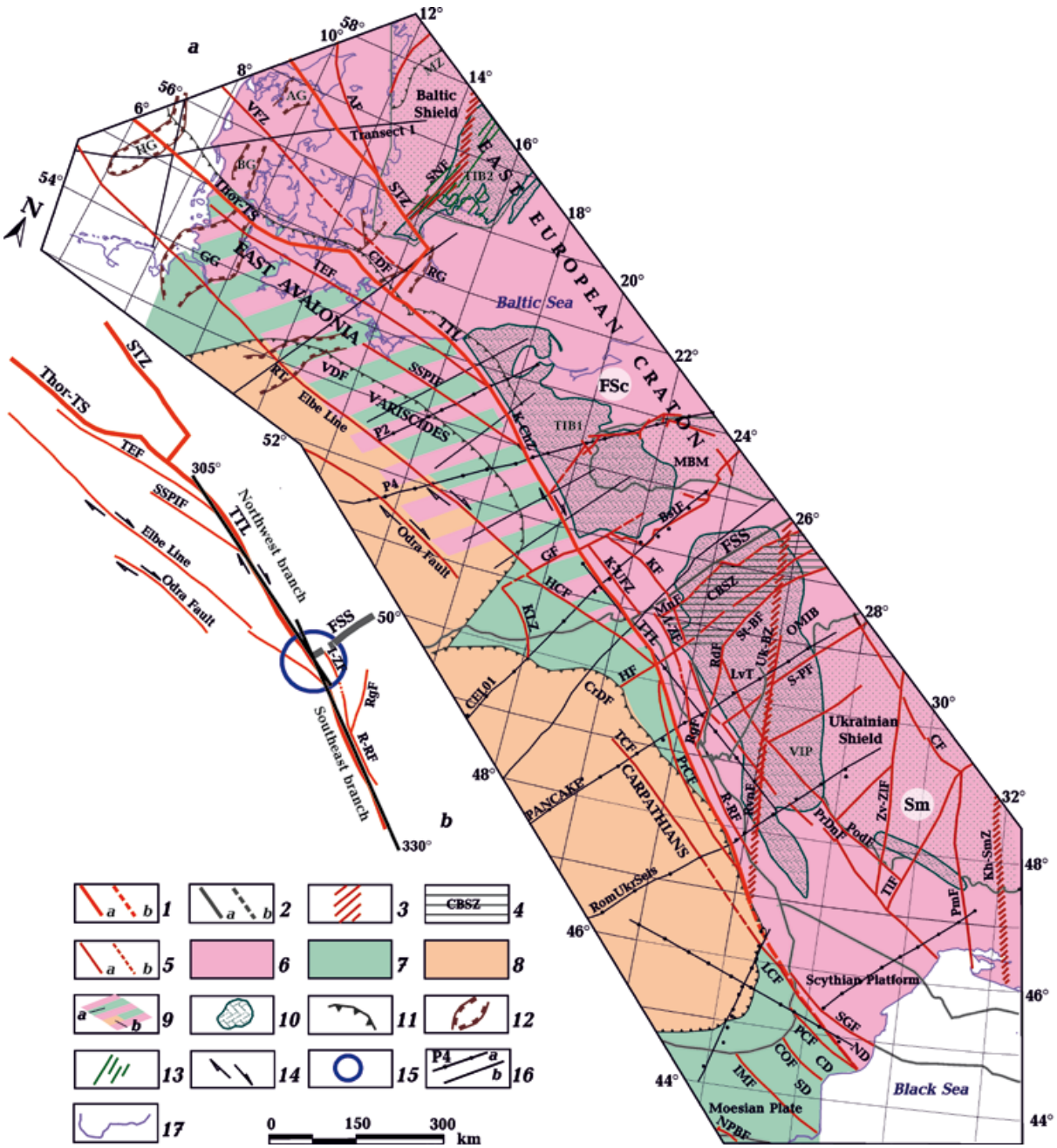

Fig. 2. Diagram of the main tectonic elements of the SW part of the EEC and its surroundings (*a*), change in the strike of the TTL (*b*), triple junction of the FSS and branches of the TTL: *1* — crystalline basement positions of the Teisseyre-Tornquist Line (TTL), the Sorgenfrey-Tornquist Zone (STZ) and the Thor-Tornquist Suture (Thor-TS) projected onto the Earth's surface (*a*), the projection's possible continuation (*b*); *2* — the Fennoscandia-Sarmatia Suture (FSS) (*a*) and its possible continuation (*b*); *3* — transregional zones of activation: Ukrainian-Baltic (Uk-BZ), Kherson-Smolensk (Kh-SmZ), Sveconorwegian Front (SNF); *4* — Central Belarusian Suture Zone (CBSZ); *5* — main faults (*a*) and their possible continuation (*b*); *6* — EEC crust; *7* — WEP crust; *8* — Variscan and Carpathian crust; *9* — Avalonian crust underlain by high-velocity EEC lower crust (*a*), Variscan crust underlain by EEC lower crust (*b*); *10* — Igneous formations: Volyn' Igneous Province (VIP), Transscandinavian Igneous Belt (TIB1, TIB2); *11* — deformation fronts: Caledonian (CDF), Variscan (VDF), Carpathian (CrDF); *12* — graben boundaries: Alborg Graben (AG), Brande Graben (BG), Glückstadt Graben (GG), Horn Graben (HG), Rønne Graben (RG); *13* — large swarm of dolerite dikes; *14* — direction of displacement along faults; *15* — intersection of FSS and TTL branches; *16* — seismic profiles (*a*), including reference profiles used in 3D modeling (*b*); *17* — coastline. For other abbreviations: CD — Central Dobrogea, ND — North Dobrogea, SD — South Dobrogea, BstF — Bialystok

Fault, COF — Capidava-Ovidiu Fault, GF — Grójec Fault, HCF — Holy Cross Fault , HF — Hrubieszów Fault, IMF — Intra-Moesian Fault, I-ZF — Izbica-Zamość Fault, K-ChZ — Koszalin-Chojnice Zone, KF — Kock Fault, KLZ — Kraków-Lubliniec Zone, K-UFZ — Kazimierz-Ursynow Fault Zone, LCF — Luncaviţa-Consul Fault , LvT — L'viv Trough, MBM — Mazur Belarusian Massif, MnF — Minsk Fault, MZ — Mylonite Zone, NF — Nemyriv Fault, NPBF — North Pre-Balkan Fault, OMIB — Osnyts'k-Mikashevichi Igneous Belt, PCF — Peceneaga-Camena Fault, PmF — Pervomays'k Fault, PodF — Podillia Fault, PrCF — Pre-Carpathian Fault, Pr-DnF — Pre-Dniester Fault, RdF — Radekhiv Fault, RgF — Rogatin Fault, R-RF — Rava-Rus'ka, RT — Rheinsberg Trough, RvnF — Rivne Fault, SGF — Sfantu Gheorghe Fault, S-PF — Sushchanu-Perga Fault, SSPIF — Szczecin-Stargard Szczeciński-Pila-Inowroclaw Fault, St-BF — Stokhid-Borisov Fault, TCF — Transcarpathian Fault, TEF — Trans-European Fault, TF — Teteriv Fault, TlF — Tal'ne Fault, VFZ — Vinding Fault Zone, Zv-ZlF — Zvizdal'-Zalissia Fault.

and STZ and Thor-TS, as mentioned earlier, are accompanied by a series of Carboniferous-Permian basalt dikes [Thybo, 2000, 2001].

The transition from the three-layer Baltic crust to the two-layer Avalonian crust is accompanied by a decrease in its thickness and a significant thickening of the upper crust [Williamson et al., 2002; Pharaoh et al., 2006; etc.]. The terrain bounded by STZ and Thor-TS is transitional from the Baltic to Avalonia and is characterized by a decrease in the thickness of the crystalline crust and its layers.

The work [Janik et al., 2022] describes the triple junction of the main tectonic units of Europe.The West European Platform, Fennoscandia, and Sarmatia in the Fennoscandia-Sarmatia Suture Zone (FSS, 50°), where a change in the TTL strike is observed. Thus, in the triple junction of the main tectonic units, there is a triple junction of large lineaments separating these units: two branches of the TTL with different strike directions (NW and SE) with the FSS. The change in TTL strike may be associated with repeated rotational movements of Sarmatia relative to Fennoscandia during their Late Proterozoic accretion [Bogdanova et al., 2013]. The junction of Fennoscandia and Sarmatia represents a complex structured suture zone within these two segments of the EEC. The main elements of the FSS are the Volyn'-Orsha Basin, classified as a rift structure according to deep seismic sounding data [Chekunov, 1992], the Belarusian-Baltic granulite belt, the Central Belarusian Suture Zone, and the Osnyts'k-Mikashevytshi Igneous Belt [Janik et al., 2022]. The major faults consistent with the FSS are the Bialystok, Minsk, Stokhid, Sushchany-Perga, Teteriv, and Nemyriv Faults.

The main lineaments of the WEP — Trans-European Fault (TEF), Szczecin-Stargard Szczeciński-Pila-Inowroclaw (SSPIF), Elbe Line (EL), Odra Fault (OF) — form a single system of right-lateral faults with the NW part of the TTL of varying ages of activation. EL includes the Dol'sk (DF) and Holy Cross (HCF) Faults. In addition to the lineaments flanking the TTL from the SW, there is a series of faults consistent with the strike of the TTL both from the EEC side and within the WEP. These include the Kock Fault (KF), Kazimierz-Ursynow Fault Zone (K-UFZ), and others. The FSc traces the Caledonian collision deformation front parallel to the TTL. Major faults transverse to the TTL and consistent with the Fennoscandia-Sarmatia Suture Zone include the Grojec Fault (GF), the Hrubieszow Fault (HF) and a number of smaller faults. To the southeast of the HF and the area of the aforementioned triple junction, the style of fault tectonics changes.

Under the Carpathians, the Pre-Carpathian Fault (PrCF) is considered to be TTL in the crystalline crust [Gintov et al., 2022; Orlyuk et al., 2022]. In the SW, it is accompanied by a series of faults parallel to it: Uzhok (UzhF), Chornogolovo (ChgF) and Transcarpathian (TCF). The Krakovets' Fault (KrF) and Nesteriv Fault (NtF) can be considered as TTL 'plumage'. The large Podil's'k Fault (PdF) and Rava-Rus'ka (R-RF) Fault are parallel to this part of the TTL.

In the SE, the EEC 'corner' is formed by two dominant directions of faults in the edge parts of the craton: NW-SE (TTL fault system) and W-E (the fault system of Scytho-Turanian lineament). The transition from a diagonal to an orthogonal fault system occurs along the Ukrainian-Baltic (Uk-BZ) Zone of activation,

which includes the Radekhiv (RdF) and Rohatyn (RgF) faults. Further east, within the Ukrainian Shield, the dominant meridional strike of the main deep faults and Proterozoic structures is determined by the long-lived transregional Kherson-Smolens'k (Kh-Sm) tectonic suture — a deep magma and fluid supply channel [Pashkevich, Rusakov, 2021]. The TTL position in this region has not been confirmed by seismic data and is controversial. The region has undergone a complex history of development associated with changing geodynamic conditions. This led to repeated subduction processes: southwards in the Ordovician-Silurian and northwardsin the late Permian period [Seghedi, 2012].

The authors of the works [Starostenko et al., 2013; Amashukeli et al., 2019, etc.] conclude that the position of TESZ is uncertain. Some authors consider as TESZ the Peceneaga-Camena [Hippolyte, 2002] and Sfantu Gheorghe faults [Pharaoh et al., 2006; Narkiwicz et al., 2015][1]. None of these faults meet the main criterion of TTL — a change in the thickness and composition of the crust during the transition from the EEC to the WEP. According to the Moho discontinuity relief map [Grad et al., 2009, 2016], crust changes from thick (more than 45 km) to thin in a latitudinal direction and crosses Central and Northern Dobrogea. Most likely, this direction reflects the manifestation of the southern boundary of the EEC and has no relation to the TTL. In addition, the strike of the faults (~310° PCF) does not correspond to the strike of its SE part (330°). This strike most likely corresponds to the Capidavu-Ovidiu Fault (COF) in Northern Dobrogea.

Fig. 2 shows a diagram of the typification of the consolidated crust of the EEC and surrounding structures. The EEC is characterized by a thick three-layer consolidated crust. The WEP has by a thin two-layer crust. This transition is accompanied by the uplift of the high-velocity lower crust of the EEC, traced in the southwest to EL [Thybo et al., 2002; Pharaoh et al., 2006, etc.]. The classification of the crust of the NW part of the region was carried out in [Grad et al., 2002, Fig. 6]. Using GSZ data, the authors of this work considered the types of crust determined by the ratio of the EEC, eastern Avalonian and Variscan crusts. They distinguished between the Avalonian crust, which was not subject to Variscan deformation, and the Avalonian and Variscan crusts, which are underlain by the high-velocity lower crust of the Baltic. This diagram was supplemented by us further to the SE based on the results of seismic profiles CELO2, CELO5, POLCRUST, PANCAKE, RomUkrSeis. The Avalonian crust, underlain by the lower Baltic crust, is bounded in the SW by the EL and its SE strike, by the DF, up to the GF. The Variscan crust, underlain by the Baltic crust, is bounded in the SW by the OF. Further to the SE, the crust type with the underlying EEC lower crust is shifted to the SW, probably along GF. To the SE, this crust type is bounded by HCF. Further to the southeast, the described crust type is mapped along the Carpathian front, gradually decreasing in horizontal thickness, and completely disappearing on the PANCAKE profile.

The igneous provinces of the region are directly related to the problem of deep magnetic heterogeneities in the consolidated crust (see Fig. 2, *a*). Along the border of Sarmatia, there is the Volyn' Igneous Province (VIP) of Vendian trap basalt. The maximum thickness of the basalt traps is found in the junction zone between Sarmatia and Fennoscandia. Neoproterozoic (1.81—1.75 Ga) Trans-Scandinavian Igneous Belt (TIB1) traces along the border of Fennoscandia, and the younger (1.71—1.65 Ga) TIB2 is associated with the Sveconorwegian submeridional front [Bogdanova et al., 2016].

From SWTIB1 is limited by TTL, the thickness of VIP basalt traps decreases to the NE, and the foci of these provinces are most likely associated with the formation of TTL.

In conclusion, we will highlight the main features of the structure of the crystalline crust of the region.

– The main lineament of the TTL region consists of two branches of different strikes. The NW branch with a strike of 330° trac-

[1] Once again, we note that TESZ cannot be identified with individual faults.

es along Fennoscandia, the SE one traces along Sarmatia with an azimuth of 305°. Both branches form a triple junction with FSS. The NW branch in the Tornquist Fan region is divided into Thor-TS and STZ, limiting a peculiar transitional domain from EEC to Avalonia.

– TTL represents a complex system with 'plumage' and subparallel faults. In the NW TTL branch, these are right-lateral faults within the WEP: SSPIF, EL, DF, HCF of the NW strike and subparallel to the TTL: KFZ, K-UFZ. The SE branch of the TTL is accompanied on the eastern flank by the R-RF and I-ZF, which are parallel to the TTL. The 'plumage' system is limited here by the meridional zone of activation Uk-BZ.

– The area consists of two main types of consolidated crust: high-velocity three-layer EEC crust and low-velocity two-layer thin WEP crust. To the SW of TTL, a third 'transitional' type can be traced, represented by the WEP crust underlain by the lower EEC crust. This type of crust is recorded along the NW branch of TTL, is most developed in Eastern Avalonia, decreases to SE, and shifts to SW along the presumed continuation of the GF. Along the SE branch of the TTL, its horizontal thickness decreases until it disappears in the RomUkrSeis profile area. The overall structure of this type of crust fits into a pattern typical for right-lateral shifts, disrupted by transverse faults.

– The nature of the faults associated with the TTL and the area of development of the 'transitional' type of crust indicate different geodynamic regimes of formation of TTL's NW and SE branches.

– The igneous provinces of Sarmatia and Fennoscandia, as well as the rejuvenation of the crust in the west of the Baltic Shield (Sveconorwegian orogen of 1.1—0.95 Ga), indicate different ages of activation of the NW and SE parts of the TTL.

4.2. ***Schematic representation of upper mantle heterogeneity***. According to seismotomography data [Zhu et al., 2015; Chyba et al., 2017; Tsvetkova et al., 2021; Gintov et al., 2022], upper mantle is characterized by a sharp change in seismic V_P and V_S waves in the TTZ region from high velocities under the EEC to low velocities under its young surroundings. To depths of 200—300 km under these main structures, the mantle is characterized by weak V_P velocity differentiation. Deeper down, the differentiation increases, and at depths of 450—500 km, it ends in a velocity inversion: high velocities beneath the WEP, low velocities beneath the EEC. Such velocities at these depths correspond to the layer transitioning from the upper to the middle (lower) mantle.

The high-velocity mantle EEC extends SW of TTL at depths of up to 200 km. The position of the boundary of the high-velocity subcrustal mantle is estimated in the first approximation by the zero isoline ΔV_P of horizontal velocity sections at depths of 50 and 100 km. As noted by [Gintov et al., 2022], due to the uneven observation network in this region, the ΔV_P isolines characterize only the general directions of mantle structures. Nevertheless, some mantle features correlate with the main crustal structures. At depths of 50—100 km beneath the WEP, there is a mantle of EEC, as well as one of WEP [Tsvetkova et al., 2021]. The subcrustal mantle of EEC at these depths can be traced SW of TTL (Fig. 3).

The projections of the boundaries of the EEC mantle at depths of 50 and 100 km onto the Earth's surface indicate the overthrusting of the craton mantle onto the WEP mantle. The overthrusting is confirmed in the DEKORP section [Bayer et al., 2002, see Fig. 2 and references thereto], where northern dip reflecting horizons have been discovered. In Fig. 3, the area of the overthrust EEC mantle is shown as a transition zone. The horizontal thickness of this zone varies from 50 to 100 km, except in the NW, where it is 150 km. A sharp change in the morphology of this zone occurs during the transition from the Variscides to the Eastern Carpathians in the Brunovistulian unit area. The wedge of the overthrust mantle to the southwest is marked by a narrow 'nose', the strike of which corresponds to the strike of the FSS and the axis of the local LAB deflection (see Fig. 3, *b*). The subcrustal mantle of the EEC is fixed under the NW part of the Carpathians, while in their SEpart, the mantle corresponds to a young platform. In the

area of the L'viv Palaeozoic Depression, the transition zone has its maximum width and is bounded in the east by the submeridional RF. Further, the contact between the EEC and WEP mantles occurs along a submeridional vertical section under the Carpathians to Central Dobrogea without the overthrust of the craton mantle. Within the EEC, this contact corresponds to Uk-BZ. The transition zone and, accordingly, the thrust of the

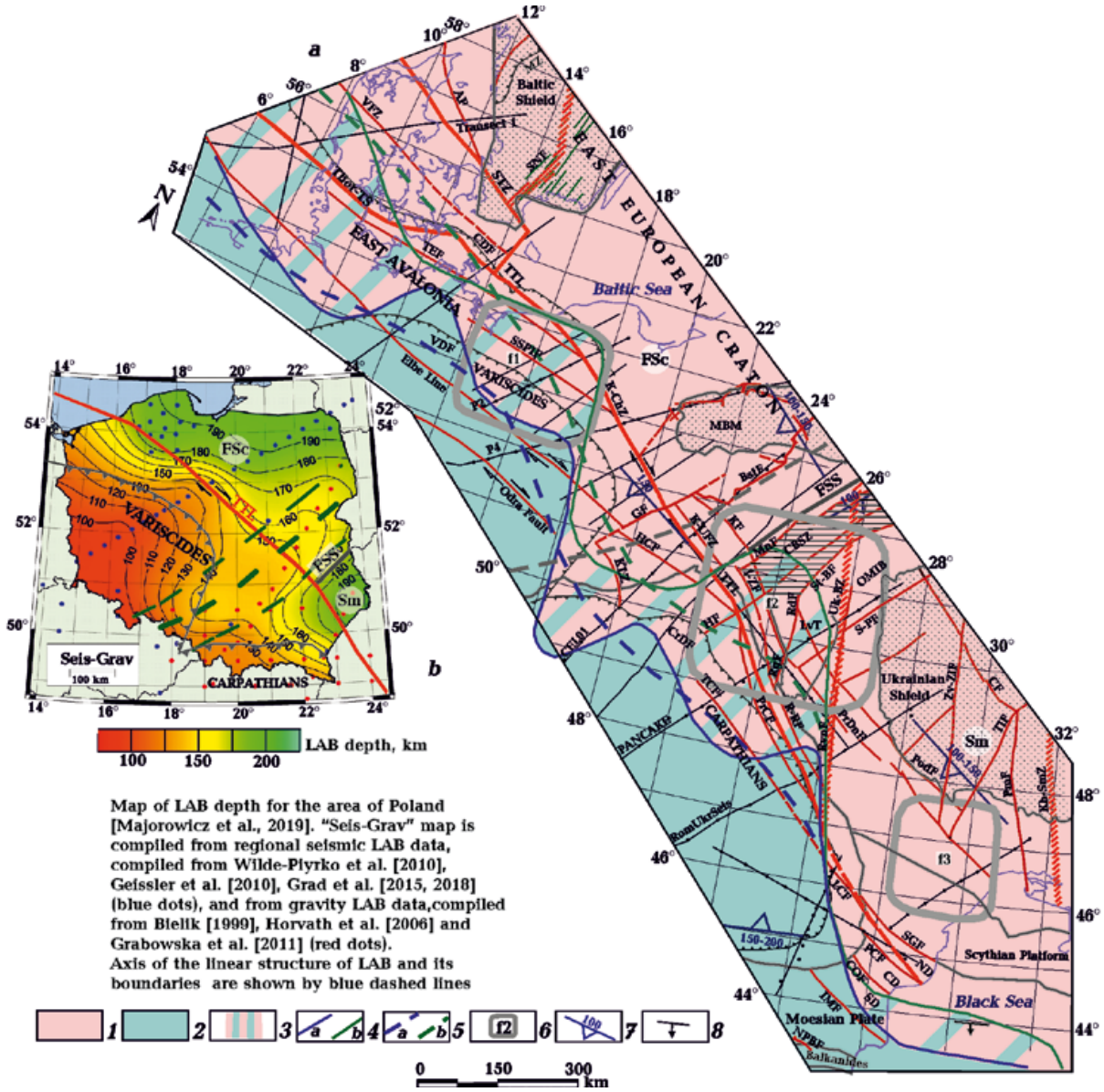

Fig. 3. Diagram of the structure of the subcrustal mantle of the EEC and its surroundings (*a*), map of the depth of the lithosphere-asthenosphere boundary (LAB) for Poland according to [Majorowicz et al., 2019] (*b*): *1* — high-velocity subcrustal mantle of the EEC; *2* — low-velocity subcrustal mantle of the WEP; *3* — zone of overthrust of the high-velocity subcrustal mantle of the EEC on the low-velocity subcrustal mantle of the WEP; *4* — projection on the Earth's surface of the boundary of the high-velocity subcrustal mantle at a depth of 50 km (*a*), the same at a depth of 100 km (*b*); *5* — 'averaged' generalized version of the projection on the Earth's surface of the boundary of the high-velocity subcrustal mantle at a depth of 50 km (*a*), the same at a depth of 100 km (*b*); *6* — projection on the Earth's surface of ultra-deep mantle fluids; *7* — projection on the Earth's surface of the upper edges of inclined lithospheric layers and the direction of their dip, the numbers (km) indicate the depth at which they are traced; *8* — dip direction of the subcrustal mantle thrust of the EEC on the subcrustal mantle of the WEP. For other symbols and abbreviations see Fig. 2.

EEC mantle onto the mantle of young structures acquires a latitudinal strike in the area of 44°N, which corresponds to the strike of the southern border of the EEC and large lineaments of the Balkanides, for example, the North Pre-Balkan Fault (NPBF).

Since, as mentioned above, the seismotopographic observation network in the study area is not sufficiently uniform, we also provide averaged projections of the upper mantle boundaries of the EEC at depths of 50 and 100 km. As can be seen, these boundaries generally reflect the strike of the TTL. In the terrain transitioning from the EEC to Avalonia, the boundary of the thrust zone is parallel to the Vinding Fault Zone (VFZ) in the centre of the terrain (see Fig. 3). In the south, the thickness of the latitudinal zone is about 50 km. However, in the V_P velocity model of the upper mantle constructed by the results of the PASSEQ experiment, no such structure was found at depths of 50—100 km. The authors [Chyba et al., 2017] believe that at depths of ~120 km, the low-velocity mantle of the WEP is thrust onto the lithosphere of the EEC.

In addition to the described features of the upper mantle, ultra-deep mantle fluids and high-velocity inclined layers have been discovered in its structure [Tsvetkova et al., 2017, 2021; Gintov et al., 2022]. The inclined layers in the work [Gintov et al., 2022, Fig. 8] are interpreted as slabs preserved since the SW subduction in the Ordovician-Silurian or Middle Ordovician. However, the identification of inclined layers along vertical velocity sections in a number of cases presents some uncertainty, associated, in particular, with the presence of ultra-deep fluids. For example, in section EW53° in [Tsvetkova et al., 2021, Fig. 3], fluid f1 is identified, but in [Gintov et al., 2022], an inclined layer is traced using a high-velocity fluid layer for the same section. The 'classical' inclined layer along the SN 27° section presented in this work can be considered quite reliable, but it was not included in the composition of the proposed slabs. Without claiming to offer a new interpretation of the seismotomography, we have attempted to identify the most reliably traceable inclined high-velocity layers. The data on the meridian seismic sections of the region were kindly provided to us by T.O. Tsvetkova with permission to use them in the study of the lithosphere. Fig. 3 shows projections onto the Earth's surface of the upper edges of only the reliably identified inclined layers, indicating the depth interval of their upper edges for each section. It turned out that the projections of the upper edges form a series of linear elements — 'traces' of the exit of inclined layers into the subcrustal mantle. Some of them are consistent with the TTL strike. The inclined layers are observed at depths ranging from 100—150 km to 300—400 km. They may represent fragments of slabs from different stages of subduction processes along the TTL, as they are recorded both to the NE and SW of the TTL and have a SW dip. In addition to the inclined layers associated with the TTL, an inclined layer with a SE dip is observed at depths of 100—250 km, the 'trail' of which is parallel to the FSS. This layer correlates with data from the EUROBRIDGE'97 seismic profile [Thybo et al., 2003] on the presence of a zone of Sarmatian thrusting onto Fennoscandia during accretion.

In the SE part of the region at 46°N (see Fig. 3), there is an outlet of the latitudinal inclined layer of northern dip into the subcrustal mantle. Most likely, the inclined layer is associated with the system of latitudinal faults of the Sarmato-Turanian Lineament and the NPBF and represents a fragment of the preserved slab. Here, in the area of 25—27.5°E and 46—47°N, there is a region of sharp dipping of the main geodynamic boundary (MGB) to a depth of more than 650 km compared to 550 km to the north. The depth interval of the main geodynamic boundary (MGB) is considered to be a sign of plate tectonic processes [Tsvetkova et al., 2019]. It is likely that the inclined layer can reflect the subduction process of the Late Permian [Seghedi, 2012].

The question of the depth of 'penetration' of the main lineaments of the region into the mantle is of fundamental importance for understanding the history of the formation of the consolidated crust. The authors [Gintov et al.,

2022] believe that the manifestation of TESZ in the mantle as a subvertical boundary of the EEC reaches a depth of 700 km. At the same time, in their opinion, its crustal structure is a trough up to 200 km wide and up to 21 km deep (on the example of the Subcarpathian Trough). Judging by the PANCAKE and RomUkrSeis seismic sections, the width of this trough under the Main Carpathian Thrust is about 40 km. It is likely that we are not talking about TESZ, but rather TTZ, and within it, about TTL as its component, limiting the consolidated crust of the EEC. TTL is clearly visible in the mantle to depths of 600-650 km as a vertical SW contact of the high-velocity mantle of the EEC with a vertical thickness of about 200 km. All troughs or depressions that are part of TESZ are located to the SW of TTL and are above the zone of the subcrustal mantle of the EEC, which is thrust onto the mantle of the WEP.

This raises the question of what causes the SW dip of the TTL in the consolidated crust with vertical mantle contact of EEC, as determined by seismic profiles (excluding P4 and P2). It is possible that the process of overthrust of the sub-crustal mantle of the EEC also involved the underthrust of the lower crust of the EEC under the crust of the WEP. This process may be associated with the stretching of the crystalline crust in the SW direction, which led to a decrease in the V_P velocity in its section, mentioned in [Gintov et al., 2022] as a general pattern.

Both NW lineaments (Thor-TS and STZ), like TTL, have a SW dip in the consolidated crust. However, the entire Thor-TS Zone is located above the zone of underthrust of the subcrustal mantle of the EEC onto the mantle of the WEP. The mantle 'trace' of its position on the surface of the crystalline crust is fixed in the form of a vertical boundary to depths of 300—600 km. STZ, like TTL, manifests itself in the mantle to a depth of 450—650 km in the form of a vertical section. The thickness of the high-velocity mantle of the EEC is 350—500 km. The vertical zone of intensively disturbed mantle beneath the TTZ branching region (12—13°E) can be traced in the middle mantle to depths of 1250—1500 km. It is quite reasonable to assume here a southern continuation of the Sveconorwegian Front, as noted in [Thybo, 2001].

An important element of the mantle structure is modern ultra-deep fluids. They represent a vertical columns of increased mantle stratification with alternating high- and low-velocity layers, identified by seismotomography in the EEC and adjacent areas [Tsvetkova et al., 2017, 2021]. These publications provide velocity characteristics of the fluids, and for the territory of our study, a connection with oil- and gas-bearing areas is established.

Three ultra-deep fluids (f1, f2, f3) were identified in the TTL region (see Fig. 3). In order to determine the relationship between magnetic heterogeneities in the consolidated crust and the structure of the lithosphere, we were interested in the tectonic position of fluids and mantle heterogeneities. As can be seen in Fig. 3, all three fluids are located into the intersections of large lineaments or close to them. From NW to SE, the positions of the fluids shift sequentially relative to the TTL: from the SW border of the TTL (f1) to the L'viv Paleozoic Trough (f2) and within the limits of the EEC (f3). At the same time, all three fluids are located in close proximity to large meridional structures of activation of the Earth's crust (SNF, Uk-BZ) and to meridional zones of displacement of the subcrustal mantle of the EEC, which is superimposed on the mantle of the WEP.

Fluid f1 is located between SSPIF and EL, bounded on the west by the supposed meridional strike of SNF, which corresponds to the TTL branching into Thor-TS and STZ. From the east of f1, there is also a meridional southward shift of the zone where the WEP mantle overlaps the EEC mantle.

Fluid f2, the largest of the fluids, is located at the triple junction of the TTL branches with the FSS (Central Belarusian Suture Zone, Osnyts'k-Mikashevichy Igneous Belt and associated faults). Within its boundaries, large faults of the TTL system (HF, I-ZF) intersect. Most of the Vendian Volyn' Igneous Province also belongs to this fluid (see Fig. 2, 3). It also corresponds to the L'viv Palaeozoic Trough,

and a deep Uk-BZ of activation related to the trans-lithosphere structures of the upper mantle has been established on the Pre-Cambrian basement.

Fluid f3 is located within the southern slope of the Ukrainian Shield. The centre of the fluid is associated with the intersection of the Podillia zone of faults, parallel to TTL, and a series of submeridional faults of the Golovanivs'k Suture Zone.

It fixes the SE angle of the EEC, formed by the junction of two main lineament systems — diagonal and orthogonal, that define the boundaries of the craton.

In conclusion, we note the main features of the upper mantle structure of the region.

– The high-velocity mantle of the EEC is in contact with the low-velocity mantle of the WEP through the transition zone of the subcrustal mantle. At depths of 50 and 100 km, the behaviour of this contact indicates that the EEC mantle is overthrusting the WEP mantle.

– The horizontal thickness of this zone varies from 150 km in the NW to 0 in the Uk-BZ activation.

– The general strike of the thrust zone corresponds to the strike of the TTL.

– East of Uk-BZ, the overthrust zone shifts southwards, acquires a latitudinal strike, and corresponds to the transition to the southern border of the EEC and the northern subduction zone along it.

– Ultra-deep fluids reveal a connection with the intersection junctions of large lineaments and the zone of triple junction of the NW branche and SE one of the TTL with the FSS.

– High-speed inclined layers, identified with slabs, are reliably traced in five cases: SW of the TTL, NE of it within the FSc, and SW of the Sm (all three with a SW dip); as well as a layer consistent with the FSS strike (SE dip) and a layer with a latitudinal strike parallel to the border of the Moesian Plate (northern dip). They can only testify to fragments of subduction slabs from different stages of tectonic processes in the region.

4.3. ***Types of transition layer from the upper to the middle mantle.*** The upper mantle of the EEC, as noted above, is characterized by increased seismic V_P velocities. The transition to the middle mantle occurs along a zone of reduced velocities, which has variable thickness. The lower boundary of the zone lies at a depth of 475—700 km and is interpreted as the main geodynamic boundary [Tsvetkova et al., 2019]. Along the TTL, this boundary dips from NW to SE from 525 to 625 km. The depth to it along the southern border of the EEC reaches 650—700 km.

The low-velocity upper mantle of the WEP is underlain by a high-velocity transition layer. As a rule, it has a complex junction zone with the low-velocity transition layer of the EEC. Sometimes this zone is overthrust-underthrust in nature and rarely has a sharp contact.

Fig. 4 shows a diagram of transition layer types. The diagram was constructed as a result of analyzing vertical meridional velocity sections, which, as already mentioned, were provided to us by T.O. Tsvetkova. The main types of transition layer are low-velocity EEC and high-velocity WEP. The boundary between these types has no direct connection with TTL. Only in the STZ region the boundary between the EEC and WEP transition layers is subparallel to this zone. In contrast to the behaviour of the subcrustal mantle at depths of 50—100 km, which is thrust onto the upper mantle of the WEP to the SW of the TTL, the WEP transition layer covers a significant area north of the TTL. It has meridional boundaries with the EEC transition layer corresponding to the SNF and Zvizdal'-Zalissia Fault.

In the transition layers of the EEC and WEP, subtypes are distinguished: a 'weakened' EEC (reduced thickness and speed) and a subtype with a 'duplicate layer' WEP. The 'weakened' transition layer shows no direct connection with TTL. It is fixed east of the 29°E meridian. A small development area of this subtype of the EEC transition layer is noted east of SNF.

The subtype of the WEP transition layer with a 'duplicate layer' is widespread to the SW of the TTL within most of the Variscan, Carpathian and Dobrogea regions. In the NW part of the region, its boundary is close to the EL. At the transition to the lithosphere of the

Western Black Sea Basin, the WEP transition layer is replaced by an area of complex junction with the EEC transition layer. The high-velocity WEP layer is thrust northward onto the low-velocity EEC layer.

From the north and south, this area is bounded by the latitudinal structures of the Scythian-Turanian Lineament and the North Pre-Balkan Fault. In the structure of the subcrustal mantle at depths of up to 100 km (see Fig. 3), the opposite picture is observed: the high-velocity mantle of the EEC is thrust southward onto the low-velocity WEP. This thrust, as noted above, accompanies the TTL to the SW and is absent under the Carpathians.

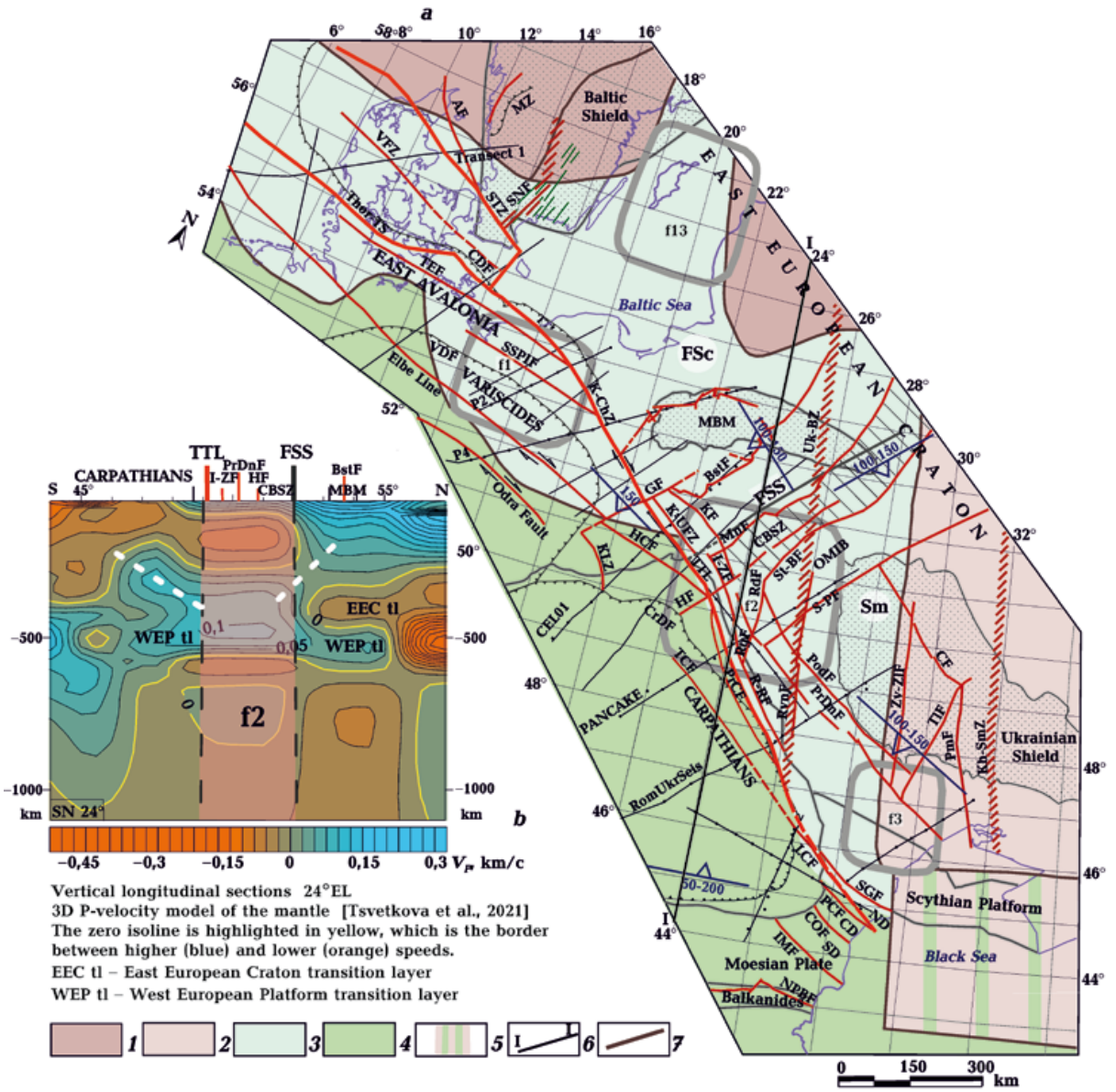

Fig. 4. Diagram of transition layer types from the upper to the middle/lower mantle (*a*), meridional velocity section at 24° E based on a 3D *P*-velocity model of the mantle [Tsvetkova et al., 2021] (*b*): *1* — low-velocity transition layer of the EEC; *2* — 'weakened' transition layer of the EEC with lower velocity and thickness; *3* — high-velocity transition layer of the WEP; *4* — area of propagation of 'duplicate layers' of the transition layer of the WEP; *5* — area of development of the WEP transition layer thrust on the EEC transition layer; *6* — position of the seismotomographic profile (ΔV_P anomalies); *7* — boundary between transition layer types. For other symbols and abbreviations see Figs. 2 and 3, *a*. The zero isoline is highlighted in yellow, which is the border between higher (blue) and lower (orange) speeds. EEC tl — EEC transition layer, WEP tl — WEP transition layer.

The development of the transitional layer subtype of the WEP with 'duplicate layers' in it deserves attention. As shown in [Pashkevich et al., 2020], 'duplicate layers' in the transition layer can be interpreted as relics of slabs that 'sank' into the transition layer in a subduction setting. In our case, this situation may be associated with subduction processes in the SW direction, assumed in the Ordovician-Silurian [Gintov et al., 2022]. It is difficult to establish the resulting picture of subduction along the entire TTL, as done in the cited work, based solely on the presence of inclined high-speed layers. Such layers can be traced most reliably (see Fig. 4) only fragmentarily. Their immersion into the transition layer is most pronounced within the fluids (see Fig. 4, *b*).

The behaviour and types of the transition layer from the upper to the middle mantle allows us to draw some conclusions:

– structural heterogeneities in the upper mantle indicate its stratification and inconsistent horizontal movement of the subcrustal mantle and lower lithosphere: thrusting of the subcrustal mantle of the EEC onto the mantle of the WEP and thrusting of the transition layer of the EEC beneath the WEP;

– subduction processes in the TTL area are evidenced by widely developed 'duplicate layers' in the transitional layer of the WEP along the entire TTL to the SW of it;

– inclined high-speed lithospheric layers are not recorded everywhere, which may be due to the ancient age of subduction;

– the above-mentioned change in the diagonal structural plan of the EEC to an orthogonal one along the Uk-BZ meridian zone is confirmed by the presence of the meridian boundary of the EEC and WEP transition layer in the zone between Uk-BZ and the transregional tectonic suture Kh-Sm.

4.4. ***Magnetic model of the Earth's crust and structure of the lithosphere.*** Before discussing the results of magnetic modelling of the region, let us consider the main features of the anomalous magnetic field caused by various deep heterogeneities of the lithosphere.

The anomalous magnetic field at ground level, as established by research within the EEC, is considered to be the combined effect of upper crustal and deep (middle-lower crustal) sources (see section 1). The differentiation of the field and the intensity of the anomalies characterize the saturation of the lithosphere with magnetic formations. The main types of magnetic sources are magmatic rocks of basic and ultrabasic composition, as well as metamorphic formations of primarily magmatic origin [Krutikhovskaya et al., 1982; Pashkevich et al., 1990 and references to it, etc.]. Therefore the field carries information about areas of different ages magmatic processing of the lithosphere. Sources associated with iron ore complexes and areas of secondary magnetic mineral development are considered exotic within the EEC. The latter are caused by metasomatic and hydrothermal processes and the influx of ultra-deep fluids.

Fig. 5 shows the near-surface anomalous magnetic field and the main tectonic elements of the region where the EEC and WEP meet. The main feature of the magnetic field is a zone of high gradient extending NW, closely correlated with the TTL and described repeatedly earlier (see, for example, [Pashkevich, 1989; Pashkevich et al., 1990 and references to it; Królikowski, 2006 and references therein]. It is caused by a sharp difference in the average magnetization of the crust of the EEC and WEP. The zone is traced from the Pomeranian Massif and the presumed southern continuation of the SNF to the junction of the TTL. Further to the SE, with a shift along the HF to the SW under the outer Carpathians, it can be traced to Uk-BZ. This zone separates the highly differentiated EEC field and the negative, weakly differentiated WEP field. The exception is Eastern Avalonia south of Thor-TS, where a positive regional field is observed with relatively low-intensity elongated positive anomalies of NNE and NW strikes.

This region belongs to the North German Basin (NGB) of the Central European Basin System. The initial rifting of the NGB in the late Carboniferous – early Permian period was accompanied by widespread volcanic activity. The newly formed meridionally trending grabens (Central, Horn and Glückstadt) are associated with the E-W strike stage. The intensity of volcanism decreases towards the SW and

disappears in the Małopolska Trough (MP) [Mazur et al., 2021].

Summarizing the history of the discovery of the TTZ, M. Grad [Grad, 2019] noted that the difference in the magnetic field between the EEC and the WEP was first discovered in publications by A. Schuk in 1899 and 1902. These publications contained maps of magnetic field's elements (declination, inclination, and horizontal component) for the pe-

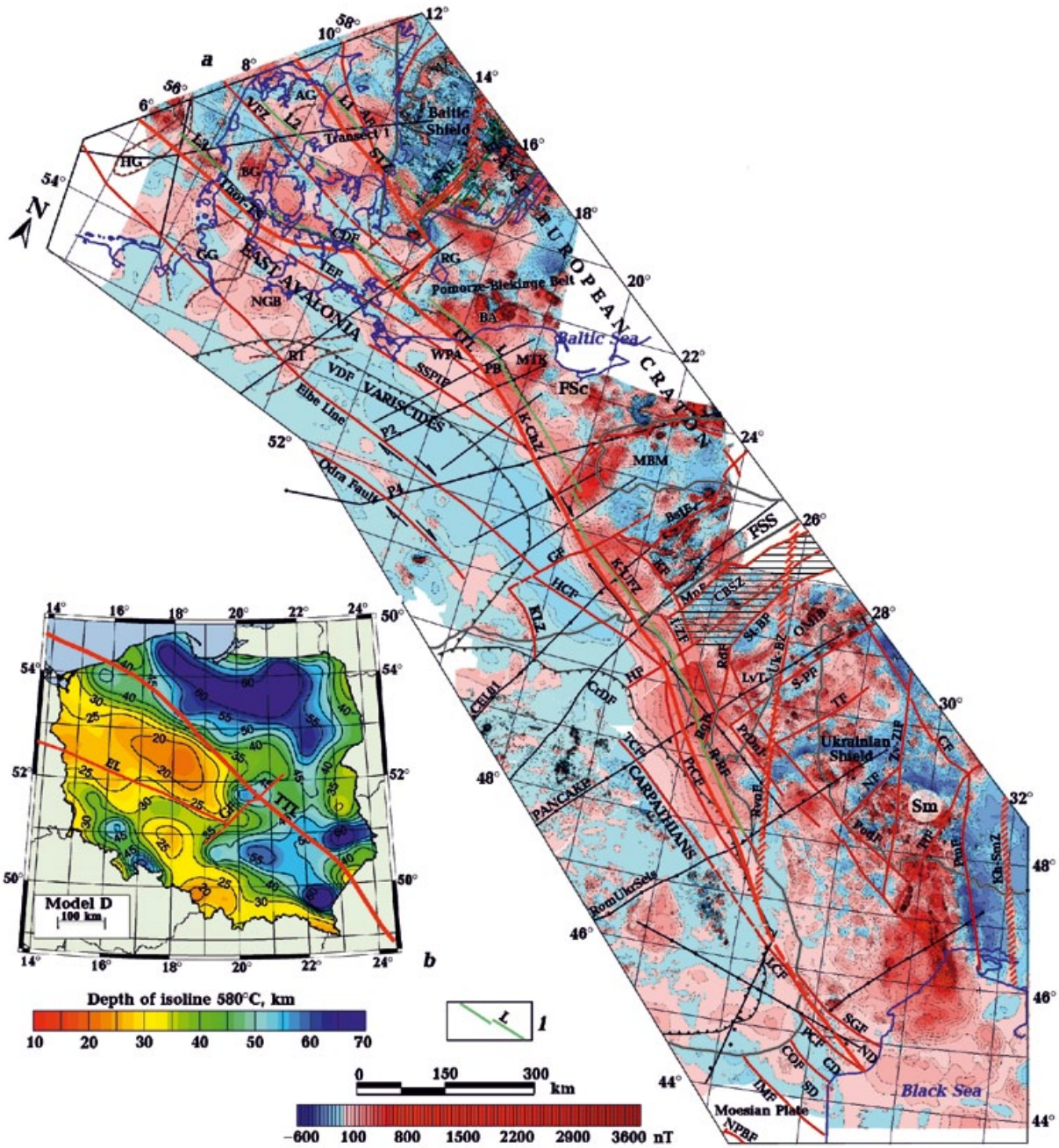

Fig. 5. Anomalous magnetic field on a scale of 1:500,000 and 1:1,000,000 compiled from data for the following countries: Ukraine [Nechaeva et al., 2002; Orlyuk et al., 2024a], Poland [Petecki et al., 2003], Germany [Gabriel et al., 2011], Denmark [Lyngsie, Thybo, 2007], Sweden [Stephens, 2020], Slovakia [Kubeš et al., 2010], Romania [Airinei et al., 1983], and Hungary [Kiss, Gulyás, 2006]. Abbreviations: BA — Baltic Anomaly, WPA — Western Pomerania Anomaly, MTK — Miastko-Tuchola-Koscierzyna Anomaly, NGB — North German Basin, PB — Polish Basin. *1* — lineament L. For other symbols and abbreviations see Fig. 2.

riod 1895.5 based on observations along the Baltic Sea coast. The first tectonic interpretation of these maps was undertaken in 1906 by W. Deecke. It is noted that the change from a calm magnetic field to a sharply differentiated one occurs along the Vistula River. A. Tornquist considered this boundary to be tectonic in 1910 and traced it to Galatz [Grad, 2019 and references thereto].

In the NW, there is no trace of a zone of continuous increased field gradient associated with TTL. The strike of individual anomalies in the region between STZ and Thor-TS corresponds to the strike of these two lineaments.

In the SE of the TTL, the zone of increased field gradient is not traced, and local magnetic anomalies, presumably associated with TTL, are noted only in Northern Dobrogea.

To the NE of the zone of increased field gradient corresponding to TTL, there are two characteristic strikes of positive anomalies: NW, consistent with TTL, and NE, consistent with FSS and the accompanying large faults (Nemyriv, Teteriv, Luts'k, Sushchany-Perga, Minsk, Bialystock, Stokhid ones). South of this series of faults and east of the meridional Uk-BZ, the structural plan of the magnetic field within Ukrainian Shield and its slope becomes meridional. It dominates on large tectonic disturbances (Pervomais'k, Tal'ne, Kryvyi Rih–Kremenchuk deep fault zones), including the transregional tectonic suture Kherson-Smolens'k.

Following changes in morphology and the strike of anomalies in the near-surface field, a lineament parallel to the TTL can be traced almost continuously, we have named it lineament L (see Fig. 5). Based on the classic signs of faults in the magnetic field, the lineament is recorded from the Pomorze-Blekinge Belt to the junction zone of Fennoscandia and Sarmatia. Along the border of the latter, it coincides with K-UFZ and R-RF. The main feature of its tracing is the change in the strikes of magnetic anomalies noted above. The lineament is most clearly expressed in the NW of the Miatko-Tuchola-Koscierzyna (MTK) anomaly within the Dobrzyn Domain, where K-ChZ is established along the described lineament. It is bounded to the NE by CDF and K-UFZ. A narrow strip of the EEC is overridden here by a deformed Early Palaeozoic fold-and-thrust sequence [Narkiewicz, Petecki, 2024 and references therein].

The TTL and lineament parallel to it limit a series of magnetic anomalies of varying intensity (from 50 to 540 nT). The band of these anomalies is complicated by disturbances of a NE strike, and south of Warsaw — by a latitudinal zone of faults in the GF area. Lineaments L1 and L2, L3 along STZ, VFZ and Thor-TS, respectively, can be distinguished as analogous to the described lineament.

In 3D modelling, the structure of the described zone of magnetic anomalies determined the geometry of deep sources. This zone can be considered as a component of 'the boundaries of the range of higher magnetic parameters of the crystalline crust' in the SE part of Poland [Grabowska et al., 2017, Fig. 14 or p. 37], detailing the 3D model of these authors. When comparing Fig. 5 of this work with Fig. 14 from the cited one, a strict parallelism of the L and TTZ lineaments according to [Narkiewicz et al., 2011] is revealed. 3D modelling of deep sources without taking into account the block structure of the crystalline basement can lead to the loss of regional features of the crystalline crust structure. In particular, a structure such as lineament L cannot be traced in the anomalous regional magnetic field obtained by various methods. For example, L cannot be traced neither in the regional field of SE Poland [Grabowska et al., 2017], obtained by low-frequency filtering with a cut-off wave number k_0=0.15 rad/km, nor in the anomalous magnetic field, recalculated to an altitude of 5 km above sea level and considered as regional. Thus, the zone of magnetic anomalies accompanying the TTL, as well as the NE-trending faults, are not taken into account in the 3D model of these authors.

As is well known, large regional features of the anomalous magnetic field are reflected in both the near-surface field and the field at high altitudes, including satellite ones. The degree of attenuation of anomalies with altitude depends on the wavelength of the

anomaly and the depth to the lower margin of the source and can be an indicator of its depth, including mantle one. The possibility of the existence of mantle magnetic sources was discussed above.

Analysis of a set of multi-scale maps of anomalous magnetic field from near-surface and satellite (Magsat, CHAMP, Swarm-A, etc.) measurements data [Langel et al., 1980, 1982; Mayhew et al., 1985; Haines, 1985; Ravat et al., 1993; Langel, Hinze, 1998; Atanasiu et al., 2005; Meyer et al., 2017; Milano et al., 2019; Liu et al., 2023; Kis et al., 2024, etc.] indicate that the TTL boundary is accompanied by an intense geomagnetic field gradient and the presence of positive anomalies in the edge part of the craton. As evidence, Fig. 6 shows the anomalous magnetic field $(\Delta T)_a$ of the EMAG model, recalculated to an altitude of 100 km, the field of the total gradient intensity of the anomalous magnetic field [Milano et al., 2019], and the Magsat field at an altitude of 400 km [Coles et al., 1982].

The main feature of the near-surface field is a zone of high field gradient associated with the TTL, traceable in the anomalous magnetic field at an altitude of 100 km within the same limits as in the near-surface field (see Figs. 5 and 6). Along the TTL at this altitude within Fennoscandia east of SNF, anomalies with an intensity of more than 60 nT are recorded. Further to the SE, the total magnetic effect of anomalies along the TTL and above the L'viv Trough persists.

The anomalous magnetic field of Magsat NE of TTL is represented by a maximum covering Fennoscandia and by a minimum over WEP. The zone of maximum gradient over TTL can be traced from SNF longitude to the FSS. To the SE, the gradient zone is 'blurred'. The maximum above the L'viv Trough is weakly manifested at satellite altitude, although according to other surveys [Atanasiu et al., 2005] and the Z-Magsat component [Langel, Hinze, 1998], it can be traced with a slight overlap throughout the entire TTL. The nature of the minimum has been debated in recent decades. However, the work [Milano et al., 2019] shows that the magnetic minimum above the WEP (Central European Minimum) is not associated with the reverse magnetization of the crystalline crust and is conjugate with the maximum above the EEC.

The most intense part of the positive satellite anomaly (>6 nT) corresponds to an area with a high-density sources of near-surface anomaly and, accordingly, to a series of field maxima at an altitude of 100 km. And the maximum satellite anomaly corresponds to the central part of the TIB1 development area (see Fig. 2).

A positive regional anomaly over Eastern Avalonia and the domain between Thor-TS and STZ is observed in the field at an altitude of 100 km, but is absent in the Magsat field.

The SE strike of the TTL zone in the form of a high-gradient zone is not traced in the magnetic field at high altitudes. The transition from the SW to the southern border of the craton is reflected in the fields at high altitudes as a latitudinal regional minimum along the southern border.

Fig. 6 also shows the intensity field of the total gradient of the anomalous magnetic field according to [Milano et al., 2019, Fig. 8, *b*].

«The total gradient modulus of the magnetic field T ($|\nabla T|$) is defined as

$$|\nabla T| = \sqrt{\left(\frac{dT}{dx}\right)^2 + \left(\frac{dT}{dy}\right)^2 + \left(\frac{dT}{dz}\right)^2}$$

where dT/dx, dT/dy and dT/dz are the partial derivatives of the total magnetic field (T) with respect to the directions x, y and z».

As noted by the authors of this work, the total gradient field anomalies are located directly above the sources and are positive regardless of whether the source is directly or inversely magnetized. The absence of a total gradient anomaly within the WEP once again indicates the weak magnetization of its lithosphere. At the same time, the authors [Milano et al., 2019] show that the WEP (Central European Minimum) magnetic minimum is not associated with the reverse magnetization of the crystalline crust. Thus, it is associated with the maximum of the EEC satellite field.

In the field of the full gradient within the EEC, large tectonic zones are clearly mapped:

the Sveconorwegian Front (SNF) and the Ukrainian-Baltic Zone of activation as a relative minimum; the FSc and Sm suture as a relative minimum consistent with the FSS strike in all fields shown in Fig. 6.

As can be seen from Figs. 2—4, the listed zones are reflected in the structure of the consolidated crust and the heterogeneity of the mantle up to the layer transitioning to the middle mantle. SNF is accompanied by TIB2, controlling the TTL separating area on Thor-TS and STZ. The zone is located above the contact between the transition layer EEC and WEP. FSS is located in the area of the triple junction of the main lineaments and is one of its components. The triple junction area is located within the ultra-deep fluid f2. FSS is associated with local LAB uplift and with changes in the lithosphere temperature regime, judging by the depths to the magnetite Curie isotherm given in [Majorowich et al., 2019]. The FSS in [Bogdanova et al., 2015, Fig. 2, *b*] corresponds to the Minsk Fault and is accompanied by a high-density lens in the lower crust, indicating palaeo- and post-collisional magmatism. The FSS is the central structure of the FSS zone, bounded to the NW by the Bialystok Fault. The FSS includes a series of deep faults and a high-velocity inclined layer of SE dip consistent with their

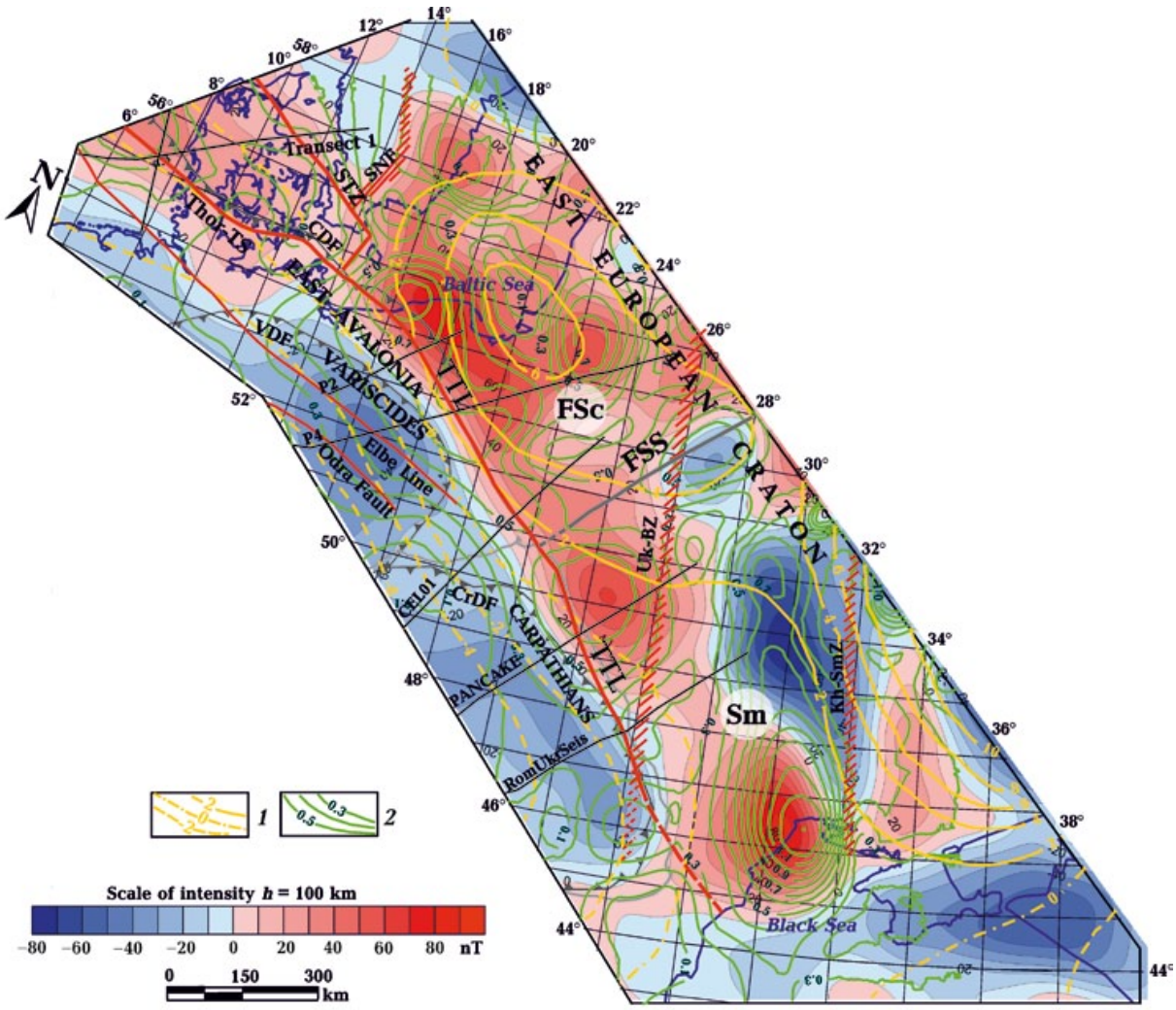

Fig. 6. Anomalous magnetic field at an altitude of 100 km [Orlyuk et al., 2025], diagram of the intensity of the total gradient of the anomalous magnetic field according to data of [Milano et al., 2019], $(\Delta T)_a$ Magsat field [Coles et al., 1982]: *1* — isodynams T of the Magsat anomalous magnetic field, nT; *2* — isolines of the intensity of the total gradient of the anomalous magnetic field, nT/km. For other symbols and abbreviations see Fig. 2.

strike (see Fig. 3). The Uk-BZ is mapped in the crystalline crust by a series of deep faults (the Rivne Fault, for example) and volcanic bodies. In the upper mantle, it corresponds to the meridional zone of displacement of the sub-crustal mantle of the EEC over the mantle of the WEP. It also forms the boundary between the low-velocity transition layer of the EEC and the high-velocity layer of the WEP. These characteristics of the zones listed serve as evidence of their mantle origin.

The analyzed fields allow the following conclusions to be drawn:

– TTL in the central part of the EEC and WEP contact in the near-surface field at an altitude of 100 km is reflected in the form of a zone of uninterrupted linear high gradient and accompanying linear anomalies from SNF in the NW to U-BZ activation in the SE;

– the Thor-TS and STZ zones, as well as the deep VFZ, are recorded in the near-surface field by intermittent linear anomalies;

– the correlation of magnetic anomalies at all altitudes, including satellite one, within the SW edge of Fennoscandia with the manifestation of TIB1 here may indicate the presence of a mantle magnetic source associated with deep magmatic foci, as well as with crustal sources;

– the attenuation of anomalies at satellite survey altitude in the area where Eastern Avalonia meets the EEC and within the L'viv Trough is evidence of the crustal origin of their sources;

– L, parallel to TTL and highlighted by the near-surface anomalous field, limits a series of magnetic anomalies along it. It can probably be considered as an element of the TTZ in the Precambrian basement. L allows the morphology of magnetic sources to be determined in 3D modelling, taking into account the structural features of the crystalline basement reflected in the magnetic field.

4.5. ***3D magnetic model.*** The object of 3D magnetic modelling was the area immediately adjacent to the TTL on the EEC side. Therefore, we will briefly discuss the nature of the anomalous magnetic field SW of the TTL, based on published data. The nature of the regional magnetic minimum and the positive West Pomeranian (WPA) regional anomaly (see Fig. 5) was discussed in [Petecki, 2001; Królikowski, 2006]. The depth to the upper edge of the WPA magnetic source was estimated using spectral analysis as 18.5 km, which corresponds to the roof of the middle crust. Thus, the source can be attributed to the middle and possibly lower crust. Further to the NW of WPA and south of Thor-TS, within the Permian-Mesozoic System of Central European Basin (CEBS), consisting of three sub-basins: Norwegian-Danish (outside our region), North German (NGB) and Polish (PB), a regional maximum of the anomalous magnetic field is recorded. The main volcanic centre of this system is located NE of NGB, where the thickness of volcanites reaches 2,300 m. To the east, the thickness of the volcanic horizon gradually decreases and blows out in the Mid-Polish Trough [Mazur et al., 2021]. In the same direction, there is a change in the intensity and sign of the anomalous magnetic field from positive regional in the NGB area to negative, weakly disturbed to the SW. Furthermore, the Carboniferous-early Permian rifting that preceded the formation of the Permian Basin was accompanied by intense volcanic activity. The nature of the positive regional anomaly may be related to a deep magma centre.

The nature of the magnetic minimum SW of the TTL remains controversial. In some cases, it is considered to be associated with a positive anomaly above the EEC, recorded by satellites [Coles et al., 1982; Heines, 1985; Taylor, Ravat, 1995; Atanasiu et al., 2005; Vervelidou, Thébault, 2015; Milano et al., 2019; etc.], or as a marginal effect of plates with different magnetizations (the EEC and the WEP) [Wonik et al., 2001, etc.]. In other cases, it is explained by the reverse magnetization of the part of the WEP crust lying above the Curie isotherm of magnetite [Królikowski, 2006 and references therein], acquired during the Illawarra magnetic inversion. Here, an interesting correlation between the magnetic minimum and the depth up to the Curie isotherm of magnetite (less than 30 km) can be noted [Majorowicz et al., 2019] (see Fig. 5). This correlation is

consistent with the findings of [Królikowski, 2006, Fig. 6] regarding the reverse magnetization of part of the WEP crust.

The results of 3D magnetic modeling of the edge part of the EEC, directly adjacent to the TTL, are presented in Fig. 7.

The diagram showing the projections of the upper edges of deep magnetic sources onto the Earth's surface contains elements of crustal tectonics (see Fig. 2). The diagram is accompanied by magnetic models based on deep seismic profiles (Figs. 8—13) showing the distribution of sources throughout the entire crystalline crust. Upper crustal sources were obtained by 2.5D modeling using GSS Potent software (https://www.geoss.com.au/index.html) under the assumption that they extend throughout the entire upper crust. Although this limitation is conditional, it does not exclude other equivalent sources. The reduced anomalous magnetic field obtained by excluding their combined effect is considered as a regional component associated with the middle and lower crust. This informal approach to assessing the combined effect of the middle and lower crystalline crust is justified in conditions of a highly differentiated basement relief. As noted earlier, under such conditions, obtaining a regional component through any transformations of a field with constant parameters is unacceptable due to the impossibility of quantitatively assessing the reliability of the result obtained. Therefore, the modeling result is only one possible scenario for the distribution of sources within the crustal section and, consequently, their magnetization values. The 3D model we present is no exception.

Let us focus on the regional patterns of the 3D magnetic model along the TTL (see Fig. 7). The main role in the zoning of magnetic heterogeneities is played by the suprastructural trans-lithospheric meridional lineaments, SNF and Uk-BZ. They delimit the region most saturated with deep magnetic sources in the junction area of Fennoscandia and Sarmatia with the WEP.

Previous studies have shown that the distribution of deep magnetic sources in the crystalline crust accompanying TTL on the side of the EEC is related to the structure and development of the NW and SE branches of the TTL (see Fig. 2, *b*, 7). The Fennoscandian and Sarmatian segments of the EEC, bounded by these branches in the SW, have different types of magnetic sources and different intensities of magnetization. Since magnetic anomalies are caused by basic and ultrabasic magmatic rocks or zones enriched with magnetic minerals, the nature of their sources in both cases is associated with deep processes and lithospheric heterogeneities.

The subduction process, which has been debated for this region for several decades, plays a special role in this regard.

The aim of our study is to establish the connection between crustal and mantle structures in terms of their contribution to the magnetic heterogeneity of the lithosphere.

The above segmentation of the TTL corresponds to the distribution pecularities of magnetic sources along it. NW of SNF, in the domain bounded by Thor-TS and STZ, deep magnetic sources are traced intermittently along both of these zones and the VFZ and correspond to their repeated activation, as does the entire domain bounded by these zones. Lineaments L1, L2, and L3 are mapped here fragmentarily, but perform the same role as L. The NW branch of the TTL is almost continuously accompanied by a strip of deep magnetic sources at the border with the FSc. From the NE, they are bounded by the L lineament. At the butt joints with them, there are heterogeneities of the Precambrian basement of the northeast-trending craton, which indicates their different ages.

In the SE branch of the TTL, SE of the HF, the distribution of deep magnetic heterogeneities takes on a different character. L can be traced here along R-RF, limiting the source associated with the TTL. The deep source of NW spreading is articulated with the source directly under the L'viv Trough and borders the meridional magnetic source west of Uk-BZ. SW of the TTL, the sources are associated with the Subcarpathian Trough and belong to the upper and middle crust.

The magnetization of deep sources, estimated through 3D modeling, ranges from 0.3

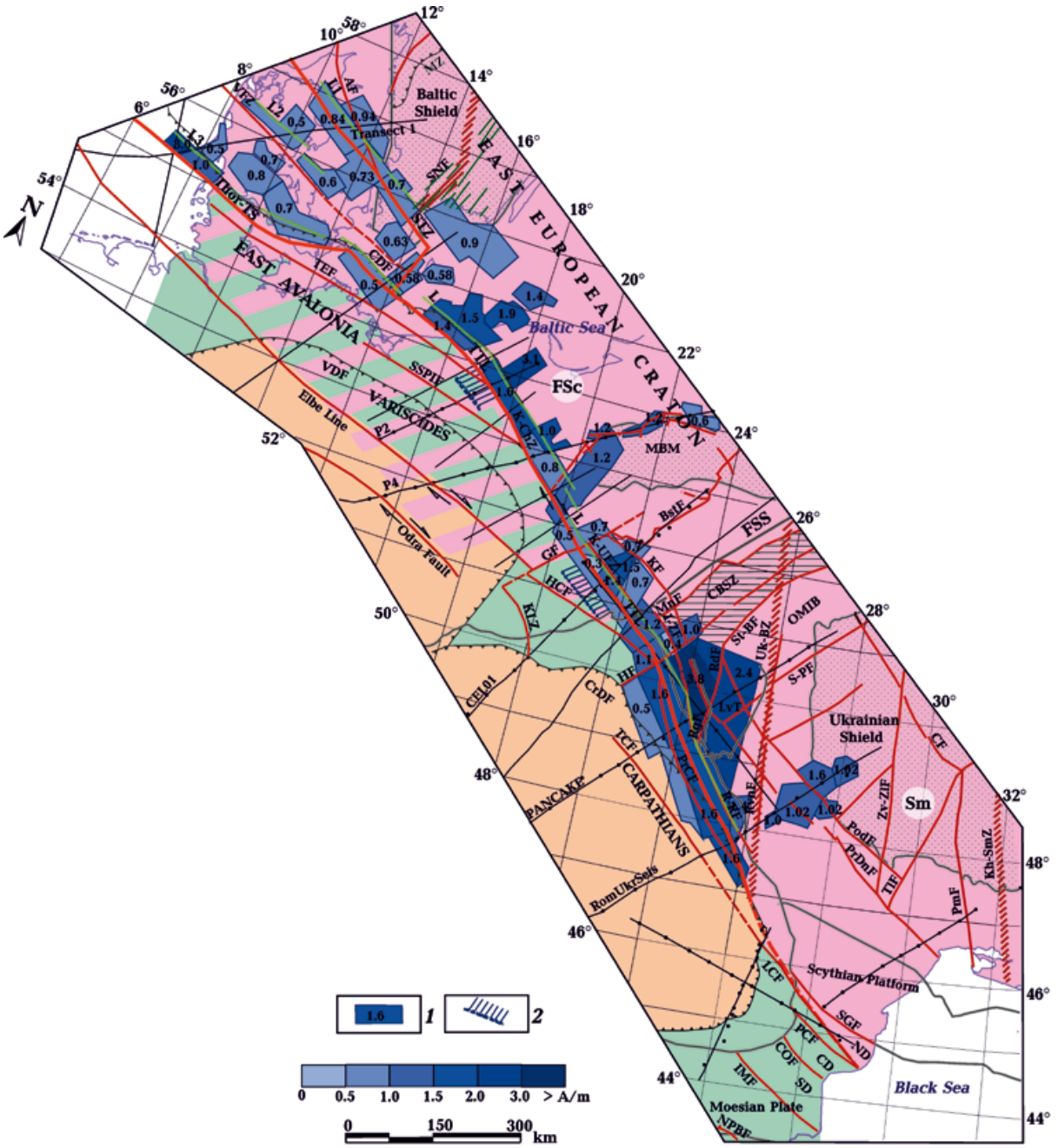

Fig. 7. 3D magnetic model of the crystalline crust: *1* — projection on the Earth's surface of the upper edge of magnetic sources; magnetization values in A/m; *2* — projections on the Earth's surface of the lower edges of magnetic sources. For other symbols see Figs. 2, 5 and for other abbreviations — Fig. 2.

to 3.8 A/m. At the same time, sources limited by TTL and L have a differentiated magnetization of 0.3 to 1.6 A/m.

The relationship between crustal and mantle structures is demonstrated by magnetic models and the lithospheric cross-section along seismic profiles Transect 1, P2, P4, Cel 01, PANCAKE, and RomUkrSeis.

Transect 1, in the extreme NW of the EEC SW, intersects the Baltica-Avalonia junction, bounded by the Thor-Tornquist Suture (Thor-TS) and the Sorgenfrei-Tornquist Zone (STZ) (Fig. 8). Profiles P2, P4, and Cel 01, shown in Figs. 9—11, characterize the magnetic heterogeneities accompanying the TTL along the Fennoscandia-WEP contact. Profiles PAN-

CAKE and RomUkrSeis (Figs. 12, 13) belong to the junction zone of Sarmatia with the Carpathian region. The Thor-TS and STZ zones were established and studied on the base of seismic data [MONA Lisa Working group, 1997a, b; Van Hoorn, 1987] and magnetic and gravity modeling [Thybo, 2001; Williamson et al., 2002; Lingsly, Thybo, 2007, etc]. Along

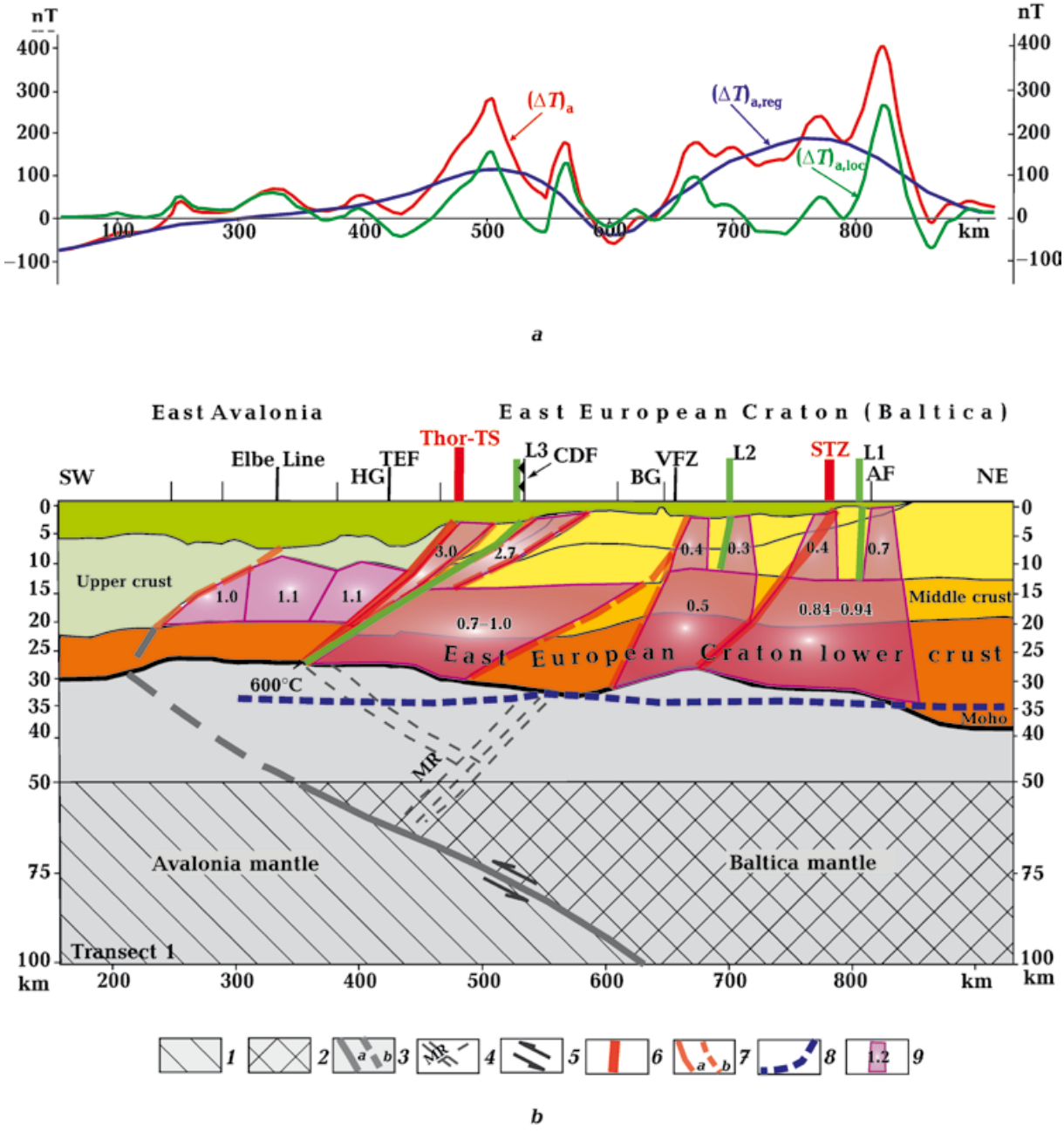

Fig. 8. Magnetic model of the crystalline crust according to Transect 1. Graphs of the anomalous magnetic field (*a*), cross-section of the crystalline crust according to [Williamson et al., 2002] and subcrustal mantle (*b*): *1* — low-velocity subcrustal mantle of the WEP; *2* — high-velocity subcrustal mantle of the EEC; *3* — boundary of high-velocity and low-velocity subcrustal mantles at depths from 50 to 100 km (*a*), its eventual continuation (*b*); *4* — mantle reflectors (MR); *5* — displacement direction along the mantle boundary of EEC and WEP; *6* — Thor-Tornquist Suture as EEC boundary; *7* — main faults (*a*) and their eventual continuations (*b*); *8* — Curie isotherm of magnetite; *9* — magnetic sources; magnetization values in A/m. For other abbreviations see Fig. 2. Seismic model according to [Van Hoorn, 1987; EUGENO-S Working Group, 1988; Thybo, Schönharting, 1991]. The section of crystalline crust is completed by us.

Thor-TS, there is a transition from the three-layer crust of Baltica to the two-layer crust of Avalonia with a decrease in crustal thickness and a significant thickening of its upper part between STZ and Thor-TS.

As noted above, a number of studies have established a sharp decrease in crustal magnetization during the transition from the EEC to the Paleozoic crust. This feature is essential in substantiating the Thor-TS as the boundary of the EEC's SW margin. The zone has a gently sloping southwest ward cross-crustal dip (Fig. 8). The authors [Williamson et al., 2002] propose a layered 2.5D magnetic model of the crystalline crust, constructed using interactive modeling software (GRAVMAG). In the three-layer model, all three layers are considered magnetic. The upper crust of Baltica is uniformly magnetized with a magnetic susceptibility of $60 \cdot 10^{-3}$ SI, the middle crust has a magnetic susceptibility of $60 \cdot 10^{-3}$ SI in the SW and $130 \cdot 10^{-3}$ SI in the NE, and the lower crust has a magnetic susceptibility of $(50—60) \cdot 10^{-3}$ SI. The two-layer crust of Avalonia is non-magnetic, with the exception of a magnetized object (χ=$50 \cdot 10^{-3}$ SI) in the upper crust between the EL and Thor-TS. The initial modeling assumption was an anomalous magnetic field recalculated to an altitude of 3 km, which is not an optimal filter for separating short- and long-wave components. As the experience of constructing magnetic models of the crystalline crust of the EEC has shown, the upper crust as a whole is weakly magnetic, magnetized inhomogeneously, and the magnetic sources are represented by local bodies, which, accordingly, cause local anomalies. Long-wavelength anomalies of the EEC are associated with the inhomogeneity of the middle and lower crust [Krutikhovskaya et al., 1982; Pashkevich et al., 2014; Orlyuk et al., 2017, etc.]. Therefore, for the transition zone from the EEC to the WEP, an alternative magnetic model can be proposed that reduces the contribution of local sources of the upper crust to obtain a regional component associated with the middle and lower crust. The Moho discontinuity is taken as the bottom of the lower magnetoactive layer, since, according to [Gemmer, Nielsen, 2001], the Curie temperature of magnetite is reached at a depth below this discontinuity. Fig. 8 shows such a model for Transect 1, combining the GECO SNST 83-07 reflection seismic line and the EUGENO-2 reflection profile. The section is borrowed from [Williamson et al., 2002] with our additions. Regarding the fault tectonics, the CDF and the STZ, VFZ, and EL zones form a single system with the Thor-TS, with a SW-dipping fault, consistent with the dip of the Thor-TS. All of the listed fault zones, like the STZ, are trough crustal by nature and determine the geometry of deep magnetic sources.

Transect 1 intersects two long-wavelength anomalies within Baltica. The total effect of sources in the middle and lower crust with magnetizations of 0.5, 0.84, and 0.94 A/m, located between the VFZ and AF, causes the NE anomaly. Sources with magnetizations of 0.5 and 0.84 A/m accompany the VFZ and AF from the NE and are bounded by L2 and L1, respectively.

In the upper crust above the deep sources, four local anomalies correspond to sources with magnetization of 0.3—0.7 A/m; they correspond to swarms of dolerite dikes of Carboniferous-Permian age striking NW and extending for hundreds of kilometers. The dike thickness in the STZ zone is 10—50 m. The magnetic susceptibility of the dikes ranges from $(3.3—24.3) \cdot 10^{-3}$ SI [Malehmir et al., 2018]. The dikes are intruded along faults formed in the extensional phase regime. In the center of the block between Thor-TS and STZ, a VFZ stands out [Thybo, 1997], which in our model is associated with a source having a magnetization of I=0.4 A/m, possibly caused by dikes.

The anomaly above Thor-TS, caused by a deep source with a magnetization of 0.7—1.0 A/m, between Thor-TS and the VFZ indicates a large spreading zone favorable for the formation of mafic magnetic sources of basic composition subducting beneath the crystalline crust of Avalonia. The source follows the strike of Thor-TS, is bounded to the NE by the L3 lineament (see Fig. 7), and is accompanied by a local upper crustal source between faults with an intensity of 2.7 A/m. A troughcrustal source with a magnetization of

3.0 A/m is adjacent to the Thor-TS Zone from the NE (see Figs. 7, 8).

The gradual decrease in the intensity of the regional magnetic field SW of Thor-TS in the work [Williamson et al., 2002] is explained by a source in the upper crust beneath the Horn Graben (HG) with a magnetic susceptibility of $50 \cdot 10^{-3}$ SI. In our model, this corresponds to a source with a magnetization of 1.0—1.1 A/m. Most probably, it is bounded from the south by the EL. The authors of the mentioned work presumably associate the nature of this magnetic body with a buried igneous complex. «This might represent the missing arc related to inferred southward subduction of the Tornquist Sea, or an exotic element emplaced during the collision between Avalonic and Baltica» [Williamson et al., 2002, p. 47].

The junction of Baltica and Avalonia in the subcrustal mantle is manifested as a transition from the high-velocity mantle EEC, thrusted at depths of 50—100 km, onto the low-velocity mantle of Avalonia. The projection of this thrust region onto the Earth's surface is shown in Fig. 3. Thesupposed continuation of the overthrust to the Moho discontinuity in the SW part of the section articulates with the EL at the bottom of the crust. The overthrust is confirmed by mantle reflectors MR installed along the DEKORP profile, Fig. 7 [Bayer et al., 2002; Pharaoh et al., 2006]. In our case, the crystalline crust of Avalonia is obducted onto the EEC crust along the Thor-TS, and the lithospheric mantle of Avalonia immerges beneath the Baltica mantle. This immersion corresponds to the domain between the Thor-TS and STZ, i.e., the transition zone between Baltica and Avalonia. Deep magnetic sources correspond to the middle and lower crust of the EEC and, like the consolidated crust of the EEC, are thrusted beneath the lower crust of Avalonia along the Thor-TS, forming an overthrust-underthrust structure. The magnetized portion of the EEC crust is underlain by the high-velocity EEC mantle.

Profile P2 is located in NW Poland and intersects the main structures of the region — the WEP and the EEC, separated by the TTL (see Fig. 5). The Polish part of the EEC is represented by the Dobrzyn Domain, in which «the TTZ and an adjoining narrow strip of the EEP are overridden by deformed Lower Paleozoic strata forming a fold-and-thrust complex referred to as the Koszalin-Chojnice Zone» (K-ChZ) [Narkiewicz, Petecki, 2024, p. 3 and references therein]. The K-ChZ is bounded by the CDF in the NE and by the TTL in the SW. Near the CDF, we identified L, described above. In this case, it is clearly mapped within the complex structure of the MTK anomaly (see Figs. 5, 6). Here it separates its NE part, which has the same strike, from the SW one, conjugated with the TTL strike. The Late Permian-Mesozoic Polish Basin is developed along the TTL to the SW of it. The latter, as a result of Alpine inversion, led to the formation of the Mid-Polish Swell. The Dobrzyn Domain is composed of synorogenic granites and paragneisses. Within the domain, the Mesoproterozoic anorthosite-mangerite-charnockite-granite (AMCG) complex is developed, marked in the magnetic field by positive and negative anomalies [Krzemińska et al., 2017; Narkiewicz, Petecki, 2024]. When constructing the magnetic model, we used data on the depth to the Curie isotherm of magnetite [Majorowicz et al., 2019, Fig. 12, Model D]. As can be seen in Fig. 9, the depth to it varies from 23 km beneath the WEP to 60 km beneath the EEC. Due to this behaviour, within the WEP there is only one magnetic source in the middle crust with a magnetization of 1.07 A/m, limited by assumed faults (the West Pomerania anomaly according to [Królikowski, 2006] with an intensity of up to 35 nT). The upper edge of this source, according to [Petecki, 2001; Petecki, Rosowiecka, 2017], is located at a depth of 18.5 km. In our model, it is attributed to the boundary of the upper and middle crust at a depth of 22 km beneath the Polish Basin. As a whole, the magnetic field beneath the WEP is represented by a broad minimum with an intensity of up to (–60) nT. In the middle and lower crust, immediately SW of the TTL, beneath the Mid-Polish Swell, a source with a magnetization of 0.25 A/m and a SW dip has been identified, likely related to the TTL. The lower magnetic crust of the EEC is thrusted beneath the lower crust of the WEP below the

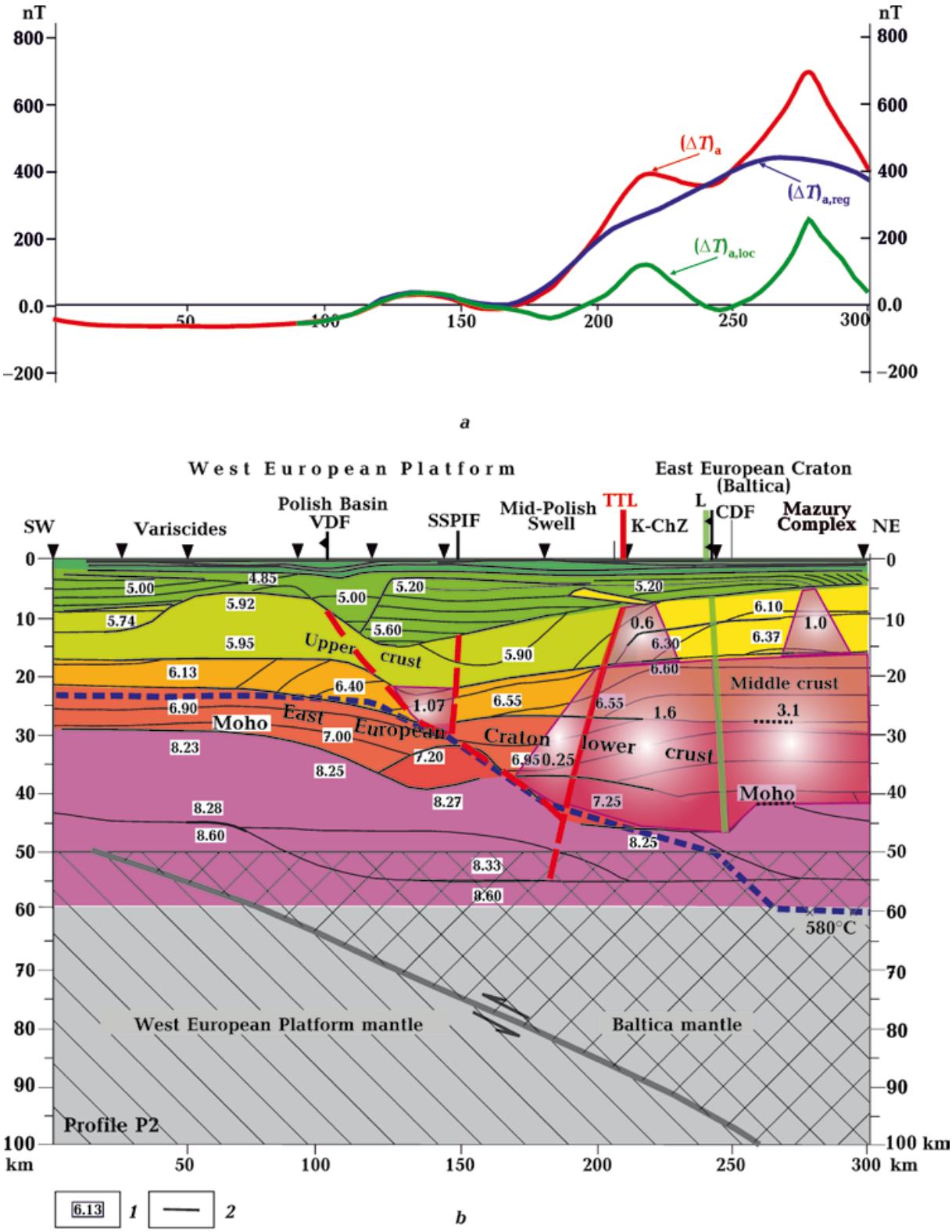

Fig. 9. Magnetic model of the Earth's crystalline crust based on seismic profile P2. Graphs of the anomalous magnetic field (*a*), magnetic model and subcrustal mantle structure (*b*). Seismic model according to [Janik et al., 2002], cross-section of the crystalline crust according to [Petecki et al., 2003; Petecki, Rosowiecka, 2017; Krzemińska et al., 2017]: *1* — seismic velocity V_P; *2* — reflective horizons of the mantle. For other symbols, see Fig. 8 and for other abbreviations — Fig. 2.

Curie isotherm of magnetite, resulting in its non-magnetic nature.

A magnetic source with a magnetization of 1.6 A/m and a source in the upper crust with a magnetization of 0.6 A/m are related to the K-ChZ, accompanying the TTL with NE and bounded by the CDF and the L. A source with a magnetization of 3.1 A/m within the Dobrzyn Domain and a source in the upper crust with a magnetization of 1.0 A/m are related to the Mazury Complex. The combined effect of sources in the middle and lower crust and sources associated with them in the upper crust corresponds to the MTK anomaly [Królikowski, 2006]. The deep sources likely have different origins, as they relate to the junction of NE-striking cratonic structures and NW-striking K-ChZ sources associated with the TTL. As in the previous case, the profile intersects the thrust of the cratonic subcrustal mantle onto the subcrustal mantle of the WEP. Seismic velocities V_P at a depth of 50—55 km reach 8.6 km/s, confirming the presence of high-velocity mantle of the EEC beneath the WEP. The mantle overthrust is likely also associated with the underthrust of the lower crust of the EEC beneath the crust of the WEP.

Profile P4 (Fig. 10) intersects Variscides, WEP and is almost orthogonal to the edge of the EEC.

Profile P4 is a representative seismic profile comprehensively studied in the region [Grad et al., 2003, 2018; Grabowska, Bojdys 2004; Wilde-Piórko, 2010; Grabowska et al., 2017; Grad, 2019 and references therein; Majorowicz et al., 2019, etc.]. The work [Grad et al., 2018] presents generalized data on lithospheric heterogeneities, including the LAB boundary, based on the results of the passive seismic experiment «13 BB star». As for magnetic modeling, it has been carried out since 1932. The version proposed in the work [Grabowska, Bojdys 2004] is based on the following assumptions. The sedimentary layer is considered as non-magnetic. The top of the magnetoactive layer is attributed to the surface of the crystalline basement based on seismic (V_P=6.0 km/s) and geological data. The bottom of the magnetoactive layer is identified by the position of the 600° isotherm, within the EEC — by the Moho discontinuity. The upper crust is divided into two magnetoactive levels: 1) from the basement surface to 8 km with magnetic properties based on rocks uncovered by boreholes; 2) in the depth range of 8—20 km (V_P=6.5 km/s) with less differentiated properties. The lower layer is bounded by V_P=6.5 km/s and the Moho discontinuity or the 600° isotherm. 2D magnetic modeling was performed using two computer programs: interactive and iterative, assuming constant inductive magnetization. The magnetization of the first layer of the crystalline crust of the EEC is estimated in the range from –1.0 to 3.4 A/m, of the second one — from 0.4 to 4.0 A/m, of the lower one — 4.6 A/m. Within the WEP, the magnetizations of the corresponding layers are: 0.4—2.5; 0.4; 3.0—6.0 A/m [Grabowska, Bojdys, 2004, Fig. 6, p. 24].

We propose a magnetic model for profile P4 within our study area from 0 to 700 km along the profile, constructed on the results of 3D modeling under the following assumptions. Two magnetoactive layers are considered: the upper crystalline crust in the depth range from the surface of the crystalline basement (V_P=6.0 km/s) to the top of the middle crust (V_P=6.3 km/s). The middle and lower crust up to the Moho discontinuity beneath the EEC and the Curie isotherms of magnetite 580° [Majorowicz et al., 2019, Fig. 12, Model D] beneath the WEP are taken as the lower magnetoactive layer.

In the SW part of the profile, the anomalous magnetic field is negative, weakly differentiated, with an intensity of up to –100 nT. The minimum is caused by the non-magnetic crust of the WEP above the position of the Curie isotherm of magnetite, as a result of which the lower crust of the craton and part of the middle one, thrusted under the crust of the platform, appear non-magnetic. Modeling along the P4 profile showed that the eastern part of the minimum satisfies the marginal magnetic effect of the inhomogeneities of the middle and lower crust of the EEC, and does not require the introduction of either the reverse magnetization of the WEP section into

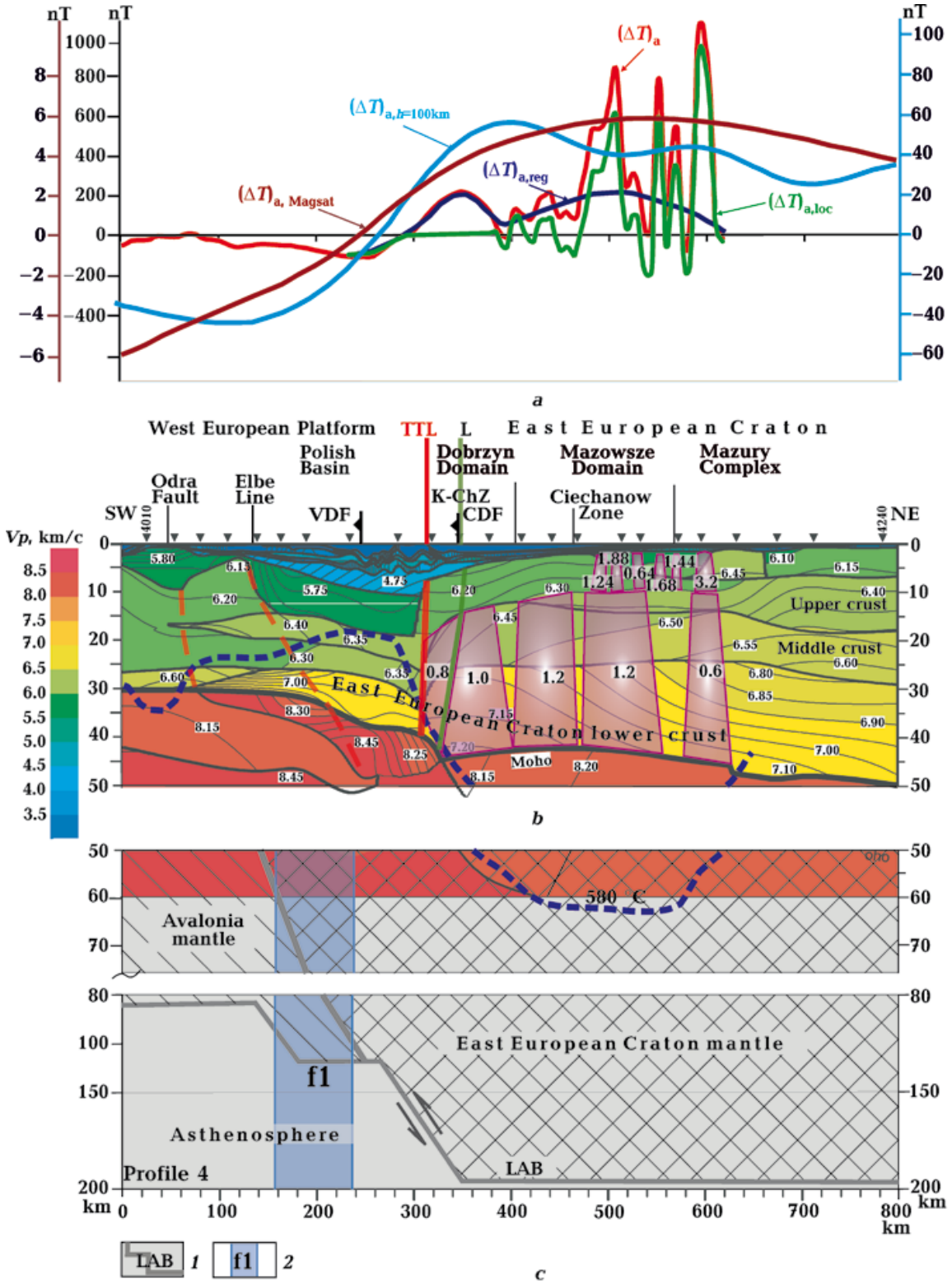

Fig. 10. Magnetic model of the Earth's crystalline crust based on the seismic profile P4. Graphs of the anomalous magnetic field (*a*), magnetic model and subcrustal mantle structure (*b*), relief of the lithosphere-asthenosphere boundary according to [Majorowicz et al., 2019] (*c*): *1* — lithosphere-asthenosphere boundary (LAB); *2* — ultra-deep mantle fluid f1. Graphs of anomalous magnetic field: observed — $(\Delta T)_a$, regional — $(\Delta T)_{a,reg}$, local — $(\Delta T)_{a,loc}$, at an altitude of 100 km — $(\Delta T)_a$, h=100 km and satellite field Magsat — $(\Delta T)_a$, Magsat. Seismic model according to [Grad et al., 2003]. For other symbols, see Figs. 8, 9 and for other abbreviations — Fig. 2.

the magnetic model, or such high values of it as in the model of [Grabowska, Bojdys, 2004]. The TTL on profile P4 has a vertical dip, which is confirmed by magnetic modeling. As in profile P2, the first source with a magnetization of 0.8 A/m marks the position of the NW-striking K-ChZ, is bounded by L from the NE, and directly accompanies the TTL. The second source with a magnetization of 1.0 A/m belongs to the Dobrzyn Domain and corresponds to the NE-striking cratonic structures. Further, the profile intersects the Ciechanow Zone (CZ), which is part of the Mazowsze Domain [Krzemińska et al., 2017], extends to the NNE (see Fig. 7) and corresponds to a positive magnetic belt with an anomaly intensity of 500—630 nT. A local anomaly with smaller values associated with the Paleozoic Mlawa syenite intrusion [Grabarczyk et al., 2022] stands out in the center of the belt. In our model, the CZ is represented by a source with a magnetization of 1.2 A/m. In the Mazowsze Domain, another deep source with the same magnetization is distinguished, as well as three upper crustal sources with magnetizations of 0.64, 1.24, and 1.88 A/m. In the NE, the profile intersects the Mazury Complex; in the magnetic field it is represented by anomalies of up to 500—900 nT, which in the middle and lower crust correspond to a weakly magnetic source (0.6 A/m).

All local anomalies in the marginal part of the profile belong to the development area of the Mazury Complex and are associated with upper crustal sources with magnetizations of 1.44—3.2 A/m.

The difference in the magnetic models described above can be considered from several positions. The division of the magnetoactive layer into two levels (upper crystalline crust, middle and lower crust) in our model is justified for the Ukrainian Shield [Krutikhovskaya et al., 1982; Pashkevich et al., 1990 and references to it; Chekunov, 1992; Pechersky, 1994, etc.].Using the correlation between the density and velocity of longitudinal seismic waves at a pressure of 4 kbar [Krasovsky, 1981], it is shown that the boundary between the upper and middle crust can be attributed to the depth where V_P=6.3 km/s, and between the middle and lower crust this velocity is V_P=6.8 km/s, which corresponds to the 3D model [Grad et al., 2018, Fig. 8]. A generalization of data on the magnetic properties and density of Ukrainian Shield rocks from outcrop and borehole samples [Krutikhovskaya et al., 1982, Figs. 17, 18] revealed a wide range of median magnetization values and magnetic susceptibility for virtually all rock types comprising the Precambrian basement. And a large number of samples (up to hundreds) for each rock type were used. This provides grounds for a wide range of magnetization for sources in the middle and lower crust. The works [Puziewicz et al., 2006; Grad, 2019, and references therein] present a petrological interpretation of the crust and upper mantle based on seismic models, geological and geophysical data. According to this model, mafic granulites predominate in the lower crust beneath the EEC and TTL. Beneath the WEP, mafic and felsic granulites with possible intrusions of mafic and ultramafic rocks are found. The middle crust beneath the EEC is composed of gneisses and amphibolites, the upper crust is composed of gneisses, granulites, granites, and charnockites. Beneath the WEP, the middle and upper crust are composed of metamorphic rocks. It should be noted that such a predicted crustal composition provides a rather generalized characteristic. In magnetic terms, for example, mafic granulites, as well as rocks of the granodiorite-diorite formation and charnockitoids, can have a wide range of magnetization (from non-magnetic to 6 A/m) [Krutikhovskaya et al., 1982]. It has also been shown that orthorocks of the granulite and amphibolite facies of metamorphism have higher magnetization compared to pararocks.

Our model uses data on the depth to the Curie isotherm of magnetite [Majorowicz et al., 2019], which, as noted above, excludes the presence of highly magnetic rocks beneath the WEP at depths greater than 20—25 km.

The differences in magnetization of the lower and middle crustal sources in the discussed models are related to the different parameters of the magnetoactive layer adopted

and the interpretation methods used in 2D and 3D modeling.

Let us consider which crustal magnetic heterogeneities correspond to lithospheric heterogeneities. The sources of the middle-lower crust of the EEC belong to the region of thrusting of the craton's high-velocity mantle onto the WEP mantle (see Section 4.2, Fig. 3). In the velocity section, the craton's subcrustal mantle at a depth of up to 60 km is characterized by velocities of V_P=8.15÷8.28 km/s. To the NE of the TTL, it is underlain by high-velocity mantle (V_P=8.30÷8.47 km/s) thrust together with the craton's lower crust onto a low-velocity layer (V_P=8.15 km/s) of the WEP mantle up to the Odra Fault. The low-velocity layer to the SW of the TTL is again underlain by a high-velocity one, which can be interpreted as a layered subcrustal mantle.

The described situation may justify a regional thrust of the EEC subcrustal mantle onto the WEP mantle as a result of a common process of their formation with dynamic stresses directed from NE to SW. Furthermore, deep magnetic sources record an extension zone. LAB data [Mazur et al., 2015] indicate a correlation between crustal and mantle structures. The greatest depth variations to the LAB beneath the EEC lower crust, which is thrusted beneath the WEP crust, are also indicative. The sharp rise of the magnetite Curie surface in the transition zone from the EEC to the WEP closely correlates with the position of the ultradeep fluid f1. It is located in the transition zone from the LAB of the craton to the LAB of the platform. The thrust of the EEC subcrustal mantle onto the WEP subcrustal mantle is also located within the fluid. The latter is likely related to the aforementioned mantle layering. Thus, the craton's magnetic sources are related to the zone of subcrustal mantle layering, while the nonmagnetic crust of the WEP is related to the rise of the magnetite Curie isotherm above the ultradeep mantle fluid and to the zone of abrupt change in lithospheric thickness.

We will also note the close correlation between the positive satellite field anomaly and the lithospheric thickness, which may suggest the presence of mantle magnetic sources.

Profile Cel 01 (Fig. 11) traces from the SW margin of the EEC to the Pannonian Basin system.

A magnetic model for the profile Cel 01 was constructed within our study area. The profile intersects the Outer Carpathians and the Pre-Carpathian Trough, the WEP, the TTL, and the Mazowsze Domain within the EEC. The WEP magnetic field is characterized by a weakly differentiated regional minimum with an intensity of up to –135 nT, caused by the marginal effect of the EEC crystalline crust and the weakly magnetic crystalline crust of the platform. The EEC's complexly differentiated magnetic field includes regional component and local one. In accordance with the purpose of this article, the magnetic model is presented only for the SW margin of the EEC in close proximity to the TTL.

The 2D magnetic model for the Cel 01 profile was previously discussed in [Grabowska et al., 2011, 2017 and references therein]. In the fundamental work [Grabowska et al., 2011], an interactive 2D magnetic model was constructed in conjunction with a density model based on the V_P velocity model [Środa, 2006], taking into account the temperature regime of the lithosphere and the seismic-petrological model [Puziewicz, 2008]. The magnetoactive layer is attributed to the entire section of the crystalline crust, for which inductive magnetization is adopted. From the presented model, it follows that the authors adhere to the opinion that magnetization increases with depth from layer to layer both within the EEC and its SW surroundings. The magnetization of the lower crust is generally accepted to be equal to 2 A/m, with the exception of two blocks: beneath the Malopolska Unit and beneath the Lublin Trough. A unique block of the middle crust (V_P=7.15; ρ=2.94 Mg/m^3 and magnetization of 2.5 A/m) is interpreted as a garnet and/or pyroxene granulite diapir (note, «without root»), or a zone rich in gabbro and cumulate ultrabasic igneous rocks). In the magnetic model, this block has a continuation in the lower crust, which appears as a supply channel. However, there is no high-velocity and density body here, which, similar to the middle crust, could be associated with a magnetic

source. The magnetic model of the lower crust includes a body with a density of 3.09 Mg/m^3 in the Moho keel region. Such a density can characterize practically non-magnetic eclogites, which suggests a shallower depth to the bottom of the magnetoactive layer.

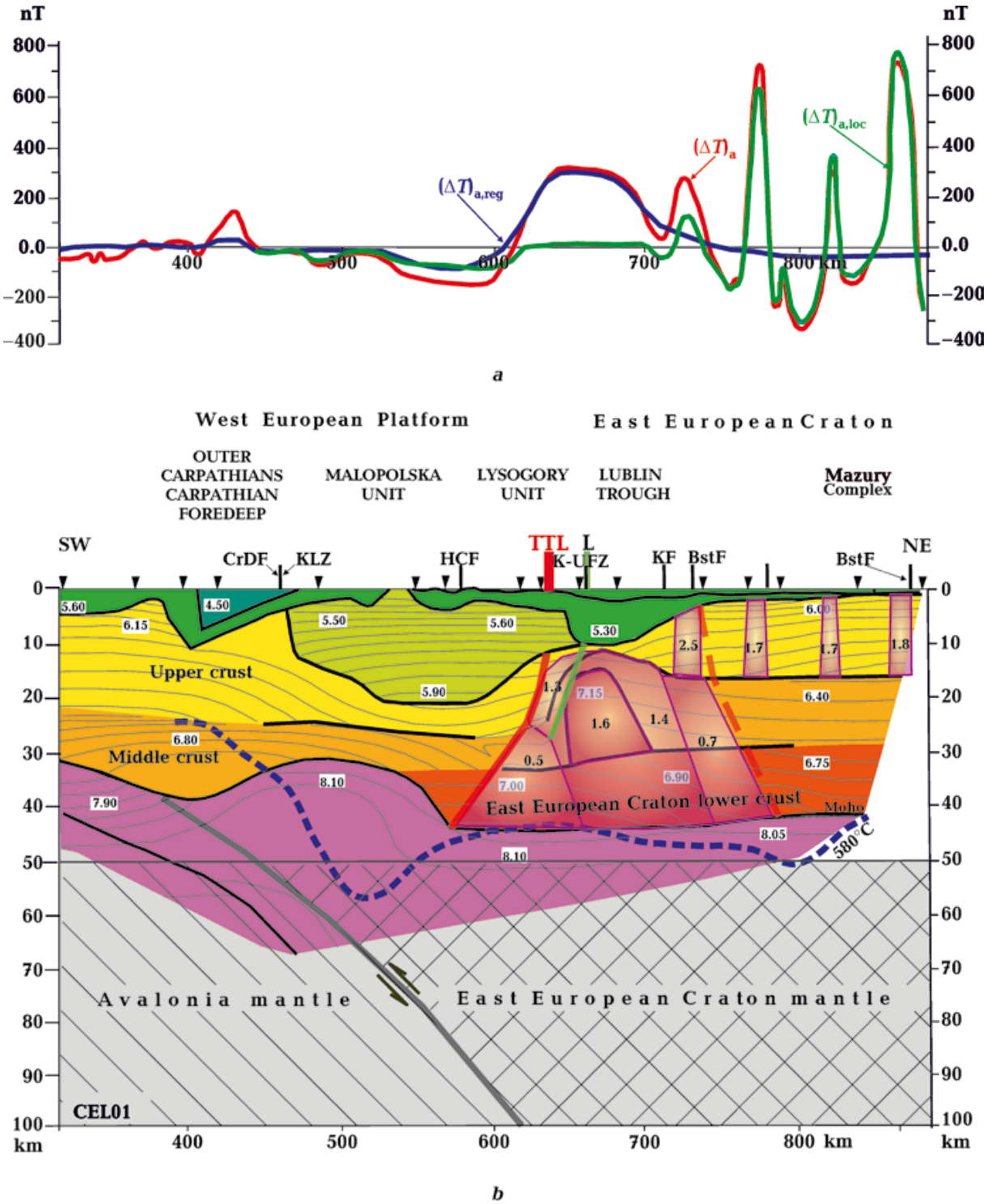

Fig. 11. Magnetic model of the Earth's crystalline crust based on seismic profile Cel 01. Graphs of anomalous magnetic field (*a*), magnetic model and subcrustal mantle structure (*b*). Seismic model according to [Środa, 2006], cross-section of the crystalline crust according to [Grabowska, Bojdys, 2001; Grabowska et al., 2011, 2017, etc.]. For other symbols, see Figs. 8, 9 and for other abbreviations — Fig. 2.

We propose an alternative magnetic model for the Cel 01 profile based on the 3D magnetic model (see Figs. 6, 11). It is constructed with different initial parameters and different distribution of sources for local magnetic anomalies in the upper crust and regional magnetic anomalies in the middle and lower crust (see Data and Methods). This resulted in a redistribution of the magnetization of regional anomaly sources, which differs from the estimates in the model by T. Grabowska et al. Presented magnetization values correspond to the average values at the source. The magnetic model of the middle and lower crust of the EEC is represented by three sources. A broad positive magnetic field anomaly with an intensity of up to 315 nT is recorded above the Lublin Trough and is caused by a complex magnetic source. At its centre, a source associated with a high-speed body with a magnetization of 1.6 A/m is allocated. Beneath the trough, the boundary between the upper and middle crust, and consequently the upper edge of the source, rises to 12 km, forming an anticline. The magnetization of the source is 1.4 A/m. Its SW edge corresponds to the K-UFZ and the L. In the middle crust, it has a dip close to the TTL one. In the lower and partly middle crust, its dip becomes NE. In the Moho keel region, the described source contacts a body of low magnetization (0.5 A/m). In the middle crust between TTL and L, a source with a magnetization of 1.3 A/m was identified, which is part of the source band along the TTL. A similar source at the same depths is recorded in the magnetic model along the POLKRUST profile to the SE of the Cel 01 profile between the Tomaszow Fault, identified with the TTL, and the I-ZF with a magnetization of 0.035 SI [Malinowski et al., 2015]. The NE face of the source with a magnetization of 1.4 A/m has a NE dip in the KF region. This source, consistent with the TTL strike (see Fig. 7), is part of the «range of the higher magnetic parameters of the crystalline crust» [Grabowska at al., 2017], traced along the TTL. This band is similar to the K-ChZ source band described above (see profiles P2, P4, Figs. 8, 9). Further to the NE, a weakly magnetic source (0.7 A/m) is located between the KF and BstF with NE-dipping lateral faces, consistent with the BstF dip [Belinsky et al., 2003, etc.] and extending beneath the Mazury Complex. Above it, a local source in the upper crust with a magnetization of 2.5 A/m is identified. In the NE, the profile intersects the belt of alkaline intrusions of the Mazury Complex, presumably determining the sources of local anomalies in the upper crust with magnetizations of 1.7 and 1.8 A/m. A connection between these local sources and a deep source, apparently reflecting the magmatic centre of the intrusions, is possible.

As in all previously described profiles, deep sources are located above the subcrustal mantle of the EEC, which is thrust over the mantle of the WEP. The thrust is confirmed by a conformable reflection/refraction boundary separating the high-velocity subcrustal mantle from the low-velocity mantle.

The PANCAKE profile intersects the Pannonian Basin, a segment of the East Carpathian Orogen, including the Pre-Carpathian Trough, and the SW part of the EEC within Sarmatia (Fig. 12).

The L'viv Paleozoic Trough adjoins the TTL on the Sarmatian side. A seismic section [Starostenko et al., 2013, 2022] and distribution data on the Earth's crustal temperature [Kutas et al., 1996] were used to construct the magnetic model.

The weakly differentiated magnetic field in the SW part of the profile up to the Transcarpathian Fault within the Alcapa corresponds to non-magnetic crust. Based on 3D modeling, a source with a magnetization of 1.07 A/m was identified beneath the Pre-Carpathian Trough. It is bounded by the TCF to the SW and by the TTL to the NE. The source is located in the middle crust and is most likely related to the formation of the Pre-Carpathian Trough. Three deep sources were identified distribution further beneath the EEC. A source with a magnetization of 1.6 A/m has SW-dipping faces corresponding to the dips of the TTL, Rava-Rus'ka (R-RF), and Rohatyn (RgF) Faults. On the basis of seismic boundaries distortion along the R-RF and considering that it is the NE boundary of the Rava-Rus'ka block of the Caledonides (we

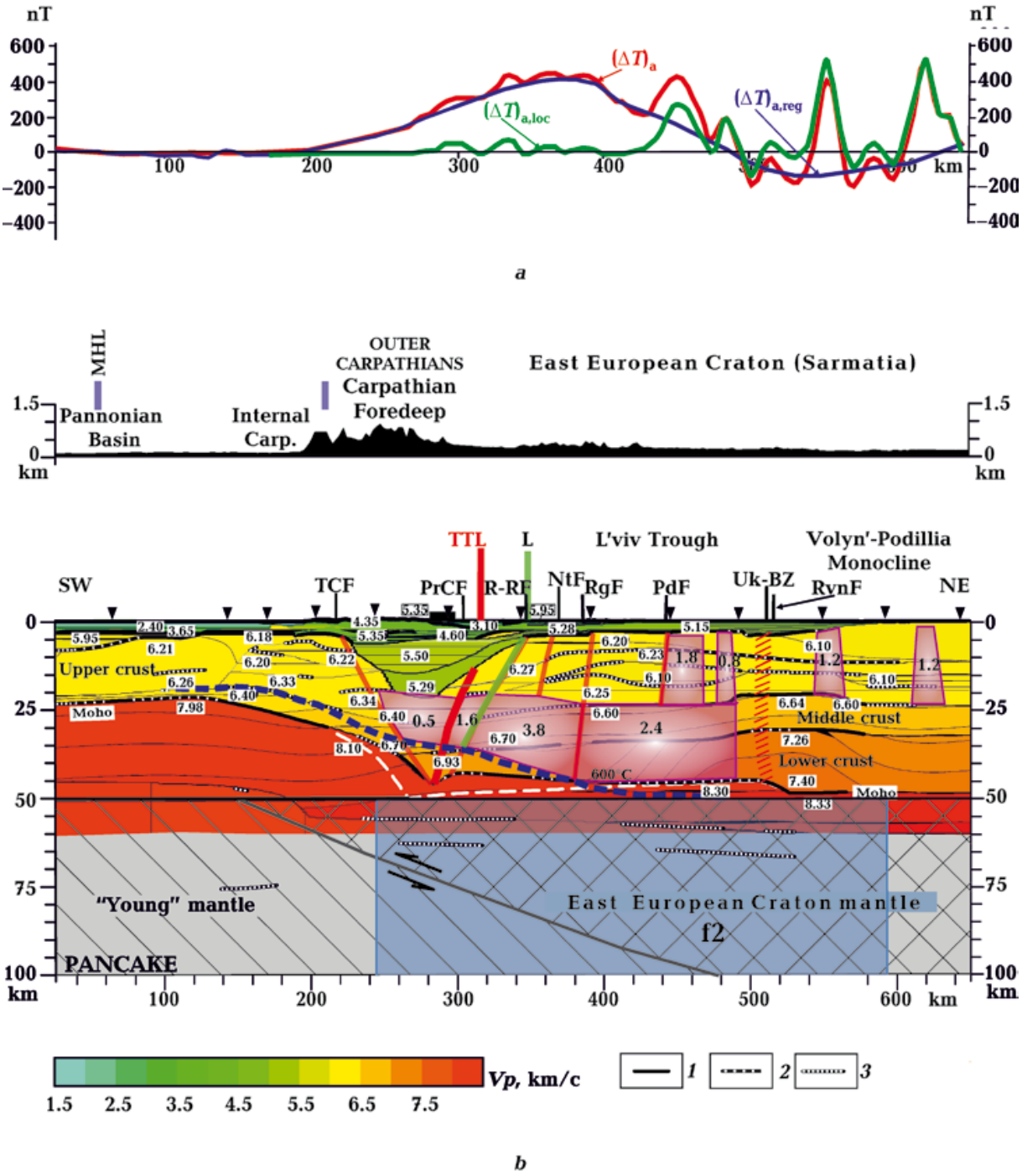

Fig. 12. Magnetic model of the Earth's crystalline crust based on the PANCAKE seismic profile. Graphs of the anomalous magnetic field (*a*), magnetic model and subcrustal mantle structure (*b*). Seismic model according to [Starostenko et al., 2013, 2022]. Mantle boundaries: *1* — refracted; *2* — refracted and reflected; *3* — reflected. For other symbols see Figs. 8—10 and for other abbreviations see Fig. 2.

identify it as lineament L), the SW part of the magnetic source between the TTL and R-RF may be analogous to sources in the K-ChZ zone. Sources with magnetizations of 3.8 and 2.4 A/m between R-RF and RvnF are related to the middle-lower crust beneath the L'viv Trough. The second source is bounded from the NE by a vertical face beneath the RvnF.

The total effect of these two sources is represented by the L'viv regional anomaly with an intensity of up to 400 nT. Above the deep source with a magnetization of 2.4 A/m, upper crustal sources with magnetizations of 1.8 and 0.8 A/m are identified. They are represented by basic rocks in the Rivne Fault Zone, which is part of the Uk-BZ activation zone. In the NE part of the profile, upper crustal sources with a magnetization of 1.2 A/m are identified. These sources are related to the Volyn'-Podillia Monocline (V-PM) and the margin of the Ukrainian Shield and are caused by Proterozoic mafic rocks of the OMIB (see Fig. 7).

The PANCAKE profile reveals a spatial correlation of magnetic sources with ultradeep f2 fluid in the region of the thrust and stratified subcrustal mantle of the craton onto the «young» mantle (Fig. 12). The association of trap eruption region of the Volyn' Igneous Province (VIP) with the L'viv regional anomaly may be related to fluidization processes that occurred in the upper mantle and lower crust during the Vendian. Specifically, in the trap eruption region, the mantle becomes depleted in low-melting iron, which concentrates in the Earth's crust, creating areas of increased magnetization [Orlyuk, 1986]. The depletion of the mantle in low-melting iron may be due to the presence of fluid. The presence of trap magmatism indicates intensive manifestations of basification of the V-PM Earth's crust west of the Chernivtsi-Kivertsi line, which leads to the formation of the magnetic sources described above in the lower crust under the L'viv Trough.

As shown previously [Orlyuk, 1986], a specific feature of the study region, complicating the construction of a three-dimensional model of the upper crust, is the occurrence of a basaltic component in the trap formation. However, the maximum thickness of the basalts here is approximately 350 m and does not significantly affect the effect of magnetic sources. The effect of the Vendian traps was not taken into account during magnetic modeling of the crystalline crust.

The RomUkrSeis profile crosses the Apuseni Mountains, the Transylvanian Basin, the Eastern Carpathians, the Volyn'-Podillia Monocline and the SW part of the Ukrainian Shield (Fig. 13).

Magnetic modeling in the SW was performed only in the region closest to the TTL. Unlike previous sections, the crystalline crust here is represented generally by a lower-velocity section. V_P velocities at the bottom of the crust throughout the profile do not exceed 6.57 km/s, while SW of the TTL, beneath the Pre-Carpathian Trough, within the Moho keel, velocities are minimal (6.30 km/s). Thus, the crystalline crustal section is represented only by the upper and middle crust. The position of the Curie isotherm of magnetite, according to [Kutas et al., 1996; Kutas, 2021], varies from 50 km beneath the EEC to 30 km beneath the Carpathians. In the Transylvanian Basin, it falls to subcrustal depths (42 km), and rises to 33 km at the transition to the Apuseni. Estimates of deep temperatures are ambiguous. For example, in [Gordienko et al., 2012], the Chernivtsi activation zone between R-RF and PrDnF with an assumed zone of partial melting at a depth of 25 km was identified on the Volyn'-Podilila Monocline.

The behaviour of the regional component of the anomalous magnetic field indicates a virtually non-magnetic crust NE of the TTL beneath the Volyn'-Podillia Monocline. From the TTL to PrDnF, the block of non-magnetic crystalline crust is consistent with the temperature regime described above. The center of this block includes a Uk-BZ activation zone, confirming its status as an activated zone. Furthermore, this is supported by the electrical conductivity anomaly detected on this profile between the TTL and PodF [Makarenko et al., 2025 and references therein]. A deep source with a magnetization of 1.6 A/m is identified on the profile directly beneath the Pre-Carpathian Trough in the low-velocity upper crust. In the middle crust to the NE of PrDnF, the well-known Vinnytsia regional anomaly [Krutikhovskaya et al., 1982] is caused by three closely spaced sources with a magnetization of 1.02—1.6 A/m. A series of upper crustal sources (1.5—1.6 A/m) corresponds to the main rocks of the crystalline basement of the Ukrainian Shield and its slope.

The Pre-Carpathian Trough, together

with the TTL (PrCF is considered here as a manifestation of the TTL), is a transition zone between the Carpathian-Pannonian region and the EEC and can be interpreted as the TTZ. This transition is accompanied by a decrease in the thickness of the electrical

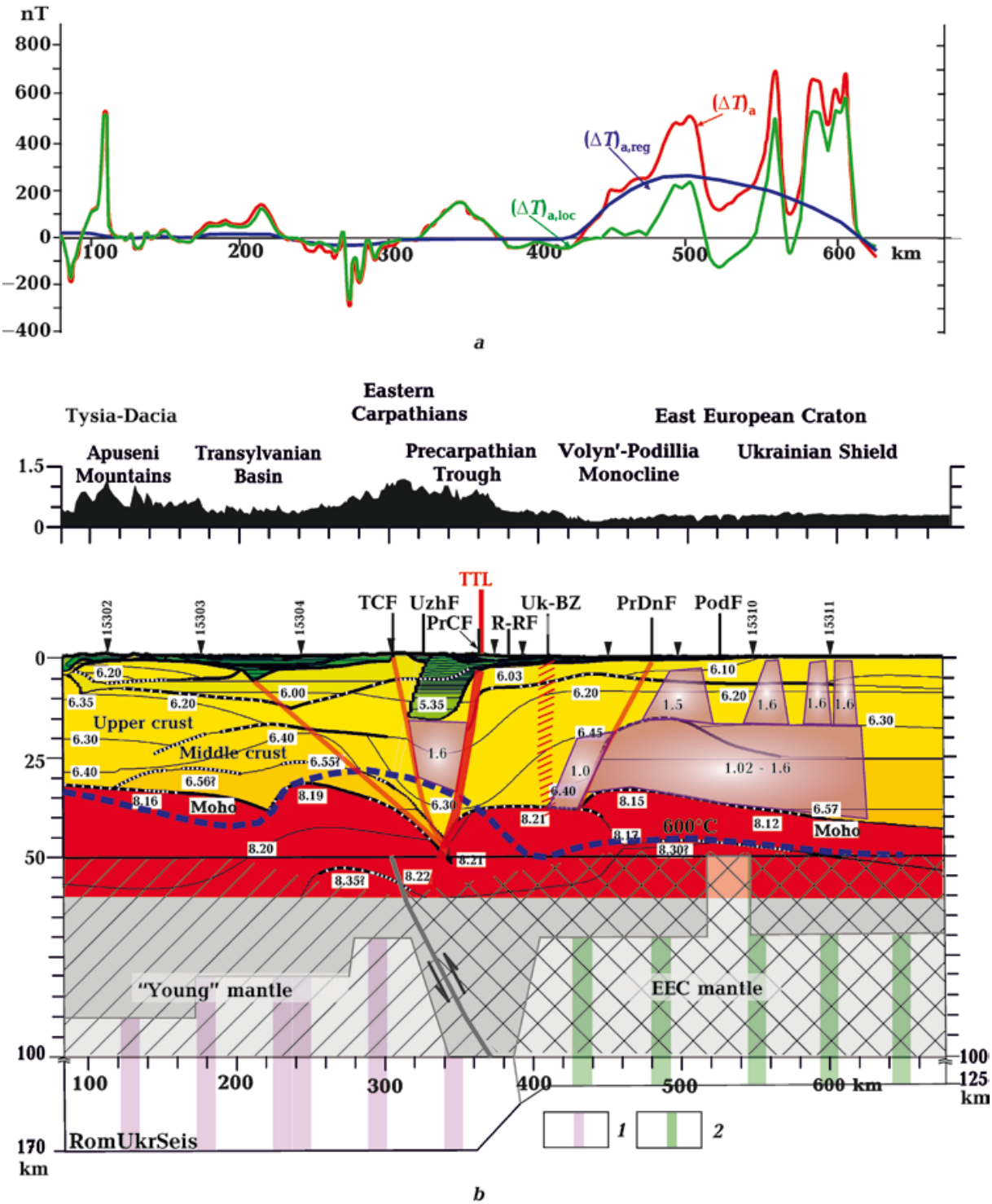

Fig. 13. Magnetic model of the Earth's crystalline crust based on the RomUkrSeis seismic profile. Graphs of the anomalous magnetic field (*a*) magnetic model and subcrustal mantle structure and 'electrical' asthenosphere by [Makarenko et al., 2025] (*b*): Total longitudinal conductivity of the asthenosphere: *1* — 6000, *2* — 2000. Seismic model according to [Starostenko et al., 2020]. For other abbreviations see Fig. 2.

asthenosphere from SW to NE from 100 to 70 km and by a change in the total longitudinal conductivity from 6000 Siemens beneath the Carpathian-Pannonian region to 2000 Siemens beneath the southern part of the Volyn'-Podillia Monocline and the western part of the Ukrainian Shield. Simultaneously, the base of the electrical asthenosphere rises from 170 to 125 km from the Carpathian-Pannonian region to the Volyn'-Podillia Monocline. The summarized data on the thermal LAB topography presented in the cited work note a sharp change in depth to the asthenosphere. Maximum depths range from 50—120 km in the SW to 140—250 km in the NE, with a zone of maximum gradients in the area of the assumed deep location of the TTZ (this term is used by cited authors). Beneath this zone, a sharp localized depression of the roof of the electrical asthenosphere is observed. It correlates with a series of faults (TCF, PrCF, R-RF, PrDnF), Uk-BZ zone and the thrust of the subcrustal mantle onto the «young» mantle, as well as a keel in the Moho relief. According to electromagnetic data, the TTL is recorded above the region of change in lithospheric electrical conductivity beneath the Eastern Carpathians and the Volyn'-Podillia Monocline. The nature of the anomalous electrical conductivity is debatable; however, it can likely be considered as the combined activity of fluidization and/or graphitization processes [Makarenko et al., 2025].

The main feature of the 3D magnetic model of the SWedge of the EEC is a band of deep sources series with magnetizations ranging from 0.5 to 1.6 A/m along the TTL, as well as along the STZ, Thor-TS, and VZF. It is bounded to the NE by L and its analogs L1, L2, and L3 in the transition domain from Baltica to Avalonia. L is identified by the change in the strike of Fennoscandia's near-surface magnetic field anomalies along the TTL within the EEC itself. Along the SW margin of Sarmatia, L corresponds to I-ZF and R-RF. Overall, L is parallel to the TTL.

The cross-sectional position of the source band concomitant with the TTL relative to the strike of the main FSc structures indicates a younger age for these sources. This conclusion is consistent with the correlation of L with CDF, the association of the source band with the K-ChZ in the Dobrzyn Domain, and the position of R-RF, which bounds the Caledonide block to the NE. The Carboniferous-Permian age of basic magmatism throughout the Tornquist Fan region, including along the STZ, VFZ, and Thor-TS, provides direct evidence of a post-Neoproterozoic age for the magnetic sources along these zones and the TTL. Thus, the TTL, the L, and the band of magnetic sources between them can be considered as TTZ. The formation of these sources may be due to the extensional regime during repeated activation of the TTZ. «The lithospheric memory of the TTZ echoed in successive stages of its reactivation in different intra-plate tectonic regimes — transpressive Variscan, mostly extensional or transtensional Permian through Early Cretaceous, compressional Late Cretaceous, and finally Neogene, related to the Carpathian orogenic compression» [Narkiewicz, Petecki, 2019, p. 937]. The formation of the TTL-concomitant magnetic anomaly sources related to mafic magmatites can be attributed to the Permian-Early Cretaceous activation phase. The emergence of an extension-transtension regime NE of the TTL, accompanied by mafic magmatism, can be explained by thrusting of the lower crust of the EEC beneath the crust of the WEP, with simultaneous thrusting of the subcrustal mantle of the EEC onto the WEP mantle and its stratification. An alternative to the magmatic origin of magnetic sources is the influx of «secondary» magnetic minerals by deep fluids due to increased mantle permeability beneath the TTL. The resulting 3D magnetic model of the consolidated crust permits the occurrence of mantle magnetic sources. Substantiating the presence of such a source in SW Fennoscandia, where a positive satellite anomaly correlating with lithospheric thickness has been recorded (see, for example, Fig. 10), is the subject of further research.

Discussion. The region, which has been studied for over 100 years, has been presented in an extremely large number of works, including a number of generalizations. Nev-

ertheless, problems of tectonics, the history of lithosphere development, and the relationship between the structure of the Earth's crust and mantle remain controversial. These include geodynamic reconstructions of the modern lithosphere, the age relationships of large domains, the structure of the crust, and others. It was not possible to cover such a broad range of problems to elucidate the relationship between magnetic heterogeneities of the crystalline crust and lithospheric heterogeneities. Therefore, the proposed results do not claim to be definitive, nor does the interpretation of any geophysical (or geological) data. However, it is possible to «link» some objectively existing geophysical and geological data, which form the basis of our conclusions.

These include: the observed near-surface anomalous magnetic field and its "structural" plan, reflecting the structure of the crystalline basement; modern data on the composition and age of the crystalline basement; and transregional tectonic lineaments reliably established from geological data (see, for example, Sveconorwegian Front). All other materials we used are ones of possible interpretation results. In particular, this applies to the depth to the Curie isotherm of magnetite, heat flow, seismic data (velocity and structural sections of the Earth's crust), seismotomographic data (vertical and horizontal velocity sections, superdeep fluids, inclined high-velocity layers interpreted as slabs), depth to the boundaries of the lithosphere and asthenosphere according to a set of geophysical data.

Tectonic zoning is not an exception. It is enough to recall how the position of the Fennoscandia-Sarmatia junction zone was revised as there appeared new data on the age, composition, and metamorphism of Precambrian rocks and seismic data on the structure of the Earth's crust [Bogdanova, 1993; Bogdanova et al., 2001, 2015, 2016; Krszemińska et al., 2017, etc.].

The character of subductive processes that formthe EEC boundary has been the subject of a long-standing debate. The geophysical signs of these processes are generally considered to be the presence of high-velocity layers in the mantle, interpreted as slabs. Available data do not provide a comprehensive justification for the subduction in the region, although geodynamic reconstructions suggest SW and NE subductions of different ages [Gintov et al., 2022 and references therein]. The presence of slabs in the lithospheric section is also of interest for substantiating possible mantle magnetic sources.

In this regard, it should be noted that slabs with a thickness of tens of kilometres can retain their magnetization for a long time due to the conservation of the thermal regime up to the Curie temperatures of magnetic minerals (magnetite with a Curie temperature of 580 °C and presumably native iron with T_C=760 °C). Such magnetic heterogeneities were discovered in the modern subduction joint zone of the Eurasian and Pacific plates [Orlyuk et al., 2016]. In our case, against the background of strongly magnetic crustal sources, it is not possible to isolate the effect of mantle slabs.

Regarding the 3D magnetic model of the crystalline Earth's crust, methodological issues play a special role in its construction. This primarily concerns methods for separating the observed magnetic field into local and regional components, as well as parameterization of the model. Long-standing practice of eliminating local anomalies demonstrates the validity of using formal methods for field separation only in conditions of virtually constant bedding depth of crystalline crust roof (shield and massif regions). Under such conditions, the attenuation of local anomalies, regardless of the filter type, does not distort the regional component. However, even under such favorable conditions, there is a risk of obtaining false regional anomalies in areas with a high concentration of local anomalies. In our case, with a sharp change in depth to the crystalline basement, the use of formal field filtering is unacceptable. Therefore, we concluded that it was necessary to construct a magnetic model of the entire crystalline crustal section. The upper edges of local sources are assigned to the surface of the crystalline basement, while the lower edges are assigned to the boundary of the upper and middle crust. The lower boundary of the magnetoactive layer is tradi-

tionally assigned to the Moho discontinuity or to the isothermal Curie surface of magnetite.In the 3D magnetic model, deep sources, unlike previous models, are represented as blocks with uniform equilibrium magnetization constant up to the Curie temperature of magnetite. This is based on experimental data under a quasi-universal pressure of 700 MPa [Pechersky, 1994]. However, such magnetic sources may represent areas of concentration of smaller sources.

With the adopted model parameterization, magnetization values for deep magnetic sources are generally lower than those obtained by previous researchers. It is important to emphasize that the magnetic model reflects the structural features of the source distribution, particularly those associated with TTL.

During the preparation of this article, a number of questions arose that require detailed study. We will highlight just a few of them.

1. Could the thrust of the lower crust of the EEC beneath the crust of the WEP and the thrust of the craton's subcrustal mantle onto the mantle of the WEP be the result of a single geodynamic process leading to the formation of an extension zone and the generation of magnetic sources within it?

2. What are the signs of crustal fluidization (besides seismotomographic data and oil- and gas-bearing along the border of Fennoscandia), which may be associated with the formation of secondary magnetic minerals and, accordingly, magnetic anomalies?

3. With which stage of the TTL activation can the band of magnetic sources accompanying TTL be associated?

4. Can the existence of a nearly uniformly reverse magnetized crystalline crust of the WEP along the TTL explain the Central European Magnetic Minimum?

5. To which stage of the tectonic development of the region can we attribute the linear uplift of the modern LAB under the junction zone of Fennoscandia and Sarmatia and the deflection of this border under the junction of the Bohemian Massif with the Carpathians?

6. What is the reason for the vertical position of the supposed deep part of the TTL under the thrust of the subcrustal mantle of the EEC onto the mantle of the WEP with the predominantly inclined SW dip of this lineament in the Earth's crust?

7. What contribution to satellite anomalies can be made by crustal sources and slabs' superposition? To resolve this issue, additional data is needed, primarily on the petromagnetism of mantle rocks, since at such altitudes, slabs and crystalline crust sources can cause the anomalies of identical wavelengths.

Conclusions. Based on a comprehensive analysis of geomagnetic, seismic and seismological data, a connection was demonstrated between the magnetic heterogeneities of the crystalline crust of the SW edge of the EEC, directly adjacent to the TTL and its NW branching at Songenfrei-Tornquist Zone and Thor-Tornquist Suture, with the structural features of the crystalline crust and upper mantle. The results obtained are substantiated by qualitative and quantitative analysis of the geomagnetic field and 3D magnetic modelling, as well as a series of diagrams, namely: diagrams of the main tectonic elements of the crystalline crust of the SW part of the EEC and its surroundings; diagrams of seismic heterogeneity of the subcrustal mantle; diagrams of types of transition layers from the upper to the middle/lower mantle.

• Diagram of the main tectonic elements of the crystalline crust, summarizing of published materials, reveals the following features.

In the TTL structure, as the main repeatedly activated lineament of the crystalline crust, two branches of different strike are distinguished: the NW one with a strike of 305° along the SW border of Fennoscandia and the SE one with a strike of 330° along Sarmatia. They form a triple junction with the Fennoscandia-Sarmatia accretion zone (strike ≈50°). The change in TTL strike is presumably associated with repeated rotational motion of Sarmatia relative to Fennoscandia during the accretion of these EEC segments [Bogdanova et al., 2013]. The volcanic provinces Sarmatia and Fennoscandia (Neoproterozoic Transscandinavian Igneous Belt 1 along the NW branch of TTL and Vendian Igneous Province

along its SE branch), as well as the rejuvenation of the crust in the west of the Baltic Shield (Sveconorwegian orogeny 1.1—0.95 Ga) indicate different ages of activation of the TTL branches.

TTL represents a complex, repeatedly activated system with 'plumage' and subparallel faults characteristic of right-lateral shifts. In the NW branch of the TTL, these are right-lateral shifts within WEP of the NW strike, traced to the HF fault in the triple junction zone of the TTL and Fennoscandia-Sarmatia Suture branches. The SE branch has a similar 'plumage' from the eastern flank of the TTL.

In addition to the main types of crystalline crust in the region (thick, high-velocity three-layer EEC crust and thin, low-velocity WEP crust), a transitional type of crust, previously identified by a number of researchers, has been traced along the Fennoscandia-Sarmatia Suture to the triple junction. It is characterized by the thrust of the lower EEC crust beneath the WEP crust. In the domain bounded by Songenfrei-Tornquist Zone and Thor-Tornquist Suture, seismic data show a three-layer thinned EEC crust, which indicates its transitional type and the EEC boundary along Thor-Tornquist Suture.

• In the subcrustal mantle at depths of 50—100 km, a thrust of high-velocity EEC mantle onto low-velocity WEP mantle has been traced. The mantle overthrust along Fennoscandia correlates with the underthrust of the lower crust of the EEC beneath the crust of the WEP and is probably associated with it by the synchronous movement of the lithosphere in a SW direction with the formation of a zone of extension to the NE of the TTL. The horizontal thickness of the mantle overthrust at these depths, projected onto the Earth's surface, varies from 150 km in the NW to 0 in the Ukrainian-Baltic activation area. The general strike of the thrust corresponds to the strike of the TTL.

TTL, which has a SW or near-vertical dip in the upper mantle section, corresponds to the vertical boundary of areas with different seismic velocities under the overthrust of the EEC subcrustal mantle. This circumstance awaits explanation. In the region, superstructural meridional trans-lithospheric activation zones of Sveconorwegian Front and Ukrainian-Baltic Zone of activation are recorded.

• In the structure of the upper mantle, inclined high-velocity layers identified with slabs have been distinguished. They have been with confidence traced in only five cases: SW of TTL, NE of it within Fennoscandia, and SW of Sarmatia (all three of which are SW dips), as well as a layer consistent with the Fennoscandia-Sarmatia Suture strike (SE dip) and a layer with a latitudinal strike parallel to the border of the Moesian Plate of the northern dip. They may indicate fragments of slabs from different stages of subduction processes in the region.

The intersections of major lineaments and the triple junction zone of the TTL and Fennoscandia-Sarmatia Suture branches reveal a connection with ultra-deep fluids established during 3D velocity modelling based on seismotomography data.

• In the heterogeneous transition layer from the upper mantle to the middle one of WEP the 'duplicate layers' interpreted as 'sunk' slabs are traced. They indicate SW subduction from the TTL side.

• Analysis of the anomalous magnetic field has revealed a lineament L, parallel to TTL and traced fragmentarily along Songenfrei-Tornquist Zone, Vinding Fault Zone, and Thor-Tornquist Suture. It marks the junction of the NW strike magnetic anomalies with the anomalies of the SW edge of the EEC. At the SW border of Fennoscandia, lineament L correlates with Caledonian deformation front.

• To construct a magnetic model of the crystalline crust, we consider unacceptable the use of any formal division of the anomalous magnetic field into regional and local components, which would result in the loss of the 'structural' factor of the field. Therefore, the regional magnetic anomalies are obtained by excluding the local anomalies from the observed field. Their sources are attributed to the entire upper crust section, while for the regional anomalies, sources are attributed to the middle and lower crust. Magnetization is assumed to be uniform, coinciding with the vector of the modern magnetic field, and

constant up to the Mohorovičić discontinuity or the Curie temperature of magnetite. Subject to strict limitations on the depth of the upper and lower edges of the sources, we consider the magnetic model of the crystalline crust to be one of the equivalent options. The estimated magnetization of the sources at the maximum possible depths to their lower edges turns out to be the minimum possible.

• The highest concentration of deep magnetic sources is observed in the region bounded by the meridional trans-lithospheric zones: Sveconorwegian Front and Ukrainian-Baltic Zones of activation. To the SE of Ukrainian-Baltic Zone of activation, there are no sources of anomalies associated with TTL.

• The main feature of the magnetic model of the SW edge of the EEC is the presence of sources accompanying TTL along Fennoscandia. They are recorded almost continuously, have a butt joint with the sources of the EEC itself, and are considered to be younger. The border of Sarmatia is accompanied by deep sources under the Pre-Carpathian Trough in the area of ultra-deep fluid and the L'viv Trough. We assume that part of the deep source between TTL and Rava-Rus'ka Fault, interpreted as L, refers to a band of sources similar to Koszalin-Chojnice Zone accompanying TTL. In the domain transitioning from the Baltic to Avalonia, sources associated with Songenfrei-Tornquist Zone, Vinding Fault Zone, and Thor-Tornquist Suture correlate with swarms of mafic dykes.

• The existence of multiple extension zones along the TTL, recognized by most researchers, creates favourable conditions for the introduction of mafic intrusions — sources of magnetic anomalies along the TTL. The presence of a subcrustal mantle overthrust, its association with the underthrust of the lower EEC crust beneath the WEP crust, increased permeability of the lithosphere, the 'blurriness' of the main geodynamic boundary, and the change of the structure of the thinned transition layer beneath the TTL contribute to the penetration of deep fluids into the crystalline crust and the formation of new ('secondary') magnetic minerals. Thus, the nature of deep magnetic sources associated with TTL is quite reasonably considered to be dual. Their magnetization is explained both by primary magnetic minerals of mafic rocks and by newly formed iron oxides brought from the depths.

The results obtained require further geological and geophysical analysis.

Acknowledgements. The study was carried out within the framework of the topic «Analysis of the geomagnetic field and magnetic models of lithospheric structures in connection with the solution of geological, geophysical and environmental problems» (State registration number: 0123U100234). We gratefully accept the reviewers' critical comments and have made the corrections we consider necessary to improve the article and make it easier to read.

We would like to express our special gratitude to Yevgenia Yeremenko for her technical support and assistance in compiling the article.

References

Airinei, S.T., Stoenescu, S.C., Velcescu, G., Romanescu, D., Visarion, M., Radan, S., Roth, M., Besutiu, L., & Besutiu, G. (1983). La carte de l'anomaliemagnétique DZ pour le territoire de la Roumanie: An. Inst. Geol. Geofiz. (ser. Geofiz., Hidrogeol. si Geol. Ing.), LXIII, 5—11.

Amashukeli, T.A., Murovskaya, A.V., Yegorova, T.P., & Alekhin, V.I. (2019). The deep structure of the Dobrogea and Fore-Dobrogea trough as an indication of the development of the Trans-European suture zone. *Geofizicheskiy Zhurnal*, 41(1), 153—171. https://doi: 10.24028/gzh.0203-3100.v41i1.2019.158869 (in Russian).

Arkani-Hamed, J., & Strangway, D.W. (1986). Magnetic susceptibility anomalies of lithosphere beneath eastern Europe and the Middle East. *Geophysics*, 51(9), 1711—1724. https://doi.org/10.1190/1.1442220.

Artemieva, I.M. (2019). Lithosphere structure in Europe from thermal isostasy. *Earth-Science Reviews*, 188, 454—468. https://doi.org/10.1016/j.earscirev.2018.11.004.

Artemieva, I.M. (2011). *The lithosphere: An interdisciplinary approach*. Cambridge Univ. Press, 773 p.

Artemieva, I.M., & Mooney, W.D. (2001). Thermal thickness and evolution of Precambrian lithosphere: a global study. *Journal of Geophysical Research: Solid Earth, 106*(B8), 16 387—16 414. https://doi.org/10.1029/2000JB900439.

Artemieva, I.M., & Thybo, H. (2013). EUNAseis: A seismic model for Moho and crustal structure in Europe, Greenland and North Atlantic region. *Tectonophysics*, 609, 97—153. https://doi.org/10.1016/j.tecto.2013.08.004.

Artemieva, I.M., Thybo, H., & Kaban, M.K. (2006). Deep Europe today: Geophysical synthesis of the upper mantle structure and lithospheric processes over 3.5 Ga. In D.G. Gee, R.A. Stephenson (Eds.), *European Lithosphere Dynamics* (Vol. 32, pp. 11—41). Geol. Soc. Spec. Publ. https://doi.org/10.1144/GSL.MEM.2006.032.01.02.

Atanasiu, L., Zugravescu, D., Mandea, M., & Roharik, M. (2005). Trans-European Suture Zone over the Romanian territory in the light of new satellite data. *Rev. Roum. Géophysique*, 49, 49—61.

Banka, D., Pharaoh, T.C., Williamson, J.P. and TESZ Project Potential Field Core Group (2002). Potential field imaging of Paleozoic central Europe. *Tectonophysics*, 360, 23—45. https://doi.org/10.1016/S0040-1951(02)00345-1.

Bayer, U., Grad, M., Pharaoh, T.C., Thybo, H., Guterch, A., Banka, D., Lamarche, J., Lassen, A., Lewerenz, B., Scheck, M., & Marotta, A.-M. (2002). The Southern Margin of the East European Craton: new results from seismic sounding and potential fields between the North Sea and Poland. *Tectonophysics*, 360, 301—314. https://doi.org/10.1016/S0040-1951(02)00359-1.

Bogdanova, S.V. (1993). The three-segment hypothesis for the East European Craton. *Terra Nova, 5*, 313—314.

Bogdanova, S.V., Gintov, O.B., Kurlovich, D.M., Lubnina, N.V., Nilsson, K.M., Orlyuk, M.I., Pashkevich, I.K., Shumlyanskyy, L.V., & Starostenko, V.I. (2013). Late Palaeo-proterozoic mafic dyking in the Ukrainian Shield of Volgo-Sarmatia caused byrotation during the assembly of supercontinent Columbia (Nuna). *Lithos* 174, 196—216. https://doi.org/10.1016/j.lithos.2012.11.002.

Bogdanova, S.V., Gorbatschev, R., & Garetsky, R.G. (2016). Europe/East European Craton. *In Reference Module in Earth Systems and Environmental Sciences* (pp. 1—18). Elsevier https://doi.org/10.1016/B978-0-12-409548-9.10020-X.

Bogdanova, S., Gorbatschev, R., Skridlaite, G., Soesoo, A., Taran, L., & Kurlovich, D. (2015). Trans-Baltic Palaeoproterozoic correlations towards the reconstruction of supercontinent Columbia/Nuna. *Precambrian Research, 259*, 5—33. https://doi.org/10.1016/j.precamres.2014.11.023.

Bogdanova, S.V., Gorbatschev, R., & Stephenson, R.A. (2001). EUROBRIDGE: Palaeoproterozoic Accre-tion of Fennoscandia and Sarmatia. *Tectonophysics*, *339*(1-2), 1—237. https://doi.org/10.1016/S0040-1951(01)00030-0.

Bogdanova, S.V., Pashkevich, I.K., Gorbatschev, R.M., & Orlyuk, M.I. (1996). Riphean rifting and major Paleoproterozoic boundaries in the East European Craton: geology and geophysics. *Tectonophysics, 268*, 1—22. https://doi.org/10.1016/S0040-1951(96)00232-6.

Brown, W.J., Beggan, C.D., Cox, G.A., & Macmillan, S. (2021). The BGS candidate models for IGRF-13 with a retrospective analysis of IGRF-12 secular variation forecasts. *Earth, Planets and Space, 73*, 42. https://doi.org/10.1186/s40623-020-01301-3.

Bulina, L.V. (1976). Characteristic features of the distribution of the lower edges of magnetized bodies on the territory of the USSR. In *Magnetic anomalies of the Earth's depths* (pp. 137—151). Kiev: Naukova Dumka (in Russian).

Burianov, V.B., Gordienko, V.V., Zavgorodnyaya, O.V., Kulik, S.N., Logvinov, I.M., & Shuman, V.N. (1987). *Geophysical model of the European tectonosphere*. Kiev: Naukova Dumka, 184 p. (in Russian).

Chekunov, A.V. (Ed.). (1992). *Schematic diagram of the deep structure of the lithosphere in the southwestern part of the East European Platform. Scale 1:1,000,000*. Kiev: Goskomgeologiya, 6 s. (in Russian).

Chyba, J., Plomerová, J., Vecsey, L., & Munzarová, H. (2017). Tomography study of the

upper mantle around the TESZ based on PASSEQ experiment data. *Physics of the Earth and Planetary Interiors, 266*, 29—38. https://doi.org/10.1016/j.pepi.2017.01.002.

Clark, Sh.C., Frey, H., & Thomas, H.H. (1985). Satellite magnetic anomalies over subduction zones: the Aleutian Arc anomaly. *Geophysical Research Letters, 12*(1), 41—44. https://doi.org/10.1029/gl012i001p00041.

Coles, R.L., Haines, G.V., Jansen van Beek, G., Nandi, A., & Walker, J.K. (1982). Magnetic anomaly map from 40 N to 83 N derive from MAGSAT sattelite data. *Geophysical Research Letters, 9*(4), 281—284. https://doi.org/10.1029/GL009i004p00281.

Coles, R.L., Haines, G.V., & Hannaford, W. (1976). Large-scale magnetic anomalies over western Canada and the Arctic: a discussion. *Canadian Journal of Earth Sciences, 13*(6), 790—802. https://doi.org/10.1139/e76-082.

EUGENO-S Working Group. (1988). Crustal structure and tectonic evolution of the transition between the Baltic Shield and the North German Caledonides (the EUGENO-S Project). *Tectonophysics 150*(3), 253—348. https://doi.org/10.1016/0040-1951(88)90073-X.

Ferré, E.C., Kupenko, I., Martín-Hernández, F., Ravat, D., & Sanchez-Valle, C. (2020). Magnetic sources in the Earth's mantle. *Nature Reviews Earth & Environment, 2*(1), 59—69. https://doi.org/10.1038/s43017-020-00107-x.

Gabriel, G., Vogel, D., Scheibe, R., Lindner, H., Pucher, R., Wonik, T., & Krawczyk, C.M. (2011). Anomalies of the earth's total magnetic field in Germany — The first complete homogeneous dataset reveals new opportunities for multiscale geoscientific studies. *Geophysical Journal International, 184*(3), 1113—1118. https://doi.org/10.1111/j.1365-246X.2010.04924.x.

Gemmer, L., & Nielsen, S.B. (2001). Three-dimensional inverse modelling of the thermal structure and implications for lithospheric strength in Denmark and adjacent areas of Northwest Europe. *Geophysical Journal International, 147*(1), 141—154. https://doi.org/10.1046/j.0956-540x.2001.01528.x.

Genshaft, Yu., & Pecherskyi, D.M. (1986). Petrological and petromagnetic evaluation of potential sources of regional magnetic anomalies. *Geofizicheskiy Zhurnal, 8*(5), 61—67 (in Russian).

Gintov, O.B., Tsvetkova, T.O., Bugaenko, I.V., Zayats, L.M., & Murovska, G.V. (2022). The deep structure of the Trans-European Suture Zone (based on seismic survey and GSR data) and some insights in to its development. *Geofizicheskiy Zhurnal, 44*(6), 63—87. https://doi.org/10.24028/gj.v44i6.273640 (in Ukrainian).

Gordienko, V.V., Gordienko, I.V., Zavgorodnya, O.V., Kovachikova, S., Logvinov,I.M., Tarasov, V.N., & Usenko, O.V. (2012). *Volyn-Podolian Plate (Geophysics, deep-seated processes).* Kiev: Naukova Dumka, 198 p. (in Russian).

Grabarczyk, A., Gil, G., Liu, Y., Kotowski, J., Jokubauskas, P., Barnes, J.D., Nejbert, K., Wiszniewska, J., & Bagiński, B. (2022). Ultramafic-alkaline-carbonatite Tajno intrusion in NE Poland: A new hypothesis about the massif formation and related mineralization. *Ore Geology Reviews, 143*, 104772. https://doi.org/10.1016/j.oregeorev.2022.104772.

Grabowska, T., & Bojdys, G. (2004). Analysis of geomagnetic field along seismic profile P4 of the International Project POLONAISE'97. *Tectonophysics, 383*, 15—28. https://doi.org/10.1016/j.tecto.2004.02.002.

Grabowska, T., & Bojdys, G. (2001). The border of the East-European Craton in south-eastern Poland based on gravity and magnetic data. *Terra Nova, 13*, 92—98. https://doi.org/10.1046/j.1365-3121.2001.00321.x.

Grabowska, T., Bojdys, G., Bielik, M., & Csicsay, K. (2011). Density and magnetic models of the lithosphere along CELEBRATION 2000 profile CEL01. *Acta Geophysica, 59*(3), 526—560. https://doi.org/10.2478/s11600-011-0007-3.

Grabowska, T., Bojdys, G., & Petecki, Z. (2017). Application of the magnetic anomalies for identification of structure of the crystalline basement of southeastern Poland. *Biuletyn Państwowego Instytutu Geologicznego, 470*, 17—48 (in Polish). https://doi.org/10.5604/01.3001.0010.6954.

Grad, M. (2019). Podolian, Saxonian and Baltic plates — Teisseyre-Tornquist Line and the edge of the East European Craton. *Geochemistry, 79*(3), 422—433. https://doi.org/10.1016/j.chemer.2019.03.002.

Grad, M., Guterch, A., & Mazur, S. (2002). Seismic refraction evidence for crustal structure in the central part of the Trans-European suture zone in Poland. In J.A. Winchester, T.C. Pharaoh, J. Verniers (Eds.), *Palaeozoic Amalgamation of Central Europe* (Vol. 201, pp. 295—309). Geol. Soc. Spec. Publ. https://doi.org/10.1144/GSL.SP. 2002.201.01.14.

Grad, M., Jensen, S.L., Keller, G.R., Guterch, A., Thybo, H., Janik, T., Tiira, T., Yliniemi, J., Luosto, U., Motuza, G., Nasedkin, V., Czuba, W., Gaczyński, E., Środa, P., Miller, K.C., Wilde-Piórko, M., Komminaho, K., Jacyna, J., & Korabliova, L. (2003). Crustal Structure of the Trans-European suture zone region along POLONAISE'9 L.7 seismic profile P4. *Journal of Geophysical Research: Solid Earth, 108*(B11), 2541. https://doi.org/10.1029/2003JB002426.

Grad, M., Polkowski, M., & Ostaficzuk, .R. (2016). High-resolution 3D seismic model of the crustal and uppermost mantle structure in Poland. *Tectonophysics, 666*, 188—210. https://doi.org/10.1016/j.tecto.2015.10.022.

Grad, M., Puziewicz, J., Majorowicz, J., Chrapkiewicz, K., Lepore, S., Polkowski, M., & Wilde-Piórko, M. (2018). The geophysical characteristic of the Lower lithosphere and asthenosphere in the marginal zone of the East European Craton. *International Journal of Earth Sciences, 107*, 2711—2726. https://doi.org/10.1007/s00531-018-1621-y.

Grad, M., Tiira, T. and ESC Working Group. (2009). The Moho depth map of the European Plate. *Geophysical Journal International, 176*(1), 279—292. https://doi.org/10.1111/j.1365-246x.2008.03919.x.

Gurskyi, D.S., & Kruglov, S.S. (Eds.). (2007). *Tectonic map of Ukraine.1:1000 000*. Kyiv: Publ. of the Ukrainian State Geological Prospecting Institute, 95 p. (in Ukrainian).

Hahn, A., & Wonik, T. (1990). Interpretation of aeromagnetic aniomalies. In R. Freeman, St. Mueller (Eds.), *Sixth EGT workshop: Data compilations and synoptic interpretation* (pp. 225—236). European Science Foundation, Strasbourg, France.

Haines, G.V. (1985). Magsat vertical field anomalies above 40 N from spherical Cap Harmonic Analysis. *Journal of Geophysical Research: Solid Earth, 90*(B3), 2593—2598. https://doi.org/10.1029/JB090iB03p02593.

Hall, D. (1974). Long-wavelength aeromagnetic anomalies and deep crustal magnetization in Manitoba and Northwestern Ontario, Canada. *Journal of Geophysics, 40*(1), 403—430.

Hippolyte, J.-C. (2002). Geodynamics of Dobrogea (Romania): new constraints on the evolution of the Tornquist-Teisseyre Line, the Black Sea and the Carpathians. *Tectonophysics, 357*(1-4), 33—53. https://doi.org/10.1016/s0040-1951(02)00361-x.

Janik, T., Starostenko, V., Aleksandrowski, P., Yegorova, T., Czuba, W., Środa, P., Murovskaya, A., Zayats, K., Mechie, J., Kolomiyets, K., Lysynchuk, D., Wójcik, D., Omelchenko, V., Legostaieva, O., Głuszyński, A., Tolkunov, A., Amashukeli, T., Gryn, D., & Chulkov, S. (2022). Lithospheric Structure of the East European Craton at the Transition from Sarmatia to Fennoscandia Interpreted from the TTZ-South Seismic Profile (SE Poland to Ukraine). *Minerals, 12*, 112. https://doi.org/10.3390/min12020112.

Janik, T., Yliniemi, J., Grad, M., Thybo, H., Tiira, T., and POLONAISE P2 Working Group. (2002). Crustal structure across the TESZ along POLONAISE'97 seismic profile P2 in NW Poland. *Tectonophysics, 360*, 129—152. https://doi.org/10.1016/s0040-1951(02)00353-0.

Kis, K.I., Taylor, P.T., Puszta, S., & Toronyi, B. (2024). Interpretation of magnetic measurements of the CHAMP and Swarm-A satellites over the Pannonian Basin. *Acta Geodaetica et Geophysica, 59*, 331—342. https://doi.org/10.1007/s40328-024-00445-y.

Kiss, J., & Gulyás, Á. (2006). *Magyarország Mágneses DZ-anomália térképe. 1:500 000 nyomtatott térkép*. ELGI kiadvány.

Korhonen, J., Fairhead, J.D., Hamoudi, M., Hemant, K., Lesur, V., Mandea, M., Maus, S., Purucker, M., Ravat, D., Sazonova, T., & Thébault, E. (2007). Magnetic anomaly map of the world-carte des anomalies magnétiquesdu monde. Commission for Geological Map of the World 1st Edition. Paris, France.

Kovalenko-Zavoyskiy, V.M., & Ivashenko, I.M. (2006). Mathematical provision for interpreting of ΔBa field of regional magnetic anomalies. *Geofizicheskiy Zhurnal, 28*(5), 18—30. https://doi.org/10.24028/gzh.0203-3100.v28i5.2006.215640 (in Ukrainian).

Krasovsky, S.S. (1981). *Reflection of the dynamics of the continental-type Earth's crust in the gravita-tional field.* Kiev: Naukova Dumka, 282 p. (in Russian).

Królikowski, C. (2006). Crustal-scale complexity of the contact zone between the Palaeozoic Platform and the East-European Craton in the NW Poland. *Geological Quartely, 50*(1), 33—42.

Krutikhovskaya, Z.A. (Ed.). (1982). *Anomalies of the geomagnetic field and the deep structure of the Earth's crust.* Kiev: Naukova Dumka, 172 (in Russian).

Krutikhovskaya, Z.A. (Ed.). (1984). *Study of regional magnetic anomalies of platform areas*. Kiev: Naukova Dumka, 220 p. (in Russian).

Krutykhovskaya, Z.A. (1976). The problem of creating a magnetic model of the Earth's crust of ancient shields. *Geophysical Communications*, (73), 3—25 (in Russian).

Krutikhovskaya, Z.A., Eliseeva, S.V., Markovsky, V.S., Rudakov, E.P., & Yakovlev, A.N. (1984). Study of regional magnetic anomalies of ancient shields. In *Study of regional magnetic anomalies of platform areas* (pp. 122—132). Kiev: Naukova Dumka (in Russian).

Krutikhovskaya, Z.A., & Pashkevich, I.K. (1977). Earth's crust magnetic model of the Ukrainian Shield. *Canadian Journal of Earth Sciences, 14*(12), 2718—2728. https://doi.org/10.1139/e77-239.

Krutikhovskaya, Z.A., & Pashkevich, I.K. (1979). Long-wavelength magnetic anomalies as a source of information about deep crustal structure. *Journal of Geophysics, 46*(1), 301—317.

Krutikhovskaya, Z.A., Pashkevich, I.K., & Silina, I.M. (1982). *Magnetic model and structure of the crust of the Ukrainian Shield*. Kiev: Naukova Dumka, 216 p. (in Russian).

Krutikhovskaya, Z.A., Pashkevich, I.K., & Simonenko, T.N. (1973). Magnetic anomalies of Precambrian Shields and some problems of their geological interpretation. *Canadian Journal of Earth Sciences, 10*(5), 629—636. https://doi.org/10.1139/e73-063.

Krzemińska, E., Krzemiński, L., Petecki, Z., Wiszniewska, J., Salwa, S., Żaba, J., Gaidzik, K., Williams, I.S., Rosowiecka, O., Taran, L., Johansson, A., Pecskay, Z., Demaiffe, D., Grabowski, J., & Zieliński, G. (2017). *Geological Map of Crystalline Basement in the Polish part of the East European Platform 1:1 000 000*. Polish Geological Institute, Warsaw.

Kubeš, P., Bezák, V., Kucharič, Ľ., Filo, M., Vozár, J., Konečný, V., Kohút, M. & Gluch, A. (2010). Magnetic field of the Western Carpathians (Slovakia): reflections on the structure of the crust. *Geologica Carpathica, 61*(5), 437—447. https://doi.org/10.2478/v10096-010-0026-z.

Kupenko, I., Aprilis, G., Vasiukov, D.M., Mc Cammon, C., Chariton, S., Cerantola, V., Kantor, I., Chumakov, A.I., Rüffer, R., Dubrovinsky, L., & Sanchez-Valle, C. (2019). Magnetism in cold subducting slabs at mantle transition zone depths. *Nature, 570*(7759), 102—106. https://doi.org/10.1038/s41586-019-1254-8.

Kutas, R.I. (2021). Deep degassing and oil-and-gas containment of the Eastern (Ukrainian) Carpathians: geodynamic and geothermal aspects. *Geofizicheskiy Zhurnal, 43*(6), 23—41. https://doi.org/10.24028/gzh.v43i6.251551 (in Ukrainian).

Kutas, R.I. (1993). Thermal field and geothermal regime of the lithosphere. In A.V. Chekunov (Ed.), *Lithosphere of Central and Eastern Europe* (pp. 115—132). Kiev: Naukova Dumka (in Russian).

Kutas, R.I., Krasovsky, S.S., Orlyuk, M.I., & Pashkevich, I.K. (1996). A model of deep structure and tectonic evolution of the lithosphere of western Ukraine. *Geofizicheskiy Zhurnal, 18*(6), 18—29 (in Russian).

Langel, R.A., & Hinze, W.J. (1998). *The magnetic field of the Earth's lithosphere: The satellite perspective*. Cambridge, UK: Cambridge University Press, 429 p. https://doi.org/10.1017/CBO9780511629549.

Langel, R.A., Coles, R.L., & Mayhew, M.A. (1980). Comparisons of magnetic anomalies of lithospheric origin measured by satellite and airborne magnetometers over Western Canada. *Canadian Journal of Earth Sciences, 17*(7), 876—887. https://doi.org/10.1139/e80-086.

Langel, R.A., Phillips, J.D., & Homer, R.J. (1982). Initial scalar magnetic anomaly map from MAGSAT. *Geophysical Research Letters, 9*(4), 269—272. https://doi.org/10.1029/GL009i004p00269.

Liu, P.F., Jiang, Y., Yan, Q., & Hirt, A.M. (2023). The behavior of a lithospheric magnetization and magnetic field model. *Earth and Planetary Physics, 7*(1), 66—73. http://doi.org/10.26464/epp2023025.

Lyngsie, S.B., & Thybo, H. (2007). A new tectonic model for the Laurentia-Avalonia-Baltica sutures in the North Sea: A case study along MONA LISA profile 3. Tectonophysics, 429(3), 201—227. http://doi.org/10.1016/j.tecto.2006.09.017.

Majorowicz, J., Polkowski, M., & Grad, M. (2019). Thermal properties of the crust and lithosphere-astenosphere boundary in the area of Poland from the heat flow variability and seismic data. *International Journal of Earth Sciences, 108*, 649—672. https://doi.org/10.1007/s00531-018-01673-8.

Makarenko, I.B., Burakhovych, T.K., Kozlenko, M.V., Murovskaya, G.V., Kozlenko, Yu.V., & Savchenko, O.S. (2025). RomUkrSeis profile: a model of the deep structure of the lithosphere and its geological and geophysical interpretation. P. II. The nature of geophysical heterogeneities based on complex analysis. *Geofizychnyi Zhurnal, 47*(1), 5—30. https://doi.org/10.24028/gj.v47i1.317035 (in Ukrainian).

Maksymchuk, V.Yu., Anikeyev, S.G., & Kuderavets, R.S. (2024). Reflection of the Teisseyre-Tornquist zone in gravimagnetic fields on the territory of Ukraine. *Proc. of the Scientific Conference. NAS of Ukraine, M.P. Semenenko Institute of Geochemistry, Mineralogy and Ore Formation (Kyiv, September 17—18, 2024)* (pp. 265—269). https://doi.org/10.30836/gbhgd.2024.55 (in Ukrainian).

Malehmir, A., Tryggvason, A., Wijns, C., Koivisto, E., Lindqvist, T., Skytta, P., & Montonen, M. (2018). Why 3D seismic data are an asset for exploration and mine planning? Velocity tomography of weakness zones in the Kevitsa Ni-Cu-PGE mine, northern Finland. *Geophysics, 82*, B33—B46. https://doi.org/10.1090/geo2017-0225.1.

Malinowski, M., Guterch, A., Narkiewicz, M., Petecki, Z., Janik, T., Sroda, P., Maksym, A., Probulski, J., Grad, M., Czuba, W., Gaczynski, E., Majdanski, M., & Jankowski, L. (2015). Geophysical constraints on the crustal structure of the East European Platform margin and its foreland based on the POL-CRUST-01 deep reflection seismic profile. *Tectonophysics, 653*, 109—126. https://doi.org/10.1016/j.tecto.2015.03.029.

Mayhew, M.A., Johnson, B.D., & Wasilewski, P.J. (1985). A review of problems and progress in studies of sattelite magnetic anomalies. *Journal of Geophysical Research: Solid Earth, 90*(3), 2511—2522. https://doi.org/10.1029/JB090iB03p02511.

Mazur, S., Malinowski, M., Maystrenko, Y.P., & Gągała, Ł. (2021). Pre-existing lithospheric weak zone and its impact on continental rifting — The Mid-Polish Trough, Central European Basin System. *Global and Planetary Change, 198*, 103417. https://doi.org/10.1016/j.gloplacha.2021.103417.

Mazur, S., Mikolajczak, M., Krzywiec, P., Malinowski, M., Buffenmyer, V., & Lewandowski, M. (2015). Is the Teisseyre-Tornquist Zone an ancient plate boundary of Baltica? *Tectonics, 34*, 2465—2477. https://doi.org/10.1002/2015TC003934.

Mazur, S., Porębski, S.J., Kędzior, A., Paszkowski, M., Podhalánska, T., & Poprawa, P. (2018). Refined timing and kinematics for Baltica-Avalonia convergence based on the sedimentary record of a foreland basin. *Terra Nova, 30*(1), 8—16. https://doi.org/10.1111/ter.12302.

McEnroe, S.A., Robinson, P., Church, N., & Purucker, M. (2018). Magnetism at Depth: A View from an Ancient Continental Subduction and Collision Zone. *Geochemistry, Geophysics, Geosystems*, 19, 1123—1147. https://doi.org/10.1002/2017GC007344.

Meyer, B., Chulliat, A., & Saltus, R. (2017). Derivation and error analysis of the earth magnetic anomaly grid at 2 arc min resolution version 3 (EMAG2v3). *Geochemistry, Geophysics, Geosystems, 18*, 4522—4537. https://doi.org/10.1002/2017GC007280.

Milano, M., Fedi, M., & Fairhead, J.D. (2019). Joint analysis of the magnetic field and total gradient intensity in central Europe. Solid Earth, 10(3), 697—712. https://doi.org/10.5194/se-10-697-2019.

Milano, M., Fedi, M., & Fairhed, J.D. (2016). The deep crust beneath the Trans-European Suture Zone from a multiscale magnetic model. *Journal of Geophysical Research: Solid Earth,*

121, 6276—6292. https://doi.org/10.1002/2016JB012955.

MONA LISA Working Group. (1997a). Deep seismic investigations of the lithosphere in the southeastern North Sea. *Tectonophysics, 269*, 1—19. https://doi.org/10.1016/S0040-1951(96)00111-4.

MONA LISA Working Group. (1997b). Closure of the Tornquist Sea: constraints from MONA LISA deep seismic reflection data. *Geology, 25*, 1071—1074. https://doi.org/10.1130/0091-7613(1997)025<1071:COTTSC>2.3.CO;2.

Mundt, W., Karataev, G.I., & Pashkevich, I.K. (1986). *Methodology for constructing a magnetic model of the lithosphere using geophysical methods (physical properties, seismometry, gravimetry and magne-tometry)* (pp. 131—147). Kiev: Naukova Dumka (in Russian).

Narkiewicz, M., Grad, M., Guterch, A., & Janik, T. (2011). Crustal seismic velocity structure of southern Poland: preserved memory of a pre-Devonian terrane accretion at the East European Platform margin. *Geological Magazine, 148*(2), 191—210. https://doi.org/10.1017/S001675681000049X.

Narkiewicz, M., Maksym, A., Malinowski, M., Grad, M., Guterch, A., Petecki, Z., Probulski, J., Janik, T., Majdañski, M., Sroda, P., Czuba, W., Gaczyñski, E., & Jankowski, L. (2015). Transcurrent nature of the Teisseyre-Tornquist Zone in Central Europe: results of the POLCRUST-01 deep reflection seismic profile. *International Journal of Earth Sciences, 104*(3), 775—796. https://doi.org/10.1007/s00531-014-1116-4.

Narkiewicz, M., & Petecki, Z. (2019). Teisseyre-Tornquist Zone — evolving approaches and new data. *Przegląd Geologiczny, 67*(10), 837—848. https://dx.doi.org/10.7306/2019.48 (in Polish).

Narkiewicz, M., & Petecki, Z. (2024). The Pomerania Gravity Low at the East European Craton margin — a granitic batholith or a Paleoproterozoic impact structure? *Geological Quarterly, 68*(1), 1—12. https://doi.org/10.7306/gq.1725.

Nechaeva, T.S., Shymkiv, L.M., & Gorkavko, V.M. (2002). *Map of the anomalous magnetic field* $(\Delta T)_a$ *of Ukraine, scale 1:1,000,000*. Kyiv, 1 s. (in Russian).

Orlyuk, M.I. (1986). Connection of the anomalous magnetic field with the structure of the Earth's crust of the Volyn'-Podolie Plate. *Doctor's thesis*. Kyiv, 17 p. (in Russian).

Orlyuk, M.I. (1984). Magnetic model of the Earth's crust of the Volyn'-Podolie edge of the East European Platform and petrological-tectonic interpretation. In *Study of regional magnetic anomalies of platform areas* (pp. 152—162). Kiev: Naukova Dumka (in Russian).

Orlyuk, M.I. (2000). Spatial and spatio-temporal magnetic models of different rank structures of the continental lithosphere. *Geofizicheskiy Zhurnal, 22*(6), 148—165 (in Russian).

Orlyuk, M.I. (1993). Structure of the lithosphere along geotraverse III. Magnetic model. In *Lithosphere of Central and Eastern Europe. Geotraverses III, VII, IX* (pp. 30—35). Kiev: Naukova Dumka (in Russian).

Orlyuk, M.I., Bakarjieva, M.I., & Marchenko, A.V. (2022). Magnetic characteristics and tectonic structure of the Earth's crust of the Carpathian oil-and-gas region as a component of complex hydrocarbon criteria. *Geofizicheskiy Zhurnal, 44*(5), 77—103. https://doi.org/10.24028/gj.v44i5.272328 (in Ukrainian).

Orlyuk, M.I., Drukarenko, V.V., & Shestopalova, O. Ye. (2020). Magneto-mineralogical grounds of the Earth's upper mantle magnetization. Overview. Geodynamics, 2(29), 89—96. https://doi.org/10.23939/jgd2020.02.089.

Orlyuk, M.I., Kovalenko-Zavoysky, V.M., Ivashchenko, I.M., & Marchenko, A.V. (2007). Interpretation of regional magnetic anomalies taking into account the sphericity of the Earth. *Abstracts of the VIII International Conference «Monitoring of Unsafeness Geological Processes and the Ecological State of the Environment», Kyiv* (pp. 76—77) (in Ukrainian).

Orlyuk, M.I., & Marchenko, A.V. (2008). Cartographic support for the development of a 3D magnetic model of the Earth's crust of the East European Platform (taking into account the sphericity of the Earth). *Geophysical technologies for forecasting and monitoring the geological environment. Proc. of the scientific conference, 6—10 October 2008, Lviv* (pp. 154—155) (in Ukrainian).

Orlyuk, M., Marchenko, A., & Bakarjieva, M. (2017). 3D magnetic model of the Earth crust

of the Eastern European craton with the account of the Earths sphericity and its tectonic interpretation. *Visnyk of Taras Shevchenko National University of Kyiv, Geology, 76*(4), 55—60. https://doi.org/10.17721/1728-2713.79.03.

Orlyuk, M., Marchenko, A., & Romanets, A. (2016). The connection between the Earth's seismicity and secular variations in its magnetic field. *Visnyk of Taras Shevchenko National University of Kyiv, Geology, 75*(4), 50—54. https://doi.org/10.17721/1728-2713.75.08 (in Ukrainian).

Orlyuk, M., Marchenko, A., Romenets, A., Bakarzhieva, M., & Orliuk, I. (2024a). Development of geomagnetic field induction module maps for the territory of Ukraine. *Geodynamics, 1*(36), 74—84. https://doi.org/10.23939/jgd2024.01.074.

Orlyuk, M.I., Marchenko, A.V., Romanets, A.O., Bakarzhieva, M.I., & Orlyuk, I.M. (2024b). Geomagnetic field of Ukraine. *Geological structure and history of geological development of the Ukrainian Shield (on the 100th anniversary of the birth of Academician M.P. Shcherbak of the National Academy of Sciences of Ukraine). Collection of materials from the scientific conference. National Academy of Sciences of Ukraine, M.P. Semenenko Institute of Geochemistry, Mineralogy and Ore Formation (Kyiv, 17—18 September 2024)* (pp. 285—289) (in Ukrainian).

Orlyuk, M.I., & Pashkevich, I.K. (1995). Magnetic model of the Earth's crust of the SW East European Platform (EEP). *Geofizicheskiy Zhurnal, 17*(6), 31—36 (in Russian).

Orlyuk, M.I., Romenets, A.O., Marchenko, A.V., & Orlyuk, I.M. (2025). Spatio-temporal disturbances of the Earth's magnetic field along the Struve Geodetic Arc. *Geofizychnyi Zhurnal, 47*(3), 102—118. https://doi.org/10.24028/gj.v47i3.323184.

Pashkevich, I.K. (1989). Platform boundary based on magnetic survey data. In *Lithosphere of Central and Eastern Europe: East European Platform* (pp. 18—22). Kiev: Naukova Dumka (in Russian).

Pashkevich, I.K., Kutovaya, A.P., & Orlyuk, M.I. (1985). On the southwestern edge of the East European Platform. *Geofizicheskiy Zhurnal, 7*(5), 74—82 (in Russian).

Pashkevich, I.K., Markovsky, V.S., Orliuk, M.I., Eliseeva, S.V., Mozgovaya, A.P., & Taraschan, S.A. (1990). *Magnetic model of the lithosphere of Europe*. Kiev: Naukova Dumka, 168 p. (in Russian).

Pashkevich, I.K., Markovsky, V.S., & Orlyuk, M.I. (1986). Petrological interpretation of the nature of the regional component of the anomalous magnetic field. *Geofizicheskiy Zhurnal, 8*(2), 26—36 (in Russian).

Pashkevich, I.K., Orlyuk, M.I., Marchenko, A.V., Romenets, A.O., Tsvetkova, T.O., & Bugayenko, I.V. (2020). On the possible mantle nature of the long-wave Central-European magnetic anomaly. *Geofizicheskiy Zhurnal, 42*(6), 100—130. https://doi.org/10.24028/gzh.0203-3100.v42i6.2020.222288 (in Russian).

Pashkevich, I.K., & Rusakov, O.M. (2021). Integrated geological-geophysical characterization of the zone of the Kherson–Smolemsktransregional tectonic suture — deep long-lived magma- and fluid-conducting channel. *Geofizicheskiy Zhurnal, 43*(5), 111—126. https://doi.org/10.24028/gzh.v43i5.244075 (in Russian).

Pashkevich, I.K., Sharov, N.V., Savchenko, A.S., & Starostenko, V.Y. (2014). Three-dimensional geological and geophysical model of the lithosphere of the central part of the Karelian craton. *Geofizicheskiy Zhurnal, 36*(6), 58—78. https://doi.org/10.24028/gzh.0203-3100.v36i6.2014.111024 (in Russian).

Pechersky, D.M. (Ed.). (1994). *Petromagnetic model of the lithosphere*. Kiev: Naukova Dumka, 175 p. (in Russian).

Petecki, Z. (2008). Magnetic basement in the Pomeranian segment of the Trans-European Suture Zone (NW Poland). *Prace Pañstwowego Instytutu Geologicznego, 191*, 5—72 (in Polish).

Petecki, Z. (2001). Magnetic evidence for deeply buried crystal line basement south west of the Teisseyre-Tornquist Line in NW Poland. *Acta Geophysica Polonica, 49*, 509—515.

Petecki, Z., Polechoñska, O., Wybraniec, S., & Cieoela, E. (2003). *Magnetic map of Poland at a scale of 1:500 000*. Parts A and B on CD-ROM. Pañstw. Inst. Geol. Warszawa.

Petecki, Z., & Rosowiecka, O. (2017). A new magnetic anomaly map of Poland and its contribu-

tion to the recognition of crystalline basement rocks. *Geological Quarterly, 61*(4), 934—945. https://doi.org/10.7306/gq.1383.

Pharaoh, T.C., Winchester, J.A., Verniers, J., Lassen, A., & Seghedi, A. (2006). The Western Accretion-ary Margin of the East European Craton: an overview. In D.G. Gee, R.A. Stephenson (Eds.), *European Lithosphere Dynamics* (Vol. 32, pp. 291—311). Geol. Soc. Spec. Publ. https://doi.org/10.1144/GSL.MEM.2006.032.01.17.

Purucker, M., Langlais, B., Olsen, N., Hulot, G., & Mandea, M. (2002). The southern edge of cratonic North America: Evidence from new satellite magnetometer observations. *Geophysical Research Letters, 29*(15), 8000. https://doi.org/10.1029/2001GL013645.

Puziewicz, J. (2008). Petrologic interpretation of the CELEBRATION 2000 profiles (CEL05, CEL01, CEL04). In M. Grad, A. Guterch (Eds*.), Comprehensive Interpretation of Potential Field Anomalies Along All the Deep Refraction Profiles on the Whole CEL 2000 Region*. Arch. Pol. Acad. Sci., Warsaw (in Polish).

Puziewicz, J. (2006). Skały dolnej skorupy i najwyższego płaszcza ziemi na obszarze eksperymentu POLONAISE'97 — Modele petrologiczno-sejsmiczne (Lower crust and uppermost mantle rocks in the area of the POLONAISE'97 seismic experiment — Petrologic-seismic models). *Prace Państwowego Instytutu Geologicznego, 188*, 53—68 (in Polish).

Ravat, D., Hinze, W.J., & Taylor, P.T. (1993) European tectonic features observed by Magsat. *Tectonophysics, 220*, 157—173. https://doi.org/10.1016/0040-1951(93)90229-D.

Riddihough, R.P. (1972). Regional Magnetic Anomalies and Geology in Fennoscandia: A discussion. *Canadian Journal of Earth Sciences, 9*(3), 219—232. https://doi.org/10.1139/e72-018.

Schnetzler, C.C., & Allenby, R.J. (1983). Estimation of lower crust magnetization from satellite derived anomaly field. *Tectonophysics, 95*, 33—45. https://doi.org/10.1016/0040-1951(83)90232-9.

Seghedi, A. (2012). Palaeozoic Formations from Dobrogea and Pre-Dobrogea — An Overview. *Turkish Journal of Earth Sciences, 21*, 669—721. https://doi.org/10.3906/yer-1101-20.

Sollogub, V.B. (Ed.). (1988a). *Lithosphere of Central and Eastern Europe: Geotraverses I, II, V*. Kiev: Naukova Dumka, 172 p. (in Russian).

Sollogub, V.B. (Ed.). (1988b). Lithosphere *of Central and Eastern Europe: Geotraverses IV, VI, VIII.* Kiev: Naukova Dumka, 172 p. (in Russian).

Środa, P. (2006). Seismic anisotropy of the upper crust in southeastern Poland — effect of the compressional deformation at the EEC margin: Results of CELEBRATION 2000 seismic data inversion. *Geo-physical Research Letters, 33*, L22302. https://doi.org/10.1029/2006GL027701.

Starostenko, V., Janik, T., Kolomiyets, K., Czuba, W., Środa, P., Grad, M., Kovacs, I., Stephenson, R., Lysynchuk, D., Thybo, H., Artemieva, I.M., Omelchenko, V., Gintov, O., Kutas, R., Gryn, D., Guterch, A., Hegedűs, E., Komminaho, K., Legostaeva, O., Tiira, T., & Tolkunov, A. (2013). Seismic velocity model of the crust and upper mantle along profile PANCAKE across the Carpathians between the Pannonian Basin and the East European Craton. *Tectonophysics, 608*, 1049—1072. https://doi. org/10.1016/j.tecto.2013.07.008.

Starostenko, V., Janik, T., Mocanu, V., Stephenson, R., Yegorova, T., Amashukeli, T., Czuba, W., Środa, P., Murovskaya, A., Kolomiyets, K., Lysynchuk, D., Okoń, J., Dragut, A., Omelchenko, V., Legostaeva, O., Gryn, D., Mechie, J., & Tolkunov, A. (2020). RomUkrSeis: Seismic model of the crust and upper mantle across the Eastern Carpathians — From the Apuseni Mountans to the Ukrainian Shield. *Tectonophysics, 794*, 226820. http://doi.org/10.1016/j.tecto.2020.228620.

Starostenko, V.I., Murovskaya, A.V., Yegorova, T.P., Gintov, O.B., & Amashukeli, T.A. (2022). The relationship of the oil and gas fields of the Forecarpathian region with the regional faults system and deep structure. *Geofizicheskiy Zhurnal, 44*(1), 111—123. https://doi.org/10.24028/gzh.v44i1.253713.

Stephens, M.B. (2020). Chapter 1. Introduction to the lithotectonic framework of Sweden and organization of this Memoir. In M.B. Stephens, J. Bergman Weihed (Eds.), *Sweden: Lithotectonic Framework, Tectonic Evolution and Mineral Resources* (Vol. 50, pp. 1—15). Geol. Soc., London, Memoirs. https://doi.org/10.1144/M50-2019-21.

Taylor, P.T., & Ravat, D. (1995). An interpretation of the Magsat anomalies of central Europe. *Journal of Applied Geophysics, 34*(2), 83—91. https://doi.org/10.1016/0926-9851(95)00015-1.

Thébault, E., Purucker, M., Whaler, K.A., Langlais, B., & Sabaka, T.J. (2010).The Magnetic Field of the Earth's Lithosphere. *Space Science Reviews, 155*(1-4), 95—127. https://doi.org/10.1007/s11214-010-9667-6.

Thybo, H. (2001). Crustal structure along the EGT profile across the Tornquist Fan interpreted from seismic, gravity and magnetic data. *Tectonophysics, 334*, 155—190. https://doi.org/10.1016/S0040-1951(01)00055-5.

Thybo, H. (1997). Geophysical characteristics of the Tornquist Fan area, northwest Trans-European Suture Zone: indication of late Carboniferous to early Permian dextral transtension. *Geological Magazine, 134*(5), 597—606. https://doi.org/10.1017/S0016756897007267.

Thybo, H., Janik, T., Omelchenko, V.D., Grad, M., Garetsky, R.G., Belinsky, A.A., Karatayev, G.I., Zlotski, G., Knudsen, M.E., Sand, R., Yliniemi, J., Tiira, T., Luosto, U., Komminaho, K., Giese, R., Guterch, A., Lund, C.E., Kharitonov, O.M., Ilchenko, T., Lysynchuk, D.V., Skobelev, V.M., & Doody, J.J. (2003). Upper lithosphere seismic velocity structure across the Pripyat Trough and Ukrainian Shield along the EURUBRIDGE'97 profile. *Tectonophysics, 371*, 41—79. https://doi.org/10.1016/S0040-1951(03)00200-2.

Thybo, H., Pharaoh, T., & Guterch, A. (Eds.). (2002). The Trans European Suture Zone II. *Tectonophysics, 360*. https://doi.org/10.1016/S0040-1951(02)00343-8.

Thybo, H., & Schönharting, G. (1991). Geophysical evidence for Early Permian igneous activity in a transtensional environment, Denmark. *Tectonophysics, 189*, 193—208. https://doi.org/10.1016/0040-1951(91)90496-F.

Toft, P.B., & Haggerty, S.E. (1988).Limiting depth of magnetization in cratonic lithosphere. *Geophysical Research Letters, 15*(5), 530—533. https://doi.org/10.1029/gl015i005p00530.

Tsvetkova, T.A., Bugaenko, I.V., & Zaets, L.N. (2017). Seismic visualization of plumes and super-deep fluids in mantle under Ukraine. *Geofizicheskiy Zhurnal, 39*(4), 42—54. http://dx.doi.org/10.24028/gzh.0203-3100.v39i4.2017.107506244080 (in Russian).

Tsvetkova, T.A., Bugaenko, I.V., & Zaets, L.N. (2021). Speed structure of the mantle of the border of the Eastern European and West European platforms. *Geofizicheskiy Zhurnal, 43*(5), 181—192. https://doi.org/10.24028/gzh.v43i5.244080 (in Russian).

Tsvetkova, T.A., Bugaenko, I.V., & Zaets, L.N. (2019). The main geodynamic border and seismic visu-alization of plumes under the East European Platform. *Geofizicheskiy Zhurnal, 41*(1), 137—152. https://doi.org/10.24028/ gzh.0203-3100.v41i1.2019.158868 (in Russian).

Van Hoorn, B. (1987). Structural evolution, timing and tectonic style of the Sole Pit inversion. *Tectonophysics, 137*, 239—284. https://doi.org/10.1016/0040-1951(87)90322-2.

Vervelidou, F., & Thébault, E. (2015). Global maps of the magnetic thickness and magnetization of the Earth's lithosphere. *Earth, Planets and Space, 67*, 173. https://doi.org/10.1186/s40623-015-0329-5.

Wasilewski, P.J., Thomas, H.H., & Mayhew, M.A. (1979). The Moho as a magnetic boundary. *Geophysical Research Letters, 6*(7), 541—544. https://doi.org/10.1029/gl006i007p00541.

Wilde-Piórko, M., Świeczak, M., Grad, M., & Majdański, M. (2010). Integrated seismic model of the crust and upper mantle of the Trans-European Suture zone between the Precambrian craton and Phanerozoic terranes in Central Europe. *Tectonophysics, 481*, 108—115. https://doi.org/10.1016/j.tecto.2009.05.002.

Williams, S.E., & Gubbins, D. (2019). Origin of Long-Wavelength Magnetic Anomalies at Subduction Zones. *Journal of Geophysical Research: Solid Earth, 124*(9), 1—17. https://doi.org/10.1029/2019jb017479.

Williamson, J.P., Pharaoh, T.C., Banka, D., Thybo, H., Laigle, M., & Lee, M.K. (2002). Potential field modelling of the Baltica-Avalonia (Thor-Tornquist) suture beneath the southern North Sea. *Tectonophysics, 360*(1-4), 47—60. https://doi.org/10.1016/s0040-1951(02)00346-3.

Wonik, T.K., Trippler, K., Geipel, H., Grein-

wald, S., & Pashkevich, I.K. (2001). Magnetic anomaly map of northern, western and Eastern Europe. *Terra Nova, 13*, 203—213. https://doi.org/10.1046/j.1365-3121.2001.00341.x.

Zayats, H.B. (2013). *Deep structure of the subsoil of the Western region of Ukraine based on seismic studies and directions of exploration for oil and gas*. Lviv: Centre of Europe, 79 p. (in Ukrainian).

Zhu, H., Bozdağ, E., & Tromp, J. (2015). Seismic structure of the European upper mantle based on adjoint tomography. *Geophysical Journal International, 201*, 18—52. https://doi.org/10.1093/gji/ggu492.

Магнітна модель кристалічної кори та неоднорідність літосфери в зоні зчленування Східноєвропейського кратону з навколишніми структурами. Частина 1. Південно-західна межа кратону

І.К. Пашкевич, М.І. Орлюк, М.І. Бакаржієва, А.В. Марченко, 2026

Інститут геофізики ім. С.І. Субботіна НАН України, Київ, Україна

У статті вперше зроблено спробу встановити зв'язок магнітних неоднорідностей кристалічної кори в районі лінії Тейссейре—Торнквіста південно-західної окраїни Східноєвропейського кратона з неоднорідностями мантії. 3D магнітну модель кристалічної кори побудовано з використанням приземного аномального магнітного поля, швидкісних і структурних розрізів по сейсмічних профілях. Джерела віднесені до двох поверхів: локальні до всієї товщини верхньої кори, глибинні — до середньої і нижньої кори. Намагніченість прийнята однорідною, рівноважною і постійною до глибини розділу Мохо та досягнення температури Кюрі магнетиту. Така параметризація моделі призвела до оцінки мінімально можливих значень намагніченості джерел. Збіг сумарного ефекту корових джерел зі спостереженим полем досягався методом проб і помилок з похибкою, яка не перевищувала 30 нТ. Співвідношення корових магнітних неоднорідностей і структури мантії базується на використанні складених схем головних особливостей кристалічної кори, неоднорідності підкорової мантії та перехідного шару від верхньої до середньої мантії. Головною особливістю 3D магнітної моделі є наявність глибинних магнітних тіл, супутніх лінії Тейссейре—Торнквіста, зоні Соргенфрей—Торнквіста і шву Тор—Торнквіста. Смуга магнітних тіл з північного сходу обмежена субпаралельним лінії Тейссейре—Торнквіста лінеаментом L, виділеним нами за структурою магнітного поля. Він корелює з деформаційним фронтом Каледонід у Фенноскандії та Рава-Руським розломом у Сарматії. Це дає змогу пов'язати магнітні джерела з активізацією системи лінії Тейссейре—Торнквіста та мафічними інтрузіями. Про магматичний генезис даних магнітних джерел свідчить також положення їх над насувом підкорової мантії Східноєвропейського кратона на мантію Західноєвропейської платформи. Насув встановлений за даними сейсмотомографії. Він корелює з підсувом нижньої кори Східноєвропейського кратона під кору Західноєвропейської платформи. Передбачається зв'язок цих структур із синхронним рухом їх із північного сходу на південний захід, формуванням зони розтягування та інтрузій. Режим розтягування вздовж лінії Тейссейре—Торнквіста може також бути обумовленим південно-західною субдукцією, що підтверджують виділені високошвидкісні похилі шари (слеби). Магматичне походження магнітних джерел не виключає утворення «вторинних» магнітних мінералів унаслідок проникнення в

кристалічну кору глибинних флюїдів. Цьому процесу сприяє підвищена проникність літосфери, «розмитість» головної геодинамічної межі, порушення структури перехідного шару верхньої мантії. Природа глибинних магнітних джерел, пов'язаних з лінією Тейссейре—Торнквіста, пояснюється таким чином як первинними магнітними мінералами мафічних порід, так і вторинними, привнесеними з глибин.

Ключові слова: Східноєвропейський кратон, 3D магнітне моделювання, магнітне поле, неоднорідність літосфери, магнітні аномалії, магматизм, лінія Тейссейре—Торнквіста, мантія, зони субдукції.